Petrologic Comparison of Cataclastic Rocks From Shallow and Deeper Crustal Levels Within the San Andreas Fault System of Southern California

J. Lawford Anderson
Robert H. Osborne

Department of Geological Sciences
University of Southern California

USGS CONTRACT NO. 14-08-0001-17732
Supported by the EARTHQUAKE HAZARDS REDUCTION PROGRAM

OPEN-FILE NO. 80-987

U.S. Geological Survey
OPEN FILE REPORT

I. INTRODUCTION

Studies leading to earthquake prediction and control require not only a knowledge of the causes and mechanics of earthquakes, but also an understanding of the physical, compositional, and mechanical properties of the geologic system in which they occur. Presently, little has been written about the nature of cataclastic rocks within fault zones except that it is generally markedly different from rocks on either side of the fault; that it may be fault gouge, fault breccia, cataclasite, or mylonite;[1] and that it originates from mechanical crushing of rocks and from varying degrees of secondary chemical and mineralogical alterations by fluids moving through the fault zone (Higgins, 1971).

The authors have recently completed a study of cataclastic rocks along the present trace of the San Andreas (Anderson, et al, in press) and the findings are summarized below in the section "Cataclastic Rocks within the San Andreas Fault Zone of Southern California." Our present effort has been directed at the San Gabriel Fault (Figure 1 and Plate 1) which as a deeply eroded precursor to the present San Andreas may provide intrafault material representative of deeper crustal levels. First, the physical effects of intrafault cataclastic material on rock failure characteristics will be briefly reviewed.

[1]Following the nomenclature of Higgins (1971), these cataclastic rocks have the following characteristics (1) fault breccia-no primary cohesion with more than 30% fragments which are greater than 0.3 mm in diameter (2) gouge- "paste-like" cataclastic rock with no primary cohesion and less than 30% fragments greater than 0.3 mm, (3) cataclasite-aphanitic cataclastic rock with most fragments less than 0.2 mm and constituting less than 30% and, (4) mylonite-cohesive cataclastic rock with fluxion structure and 10-50 percent porphyroclasts generally larger than 0.2 mm.

Figure 1. Map showing the San Andreas and San Gabriel Fault Zones of Southern California and sample location sites.

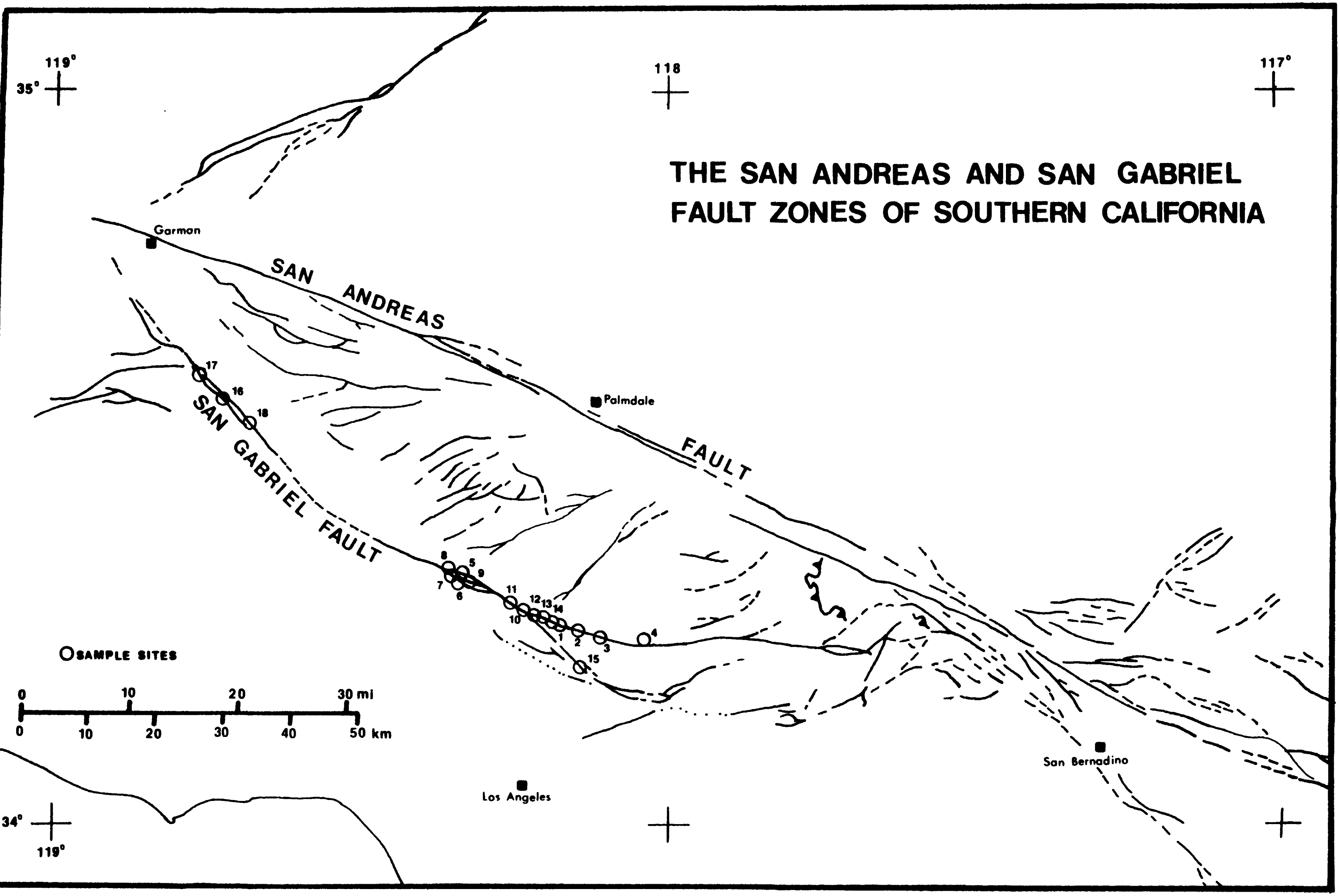
THE SAN ANDREAS AND SAN GABRIEL
FAULT ZONES OF SOUTHERN CALIFORNIA
119°
35°
118
117°
34°
119°
Garman
Palmdale
Los Angeles
San Bernadino
SAN ANDREAS FAULT
SAN GABRIEL FAULT
1
2
3
4
5
6
7
8
9
10
11
12
13
14
15
16
17
18
SAMPLE SITES
0
10
20
30 mi
0
10
20
30
40
50 km

Plate 1. Exposure of the San Gabriel Fault in Little Tujunga Canyon, San Gabriel Mountains. White rock on the left is the Josephine granodiorite and the darker rock on the right is the Mendenhall Gneiss. The fault is marked by the thin black 1-3 cm zone of cataclasite separting the two litholgies. View is to the northwest. Note person at lower right for scale.

A. Role of Intrafault Material

The importance of cataclastic intrafault material such as fault gouge in controlling the failure characteristics of rocks has been demonstrated in experimental studies. Scholz et al. (1972) noted that the development of gouge allowed the samples to reach a steady-state frictional behavior and that the gouge seems to have the effect of reducing the stress drops to a small fraction of their value for clean ground surfaces. The latter feature concurs with the suggestion by Stesky and Brace (1973) that the presence of low strength alteration materials in the San Andreas fault zone may account for the low frictional shear stress estimates provided from heat flow data relative to the much higher estimates from high-temperature frictional studies.

Wu et al. (1975) have suggested that the mineralogy of gouge may govern the type of failure (creep versus stick-slip) in fault zones. They argue convincingly that within the fault zone, to a depth of perhaps 12 km, sodic and magnesian-rich Franciscan rocks alter to expandible clay (montmorillonite) gouge which, by its strength, governs the nature of fault movement.

Recent experimental studies, however, have shown that the stablizing influence of fault gouge decreases with increasing confining pressure. Logan (1977 a,b; 1978) has shown that stable sliding is a consequence of low pressure and, even with the presence of fault gouge, the failure characteristics become increasingly unstable and change to a catastrophic stick-slip mode of displacement as the confining pressure is increased. The transition from stable to stick-slip motion is very dependent upon mineralogy. For quartz and feldspar gouge the mechanical transition is at about 2.5 kb. For soft minerals with a high degree of compaction characteristics, such as carbonates, the transition occurs only at about 1.0 kb. Although montmorillonite clay gouge certainly enhances stability (transition occurs at about 6.0 kb) other clays, particularly kaolinite, do not readily affect the sliding behavior relative to other gouge mineralogies. Byerlee _et al_. (1978) have speculated that the overriding factor governing the transition from stable to stick-slip displacement may be the compaction behavior or porosity of the fault gouge. Engelder (1974) has demonstrated that the grain size of cataclastic rocks within fault zones decreases with increasing confining pressure and the resultant loss of porosity (increased compaction) may favor unstable sliding. The prevailing geothermal gradient is also a major factor governing this transition (Brace, 1972) and Logan (1978) has demonstrated that unstable sliding becomes increasingly stable as temperature increases beyond 400^0C.

Unfortunately there have been few detailed petrologic studies of the cataclastic rocks comprising the intrafault material of fault zones. This is particularly evident for active fault zones, such as the San Andreas, where realistic modeling of rock failure is important. Nason (1972), Wu _et al_. (1975), Wu (1977), and Wang (1977) have demonstrated the existence of "clay" gouge along the trace of the San Andreas in central California where large sections of the fault exhibit creep slippage (Nason, 1973). This gouge differs from the gouge along the fault in southern California.

B. Cataclastic rocks within the San Andreas Fault Zone of southern California

As reported in Anderson, et al. (in press) and in our technical reports of last year, the principal cataclastic rock formed along the San Andreas Fault in southern California is unindurated gouge derived from a range of crystalline rocks including diorite, tonalite, granite, aplite, and pegmatite. The mineralogical nature of this gouge is decidedly different from the "clay gouge" reported by Wu (1975) for central California and is essentially a rock flour with a quartz, feldspar, biotite, chlorite, amphibole, epidote and oxide mineralogy representing the milled-down equivalent of the original rock. Clay development is minor (less than 4 wt. %) to nonexistent and is exclusively kaolinite. Alterations involve hematitic oxidation, chlorite alteration on biotite and amphibole, and local introduction of calcite. Electron microprobe analysis showed that in general the major minerals were not reequilibrated with the pressure-temperature regime imposed during cataclasis.

Petrochemically, the form of cataclasis that we have investigated is largely an isochemical process. Some hydration occurs but the maximum amount is less than 2.2% added H_2O. Study of a 375 meter deep core from a tonalite pluton adjacent to the fault showed that for Si, Al, Ti, Fe, Mg, Mn, K, Na, Li, Rb and Ba, no leaching and/or enrichment occurred. Several samples experienced a depletion in Sr during cataclasis while lesser number had an enrichment of Ca (result of calcite veining).

Texturally, the fault gouge is not dominated by clay-size material but consists largely of silt and fine sand sized particles.

An intriguing aspect of our work on the drill core is a general decrease in particulate size with depth (and confining pressure) with the predominate mode shifting sequentially from fine sand to silt size material.

The original fabric of these rocks is commonly not disrupted during the cataclasis. It is evident that the gouge development in these primarily igneous crystalline terranes is largely an *in situ* process with minimal mixing of rock types. Fabric analyses reveal that brecciation (shattering), not shearing, is the major deformational mechanism at these upper crustal levels.

C. The San Gabriel Fault

Near surface exposures along the present trace of the San Andreas yield cataclastic rocks that must characterize the more shallow levels when we consider that seismic activity exists down to 12 to 15 km. The mineralogical and physical nature of cataclastic rocks deep within the San Andreas fault zone has not been documented. However, exposures of intrafault material within abandoned and deeply eroded faults within the San Andreas system of southern California indicate rock types more indurated than the gouge exposed on the present trace and ranges to cataclasite in rock fabric and texture. In absence of very deep drill holes, we have evaluated a deeply eroded precursor to the present San Andreas, the San Gabriel fault zone of the San Gabriel Mountains. This fault was the initial trace of the San Andreas system when it was originated in the Late Oligocene to Mid Miocene (Crowell, 1952, 1954, 1968, 1973, 1975a, b, 1979; Ehlig, 1971, 1973; Dibblee, 1968).

While early workers concluded that the San Gabriel Fault was a normal or high angle reverse fault (Kew, 1924; Hill, 1930; Miller, 1934), it was not until studies by Eaton (1939) in the Ridge Basin area that a relationship between the San Gabriel and San Andreas faults was suggested. Eaton recognized that Ridge Basin was a graben between the two faults and established the antiquity of the San Gabriel Fault relative to the presently active San Andreas. However, the first solid documentation of right-lateral strike-slip displacement on the San Gabriel Fault was given by Crowell (1952). Subsequent studies by Crowell (1954, 1968, 1973, 1975a, b) show that the fault zone has had up to 60 km (38 miles) of right slip and 4.6 km (15,000 ft.) of dip slip. The fault is now locked at both ends and has been largely inactive for 4-6 m.y. (since Mid to Late Pliocene) (Crowell, 1975a, 1979) with only minor movement in the Late Quaternary (Weber, 1977).

Since the Late Pliocene, and particularly since Mid Pleistocene, the San Gabriel Mountains, as part of the Transverse Ranges, has undergone tremendous uplift (Oakeshott, 1971; Ehlig, 1971; Morton and Baird, 1971; Jahns, 1973; Dibblee, 1975; Morton 1975). As evident from its imposing mountain front and rugged internal relief (0.9 to 2.1 km or 3000-7000 ft.), erosion within the San Gabriel Mountains has been significant. Reviewed by Ehlig (1975) and Crowell (1975a, 1979), the uplift is in response to the same tectonics that led to the San Gabriel Fault being abandoned in favor of the San Andreas. The change to the San Andreas occurred when the "bend" developed. Resultant N-S shortening uplifted the San Gabriel block along the frontal fault system. This set of high angle, reverse dip-slip faults includes the

Cucamonga, Sierra Madre, Raymond Hill, Santa Monica, and Malibu Coast faults. The result has been a NW tilting of the block and maximum estimates of uplift since the Pliocene range from 4 to 9 km or 13,100 to 30,000 feet (Oakeshott, 1971; Morton and Baird, 1971). The amount of erosion has not been estimated, but using average erosion rates for this type of uplift (Blatt, Middleton, and Murray, 1972) indicates that the present exposures of the San Gabriel Fault represent crustal levels down to 2 to 5 km.

Hence, petrologic studies along such eroded San Andreas type faults should give us a more accurate picture of intrafault material in the seismically active depths of the San Andreas. We were initially attracted to this old fault for our reconnaissance studies indicate that the cataclastic rocks are much different from the unindurated gouge typical of the upper levels on the present trace. Past descriptions (Ehlig, 1973; Crowell, 1975) refer to the intrafault material as gouge, but in places this hard, black, even flinty material is strongly indurated and approaches the rock type "cataclasite" (Higgins, 1971).

II. DESCRIPTION OF LOCALITIES AND SAMPLES

Figure 1 shows the locations of the eighteen sites along the San Gabriel Fault chosen for intensive petrologic study. Below is a description of each site and a log of samples collected.

Site 1. SW¼, SW¼, Sec. 1, T.2N., R.12W. - on north branch of the San Gabriel Fault Zone at road cuts on Big Tujunga Canyon Road approximately 3½ km east of Big Tujunga Canyon.

Fault separates adamellite and tonalite. Rocks are brecciated but significant development of cataclastic rock is absent.

Samples SG1-pgr1: altered and brecciated leuco adamellite

SG1-grd: altered biotite, hornblende tonalite

Site 2. NW¼, SW¼, Sec.9, T.2N., R.12W. - Roadcut on north side of Angeles Crest Highway 1.2 km east of intersection with Angeles Forest Highway.

Fault is within a major biotite, hornblende adamellite body marked by breccia and gouge zone.

Samples SG2: microbreccia and gouge

SG2-pgr: biotite, hornblende adamellite

Site 3. NE¼, NW¼, Sec.14, T.2N., R.12W. - Exposure on southside of Angeles Forest Highway, 0.9 km northwest of Red Box Gap.

Numerous faults separate amphibolite, biotite-hornblende tonalitic gneiss, and hornblende-biotite schist: alteration involving hematization and chloritization is severe with some brecciation and minor gouge development.

Samples SG-3A: amphibolite

SG-3B, 3C, 3D: hematized biotite-hornblende tonalitic gneiss.

SG3pbs: hornblende-plagioclase schist

Site 4. SW¼, SE¼, Sec.7, T.2N., R.11W. - Exposure at crest of ridge just east of Valley Forge Canyon.

Fault separates amphibolite and leucotonalite. Other than minor brecciation there is no significant cataclasis.

Samples SG-4pa: amphibolite

SG-4pgr: leucotonalite

Site 5. NE¼, NW¼, Sec.16, T.3N., R.14W. - Exposure on Mendenhall Ridge Road, 0.6 km north of Little Tujunga Road and Dillon divide.

Extensive gouge and breccia . Rock contains abundant small porphyroclast (0.1-0.5mm) of quartz, feldspar, magnetite, and epidote in a moderately cohesive muscovite-rich matrix.

Sample SG-5: micaceous gouge

Site 6. SE¼, NW¼, NE¼, Sec.17, T.3N., R.14W. - Steep exposure on northside of Little Tujunga Road

Fault is the De Mille Fault (Oakeshott, 1958), a branch of the San Gabriel Fault, and is marked by a breccia and shear zone in leucogranite. Incipient gouge is developed within the breccia.

Sample SG-6: brecciated leucogranite

Site 7. SE¼, NE¼, NW¼, Sec.17, T.3N., R.14W. - Small roadcut on northside of Little Tujunga Road. De Mille Fault separates biotite granodiorite and breccia with clasts of biotite adamellite and is marked by a thin 1-4 cm thick cataclasite zone. Catallasite is dark brown to black in color, aphanitic, and flinty. Breccia may be part of the Paleocene Martinez Formation. Granodiorite is probably the late Cretacrous Josephine Granodiorite

Samples SG-7, 7-2: cataclasite. Sample 7-2 is of the interior of the cataclasite layer, sample SG-7 is of the less fine-grained margin of the cataclasite layer.

SG-7pb: breccia of biotite adamellite

SG-7pgr: biotite granodiorite

Site 8. NW¼, SE¼, SE¼, Sec.7, T.3N., R.14W. - Exposure at dry waterfall on north side of Little Tujunga Road.

Fault separates Josephine Granodiorite (same as at site

7) and the Precambrian Mendenhall Gneiss (Carter and Silver, 1972) and, as at site 7, is marked by a thin 2-5 cm wide cataclasite zone. Cataclasite is dense, aphanitic, and black in color. The gneiss is a quartz-plagioclase-biotite-actinocite gneiss formerly of granulite grade now retrograded to greenschist faces.

Samples SG8A, 8B, 8-2: cataclasite

SG8pgn: Mendenhall Gneiss

SG8pgr: Josephine Granodiorite

Site 9. NW¼, NW¼, Sec.22, T.3N., R.14W. - just east of Barrel Spring on Little Tujunga Canyon Road.

De Mille Fault separates diorite gneiss ("dgn" of Oakeshott, 1958) and the Martinez Formation. The gneiss is a heterogeneous diorite or amphibolite gneiss with small leucocratic granitic intrusives. The Martinez here is a tightly cemented conglomerate containing abundant clast of granite. Fault is marked by a 15m gouge zone (a black, mud-like gouge) and a wider alteration zone extending another 30m into both the gneiss and the conglomerate.

Samples SG9A-1,2: gouge

SG9B: Martinez Formation (conglomerate)

SG9C: Brecciated diorite gneiss

Site 10. NE¼, SW¼, SE¼, Sec.33, T.3N., R.13W. - on north side of Big Tujunga Canyon Road at three large, vertically stacked road cuts.

This is a major 70m thick gouge zone in heterogenous granitic gneiss and leucogranite.

Sample SG10A and B: gouge derived from granitic gneiss.

SG10C and D: white gouge from leucogranite in the gneiss.

Site 11. NE¼, SE¼, SW¼, Sec.33, T.3N., R.13W. - on north side of Big Tujunga Canyon Road at samall road cut.

Small fault in leucogranite with 4-7cm thick dense gouge or cataclasite zone.

Samples SG11A: gouge

SG11B: Brecciated leucogranite protolith

Site 12. NW¼, SE¼, Sec.3, T.2N., R.13W. - at Vogel Flat on road between Big Tujunga Canyon Road and Big Tujunga Station.

Sixteen meter wide gouge zone in granodiorite.

Sample SG-12: Sericitic gouge from fault surface

Site 13. NW¼, SW¼, SW¼, Sec.2, T.2N., R.13W. - on Big Tujunga Canyon Road 0.8km southeast of Big Tujunga Station.

The fault zone here has two faults within biotite granite. The granite contains several screens of biotite gneiss and both faults contain thin 5-10cm zones of dense gouge. Gouge derived from the fault in the granite is light colored while gouge derived from the gneiss is dark and clay-like.

Samples SG13A: granite gouge

13ap: granite protolith to 13A

13B: dark gouge from gneiss

13bp: gneiss protolith

Site 14. SW¼, SE¼, SE¼, Sec.2, T.2N., R.13W. - roadcut on Big Tujunga Canyon Road east of Fusier Canyon.

The fault here is marked by shear zone in granite and granite gneiss. Strong foliation is locally developed. Fault has 5cm wide zone of dense gouge, and granite on northwest side of the fault is shattered and friable. The exposure is quite weathered.

Samples SG14A: dense, fine grained gouge

SG14B: friable granite gouge and breccia

Site 15. SE¼, NW¼, Sec.33, T.2N., R.12W. - Millard Campground. San Gabriel (or Sierra Madre) Fault Zone separating hornblende granodiorite and granite gneiss. Gouge was sampled at two locations: one of gouge derived from granodiorite adjacent to campground parking lot, the other is of a bluish-grey clay-like gouge forming a mudslide along the fault exposed on a trail above the campground.

Sample SG15A: gouge and microbreccia from hornblende granodiotite

SG15mp: bluish-grey clay-like gouge

Site 16. NW¼, SW¼, Sec.30, T.6N., R.17W. - on unimproved road to Whitaker Peak in the Ridge-Basin Area

The San Gabriel Fault here separates Cretaceous (?) biotite adamellite and Precambrian (?) mafic, banded gneiss. Fault is marked by 1-4cm wide cataclasite zone. Cataclasite is dense, aphanitic, and dark brown in color and is similar to cataclasites of sites 7 and 8.

Samples SG16A: cataclasite

SG16B: brecciated adamelline at fault

SG16C: brecciated gneiss at fault

SG16D: banded gneiss 30m from fault

SG16E: biotite adamelline 100m from fault

Site 17. NW¼, SW¼, Sec.14, T.6N., R.18W. - on south side of Piru Creek.

Strand of San Gabriel Fault in banded biotite gneiss. Fault is marked by 1-2cm shear zone. No significant cataclasis.

Sample SG17: sheared and altered gneiss

Site 18. NE¼, SW¼, Sec.6, T.5N., R.17W. - 2.1km south of Townsend Peak on unimproved road.

San Gabriel Fault separates sedimentary clastic rocks and amphibolitic gneiss. Six meter wide gouge and breccia zone is developed within a strand of the main fault in the amphibolitic gneiss.

Sample SG18: breccia and gouge derived from amphibolite.

III. ANALYTICAL PROCEDURE

Each sample was partitioned with a sample splitter to obtain representative subsamples for the separate mineralogic, petrochemical and textural analyses.

The mineralogy of the cataclastic and related rocks was analyzed by optical examination of thin sections, X-ray diffraction, scanning electron microscopy (S.E.M.), and electron microprobe. Modal analyses and X-ray diffraction was done by subcontract to Kent State University under the supervision of Donald F. Palmer. Half of each thin section was stained for K-feldspar and modal analyses involved duplicate measurements by two observers, each counting a minimum of 1500 points per thin section. X-ray examination of bulk samples and sample separates was done with a Philips-Norelco diffractometer with a focusing monochromator and using Cu K-alpha radiation. Scans were made a 1°2θ per minute for all samples and at ¼°2θ per minutes over low angles of 2θ on all samples exhibiting alteration or cataclasis. Ultraslow scans were made to detect the natur of any existing clay minerals. X-ray analysis of grains utilized the Debye-Scherer powder camera. X-ray examination was made on bulk sample separates. Samples were separated first on the basis of the grain size by using 0.177, 0.149, and .063 mm sieves. Most of the samples also were sieved with a .044 mm screen in the hope of obtaining fine clays. In most samples, a very fine fraction was obtained by putting the whole sample into suspension and filtering out the fine suspensate.

Electron microprobe analysis was done on an automated, 3-channel MAC (Material Analysis Corporation) microprobe housed at the California Institute of Technology. Data collection and reduction were performed on-line by a Digital Corporation PDP-8/L computer utilizing the alpha correction factors of Albee and Ray (1970) and the empirical reduction scheme of Bence and Albee (1968). Operating conditions consisted of 15kv accelerating potential, 0.05 μamp current measured on brass and a 2-10 μm beam diameter. Oxides, synthetic silicates, and well characterize natural minerals were used as standards.

Petrochemical analysis of the samples was done for eight major (Si, Ti, Al, Fe, Mg, Ca, Na, and K), five minor or trace elements (Mn, Li, Rb, Sr, and Ba), and combined volatiles (H_2O and CO_2). Silicon was analyzed by UV-VIS colorimetric spectrophotometry. All other elements were analyzed by atomic absorption spectrophotometry using an HF - H_3BO_3 acid dissolution technique. Standards and blanks were made synthetically and U.S.G.S. reference samples (G-2, SY-2, and W-1) were used as internal standards as a monitor of accuracy. As a further check on accuracy, sample splits from site 4 of last year (San Andreas Fault at Lake Hughes) were also analyzed at Kent State University. Analyses from the two labs (USC and KSU) are in excellent agreement (Figure 2). Total volatile content was based on loss of ignition (L.O.I.) at 1000°C. For these samples, H_2O is the predominant volatile component with CO_2 as a very minor constituent.

Although conventional sieving and pipette methods were attempted to determine grain size characteristics of the first set of samples collected from the San Gabriel Fault Zone, petrographic analysis of resultant size fractions clearly showed that disaggregation of the cataclastic rocks was incomplete. The indurated nature of these samples necessitated that optical methods be used to obtain textural information. Consequently a Zeiss TGZ particle size analyzer was employed due to the high measurement efficiency characteristic of this instrument as compared to ocular microscopy. All photomicrographs were enlarged 143 times. The particle size analyzer was used in the standard range with the exponential, distribution mode. Inasmuch as the plane of a thin section generally does not transect the maximum grain diameters of constituent particles, grain-size measurements from thin sections tend to be smaller than corresponding measurements obtained by sieving, settling tube or pipette methods. No corrections were applied to these samples because the grain shape and packing are not known. Furthermore, this error should be small for measurements of dominantly silt-size particles. Computer software was developed to facilitate the statistical evaluation of these textural measurements. The Rosiwal-Shand method (Galehouse, 1971) was used to obtain estimates for the volume percent of measureable grains ($\geq$ 0.0078 mm in diameter)

Figure 2: Plot comparing the chemical analyses of the USC and KSU petrochemicstry laboratories.

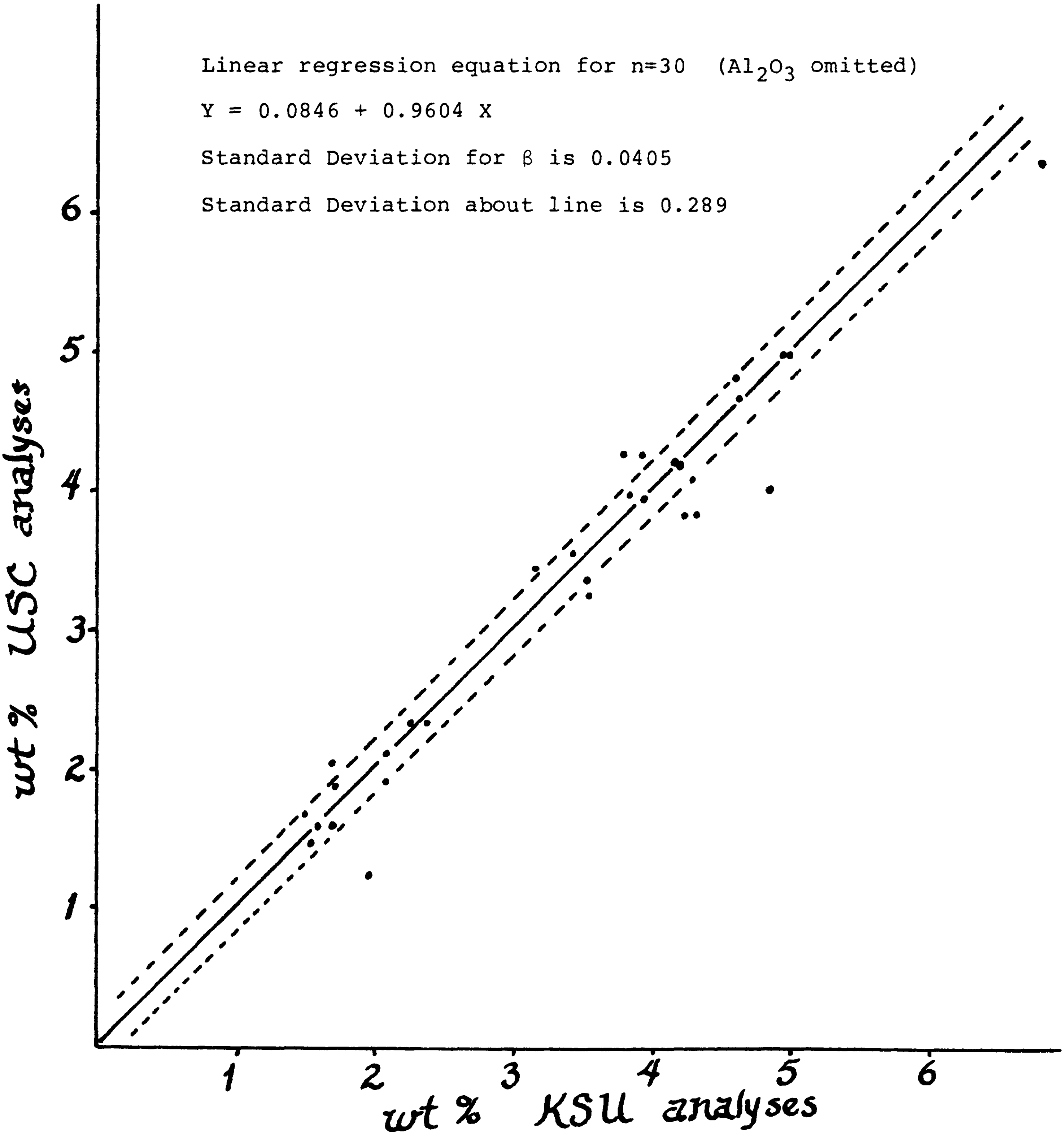

as compared with finer-grained, recrystallized matrix. The length of all measured grains along 20 parallel lines spaced at 0.4 cm intervals and each 9.5 cm long was summed for each photomicrograph and expressed as a percentage of the total length of all traverses (266 cm/photomicrograph).

IV. ANALYTICAL RESULTS

Due to the lack of intense cataclasis at sites 1 and 4 and the extreme alteration at site 3, samples from these three sites were largely excluded from study (modal analyses are included in Table 1 for these sites). Of prime interest are the cataclasites from sites 7, 8, and 16 as this dense and fine-grained cataclastic rock type does not occur along the present trace of the San Andreas and perhaps is intrinsic to more deeply eroded fault zones. Samples from the other sites are less cataclasized than those from the above cataclasite sites, but are more cohesive and finer grained than similar gouge and breccia from the San Andreas.

A. Petrography and Petrofabric Analysis

The major mineralogy and mineral percentages are presented in Table 1. The primary (pre-cataclasis) mineralogy of all samples includes plagioclase, quartz, alkali feldspar, biotite, muscovite, hornblende or actinolite, sphene, chlorite, epidote, allanite, magnetite and ilmenite. Cataclasis has not readily changed the mineralogy although associated alteration has generated calcite, sericite (celadonitic muscovite), more chlorite, hematite, and small amounts of laumontite, ferro-pseudo brookite, and zeolite (species yet unidentified).

The groundmass usually has the same modal mineralogy as is found in the larger clasts down to the limits of resolution of the optical system - 0.005 mm. However, in some samples the matrix is rich in sericite, sericite and chlorite, or is heavily veined with calcite. The term groundmass or matrix refers to areas which are so fine grained that individual minerals are not resolved. Nonetheless mats of very fine sericite or chlorite may be identified by "bulk" optical properties.

1. Cataclasites - sites 7, 8, and 16

The cataclasite at these sites consist of 10-15% porphyroclasts of feldspar, quartz, and lesser amounts of epidote, biotite, magnetite, and actinolite (SG-8 only) dispersed in an aphanitic dark-colored matrix. Typical photomicrographs are presented in Plate 2. The matrix lacks foliation or fluxion structure although a few cross-cutting slippage surfaces occur as is visible in Plate 2b. Porphyroclasts are commonly sub-angular. Although the matrix is generally opaque and too fine grained to optically detect a grain size, Plate 2b, c, and d show the matrix to be crystalline. This is more evident in scanning electron microscope (S.E.M.) photographs of cataclasite from site 8 (Plate 3) which show a recrystallized grain size of .0003-.0010 mm (Plate 3a-c). This is important as fault gouge of the San Andreas in this same region has a flour-like, particulate matrix that is not recrystallized. Also evident in the S.E.M. photographs (Plate 3c-f) is the development of post-kinematic chlorite with a distinctive "bladed rosette" habit growing on feldspar and quartz porphyroclast at the matrix/porphyroclast interface. Energy-dispersive analysis of these rosettes show them to contain

Plate 2. Photomicrographs of cataclasite from sites 7 (a and b) and 8 (c and d). Porphyroclast minerals are: Q - quartz, K - alkali feldspar, P - plagioclase, E - epidote, Z - zircon, and M - magnetite. Bar scale (0.14 mm) is the same on each. Plane light.

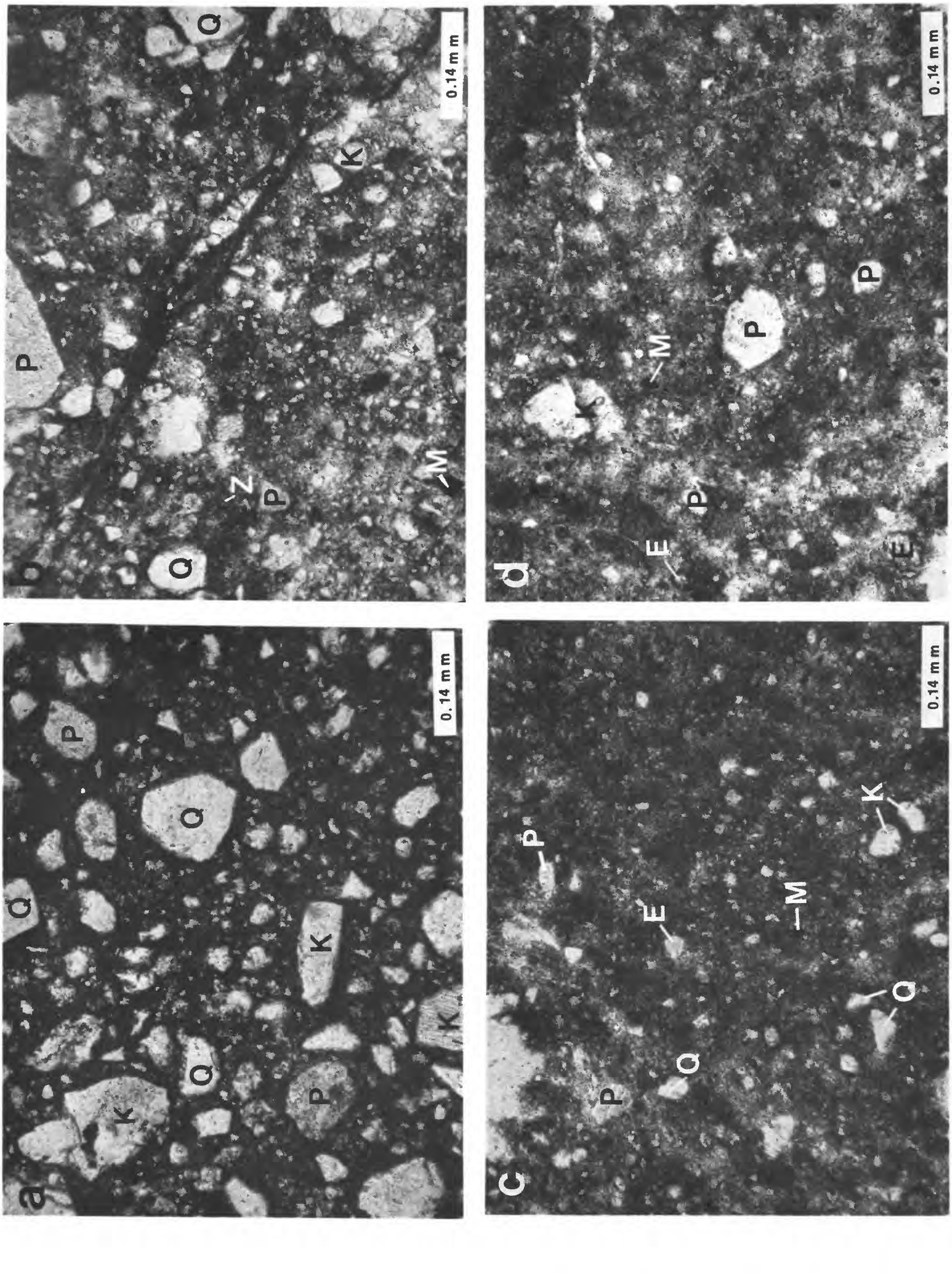
a
b
c
d
Q
P
K
M
E
Z
0.14 mm
0.14 mm
0.14 mm
0.14 mm

Plate 3. Scanning electron microscope photomicrographs of cataclasite matrix and porphyroclast from site 8; (a,b) quartz porphyroclast in cataclasite matrix; (c) edge of porphyroclast. Note crystalline nature of the matrix; (e-f) rosettes of unknown mineral growing on porphyro clast at matrix-porphyroclast interface. Sequence of photomicrographs is in increasing mignification.

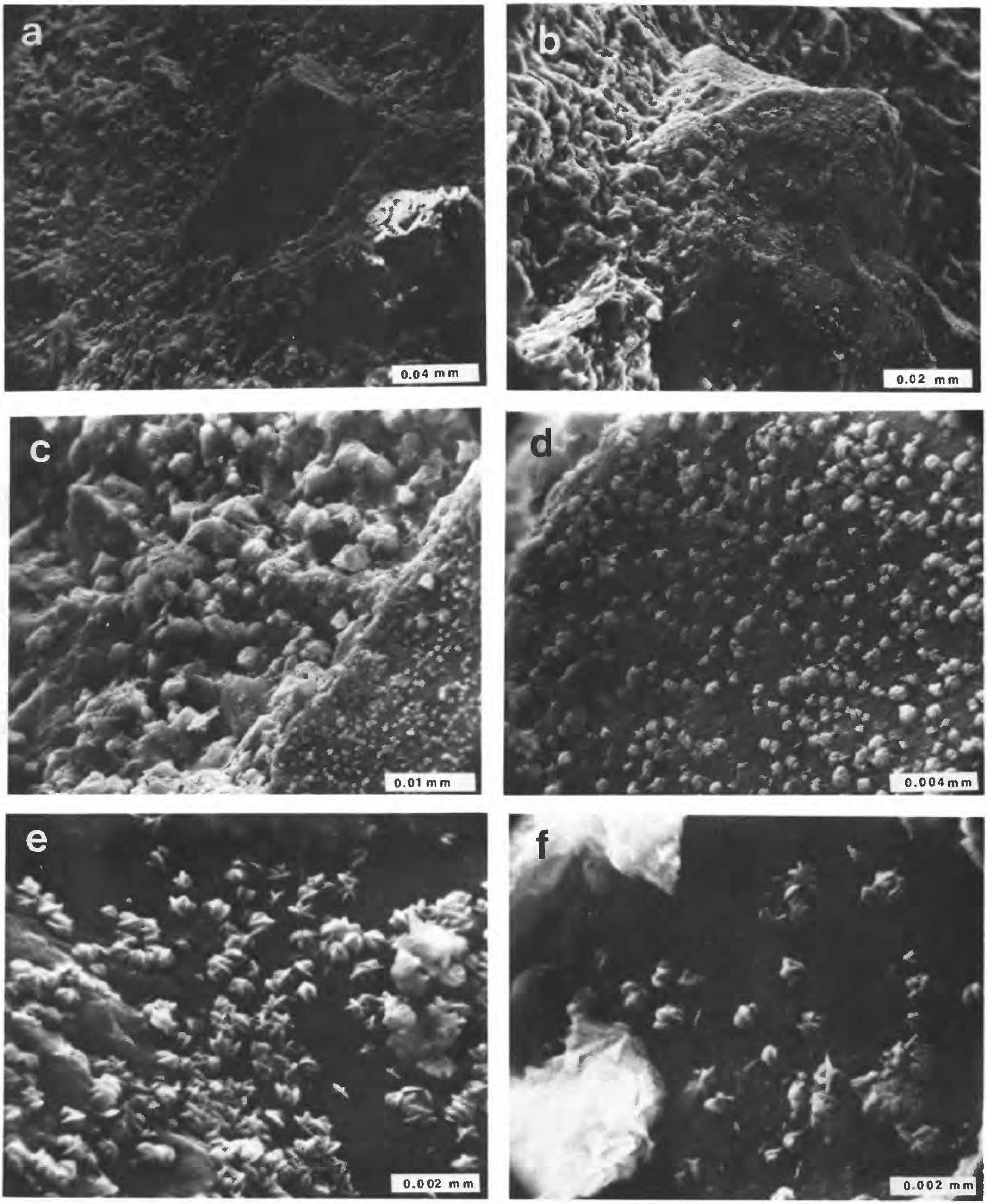
a
0.04 mm
b
0.02 mm
c
0.01 mm
d
0.004mm
e
0.002 mm
f
0.002 mm

Si, Fe, Al, and Ti in decreasing order of abundance. S.E.M. studies of the cataclasite from site 16 show a matrix rich in foliated biotite or stilpnomelane with occassional sprays of a yet unidentified K-Ca zeolite with a radiating stellated habit. These phases are in too low an amount to be detected by X-ray diffraction (next section) but is important as it is evidence of a least minor development of new minerals formed during or after cataclasis.

2. Gouge and Microbreccia

Cataclastic rocks from sites 2, 5, 6, 9-15, 17, and 18 are much coarser than the cataclasites described above and are only weakly to moderately cohesive. They range from gouge to microbreccia with interstitial gouge. Porphyroclasts are more angular than those in the cataclasites and range in percentage from 25-80%. Major porphyroclast minerals are quartz, feldspar epidote, magnetite, and chloritized biotite or biotite. The matrix in SG-2 (site 2) is weakly foliated due to the minor amounts of matrix chlorite. The matrix in SG-5, and 12, is moderately foliated and is rich in fine-grained muscovite or sericite. The matrix in samples SG-9, 13b and 14a is rich in fine-grained biotite or stilpnomelane. In addition, SG-9 contains veins of laumontite ($Ca\ Al_2Si_4O_{12}\ 4H_2O$).

B. X-ray Mineralogy

Due to the limitations of x-ray diffraction, it is not possible to clearly detect a mineral which is less than about 3% in abundance in the sample. Thus, sample separations aimed at concentrating certain phases relative to others are of primary importance. Samples were analyzed for the finer fractions down to -325 mesh. There was no consistent change in the x-ray diffractograms as a function of grain size except where the matrix is enriched in sericite and chlorite, commonly with quartz. In all cases the major minerals detected by x-ray were quartz, plagioclase, and potassium feldspar with some chlorite, biotite, and/or hornblende. The ratios of these, as measured by peak height, did not change as a function of grain size for coarser fractions.

In certain samples (SG 10b, 10d, 12, 15A, 16c, 17, and 18) the finer grain size fraction shows a significant change in the increased percentages of quartz and sericite usually with chlorite along with a decrease in the amount of feldspar. This change is noted in figure 3 for sample SG-18, but the change is characteristic of all samples which show a high sericite component in the gouge by optical examination. Here the presence of low birefringent quartz and chlorite seems to be masked by the highly birefringent sericite.

As in the case of samples from the San Andreas Fault Zone in the same region, no development of clay minerals was found (Figure 4). Even in the finest material, the gouge is dominated by sericite and chlorite. While it is possible that these phyllosilicates may be masking some clay mineral peaks, there is no evidence for any clay peaks in the present gouge samples.

Superimposed upon the peaks related to the major minerals were lesser peaks caused by the presence of calcite, epidote, and rarely actinolite. Since the larger clasts were usually completely fractured, even the largest grains could usually be forced through a fine sieve. For this reason sieving was done very gently to try to preserve the larger grains. The cloudy nature of many of

Figure 3: Comparative diffractographs of Sample SG-18 showing the increase in quartz, muscovite, and chlorite typical of gouge samples with a sericitized matrix. Diffractographs are for the bulk sample (bottom), -200 mesh (center), and -325 mesh (top).

Q = quartz, P = plagioclase, C = chlorite,
M = muscovite, and Ca = calcite

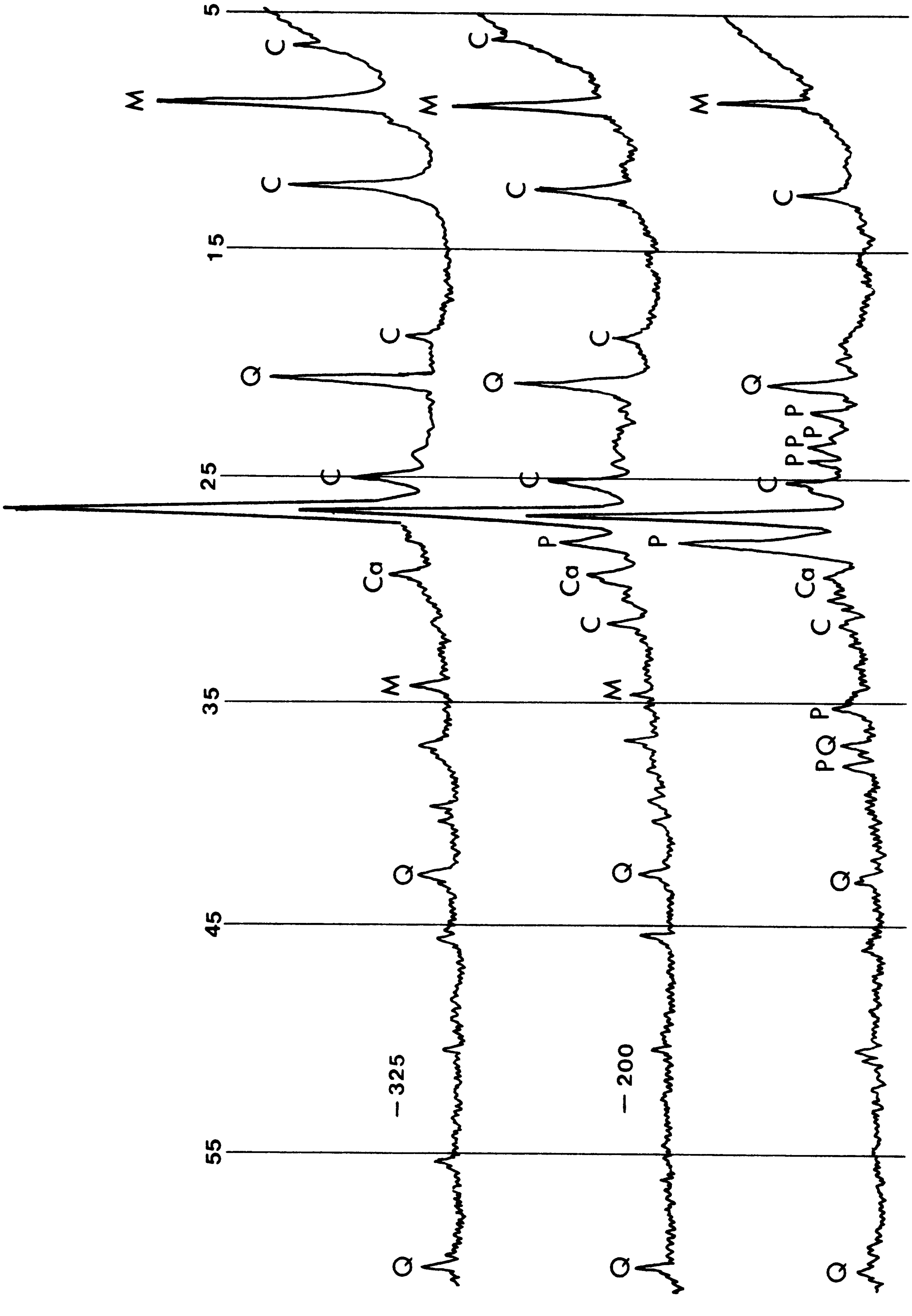
5
15
25
35
45
55
Q, M
M
C
Q
Ca
P
PQ
−325
−200

Figure 4: Comparative diffractographs of Samples SG-8A, cataclasite (center trace), SG-8pgn, Mendenhall gneiss (upper trace), and Sg-8pgr, Josephine granodiorite (lower trace) showing mixing of protolith fractions within the cataclasite. The only clear difference is seen in the potassium feldspar (K) and hornblende (H) in the Josephine granodiorite which is apparent in lesser amounts in the bulk x-ray analysis of the cataclasite but which are absent in the Mendenhall gneiss. Quartz (Q) and plagioclase (P) are seen to be common to all three rock types.

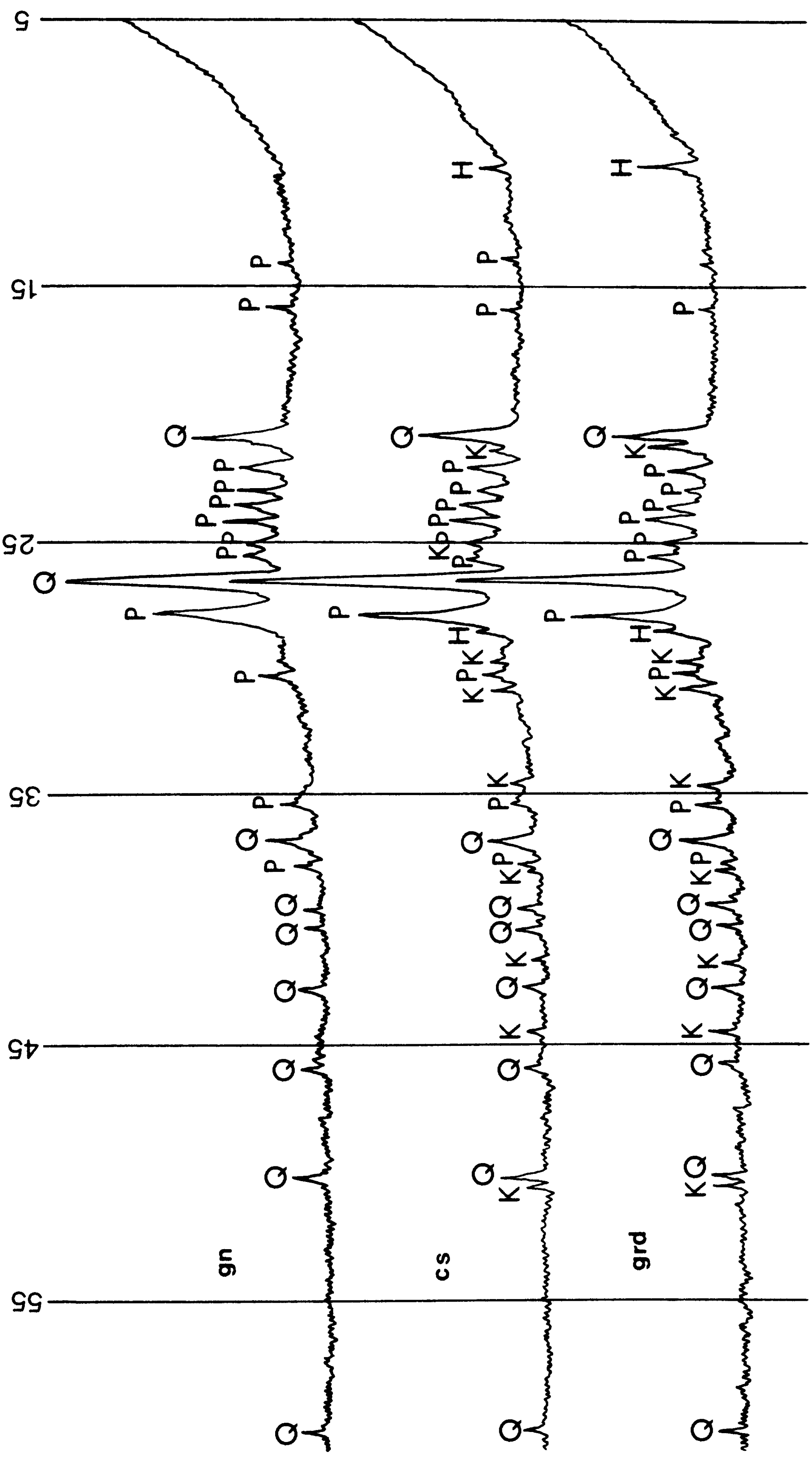
5
15
25
35
45
55
gn
cs
grd

the large feldspar grains supports the idea that much of the clay within the gouge may be on or in the larger grains. Thus the clay, while fine grained in and of itself was often segregated with the medium grained size fraction.

X-ray diffractograms show that clays are either absent or are generally not very well crystallized.

C. Detailed Mineralogy and Mineral Chemistry

Electron microprobe analysis of the major minerals (plagioclase, alkali feldspar, muscovite, biotite, chlorite, actinolite, hornblende, epidote, calcite, apatite, magnetite, and ilmenite) in the cataclastic rocks and their protoliths are presented in Table 2.

1. Cataclasites

X-ray scans from the rocks from site 8 show the cataclasite to be intermediate in modal composition between the granodiorite and gneiss juxtaposed by the fault. As shown in figure 5a, plagioclase in the cataclasite of site 8 has the same range of composition as the granodiorite and gneiss protoliths. In the presumed P-T conditions of the fault zone (which must be greenschist grade or less assuming normal geothermal gradients), plagioclase generated during cataclasis would be albite. Yet plagioclase compositions range continuously from $An_{6.5}$ to $An_{38.5}$. The more albitic compositions are evidently derived from the Mendenhall Gneiss which has the bimodal distribution of plagioclase composition - $An_{11.1-2.7}$ and $An_{22.5-31.5}$ reflecting the polymetamorphic history of this Precambrian unit (granulite and greenschist grade metamorphism); compositions in the granodiorite are more uniform being $An_{21.4-25.7}$. There is no evidence of a new feldspar compositions being generated

Figure 5. Feldspar compositions for cataclasite sites 7(a) and 8(b) of the San Gabriel Fault and Gouge (c) from the Lake Hughes area of the San Andreas Fault.

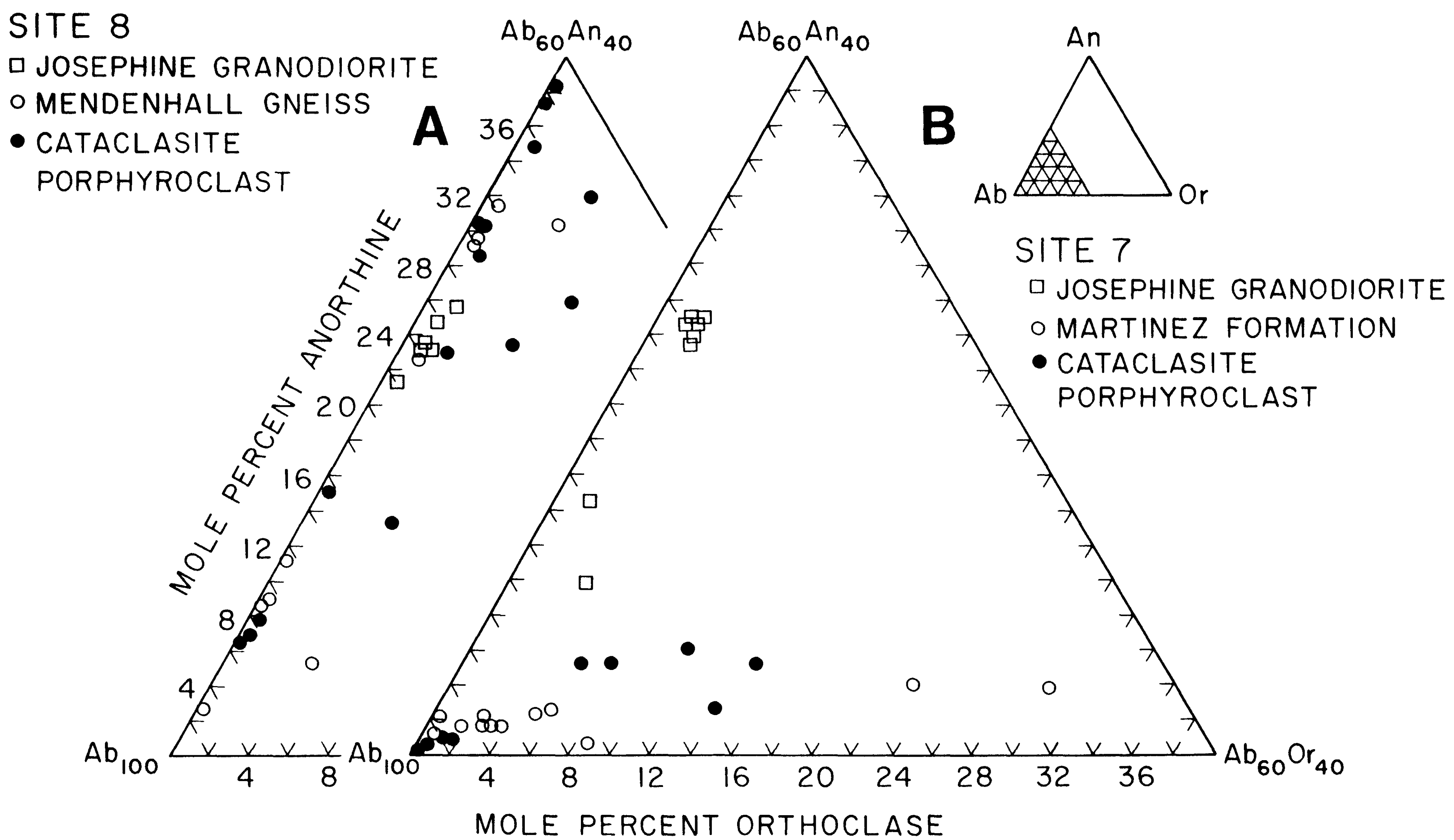
SITE 8
JOSEPHINE GRANODIORITE
MENDENHALL GNEISS
CATACLASITE PORPHYROCLAST
A
B
$Ab_{60}An_{40}$
$Ab_{60}An_{40}$
Ab_{100}
Ab_{100}
$Ab_{60}Or_{40}$
An
Ab
Or
SITE 7
JOSEPHINE GRANODIORITE
MARTINEZ FORMATION
CATACLASITE PORPHYROCLAST
MOLE PERCENT ANORTHINE
4 8 12 16 20 24 28 32 36
MOLE PERCENT ORTHOCLASE
4 8 12 16 20 24 28 32 36

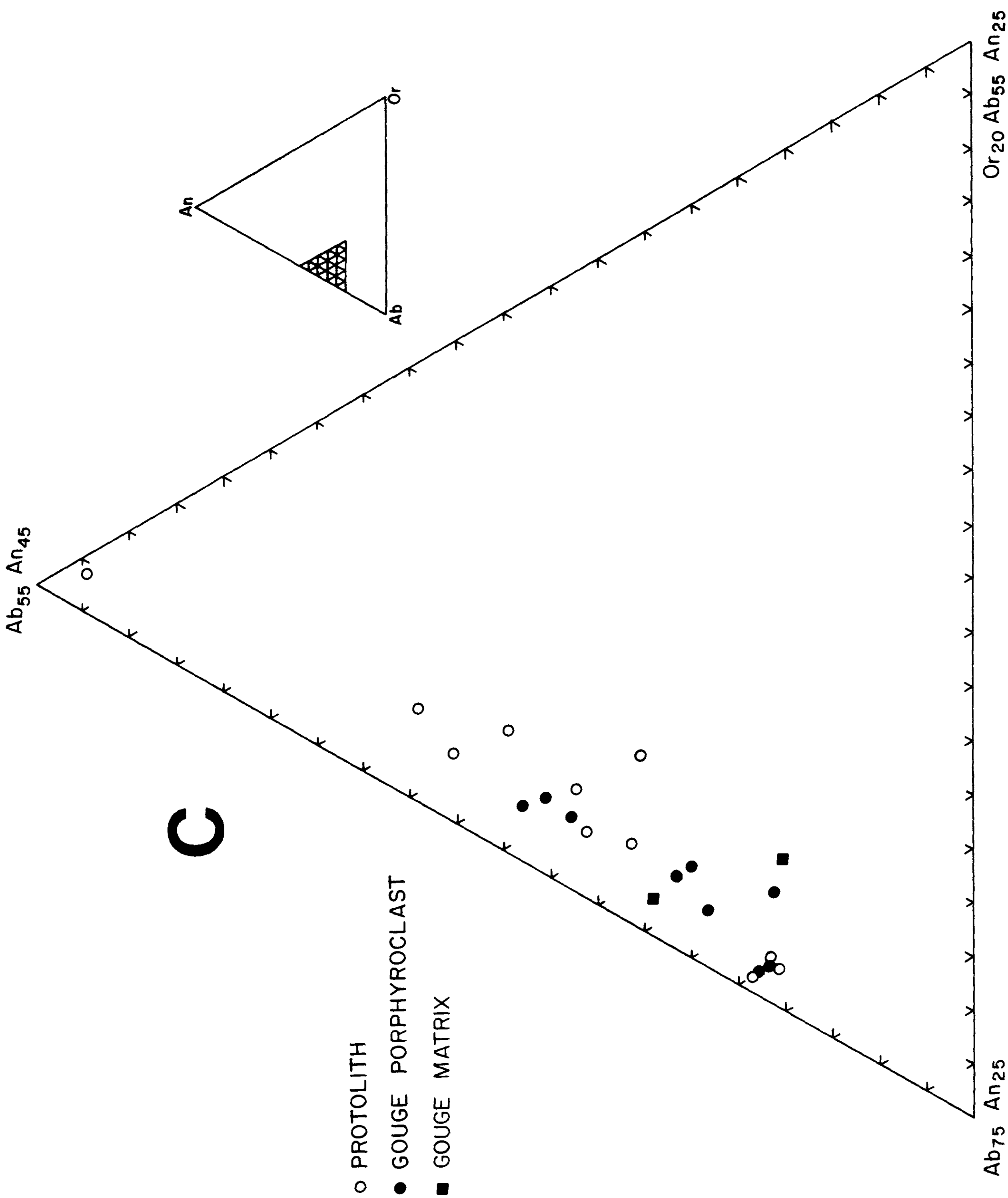
C
○ PROTOLITH
● GOUGE PORPHYROCLAST
■ GOUGE MATRIX
Ab_{55} An_{45}
Ab_{75} An_{25}
Or_{20} Ab_{55} An_{25}
An
Or
Ab

during cataclasis. This is the same conclusion reached by us for feldspars in gouge along the San Andreas Fault (figure 5c). The biotites from the site 8 samples are interesting. The composition of the biotites in the two protoliths and cataclasite are indistinquishable in terms of Al^{IV}, Al^{VI}, Fe, Mg, and Ti, yet the concentrations of Mn and F of the cataclasite biotite matches well only the biotite of the Mendenhall Gneiss. Weight percent MnO in the biotites of the gneiss and the cataclasite range from 0.20 to 0.33% and 0.25 to 0.30%, respectively, as compared to 0.66 to 0.84% for biotite of the granodiorite. Likewise, fluorine ranges from 0.00 to 0.18% and 0.11 to 0.12%, respectively, while the concentration in the granodiorite biotite is 0.17-0.75%. This implies that the cataclasite is more derived from the gneiss rather than the granodiorite, a conclusion confirmed by whole rock chemical data (next section). Moreover both the cataclasite and the gneiss contain actinolite and ilmenite which were not found in the granodiorite. Yet there has to be some component of the granodiorite in the cataclasite as both contain alkali feldspar and hornblende which does not occur in the gneiss at this locality.

There is likewise a suggestion of a larger contribution of one protolith relative to the other in the cataclasite of site 7. Plagioclase in the two protoliths are quite dissimilar (figure 5b). In the granodiorite (same unit as at site 8) plagioclase ranges $An_{14.5-25.0}$, mostly $An_{23.5-25.0}$. In the breccia (SG7-pb, presumably Martinez Formation), the plagioclase is largely low in anorthite (An) component and is primarily a solution of albite (Ab) and orthoclase (Or) end members. Most of the plagioclase is quite albitic ($Ab_{90.8-98.3}$), although some is more intermediate ($Ab_{66.2-80.3}$

$Or_{14.4-30.0}$). In the cataclasite, most of the feldspar is either albitic ($Ab_{98.3-99.0}$) or likewise of a K-Na solution ($Ab_{80.3-83.5}$ $Or_{13.9-14.4}$) which suggest that the cataclasite is derived largely from the Martinez Formation rather than the granodiorite.

At both sites, biotites show considerable chloritization. Data for partially chloritized biotites are also given in Table 2 and shows a decrease in K, Ti, and Fe and greater Mn, Mg, H_2O, and F with alteration. In sample SG8-pgr (granodiorite of site 8), biotites which are deformed, although not altered, exhibit systematic changes presumably related to cataclasis. Relative to undeformed biotite, deformed biotites are enriched in Al^{IV} and depleted in Ti, Al^{VI}, and Si. Also, on a total cation basis, the overall charge of the deformed biotites is less requiring an increase in the ratio of Fe^{3+}/Fe^{2+} (the charge of all of the biotites is less than the ideal charge of 22 due either to the presence of Fe^{3+} or a vacancy in the octahedral and/or interlayer sites). This suggest coupling of the following solution mechanisms during cataclasis: (1) $4Al^{IV} = 3Si$ (2) $2Fe^{3+} = Fe^{2+} + Ti$, and (3) $Fe^{3+} = Al^{IV}$. Lower temperature biotites are commonly depleted in Ti (Guidotti, et al., 1976) and the increase in Fe^{3+}/Fe^{2+} implies also an increase in oxidation. The latter is consistent with the observed hematization. Also indicative of low temperature is the coexistence of magnetite and ferro pseudo-brookite in SG-7pb requiring that ilmenite, under these low temperature-oxidizing conditions, is a relict, unstable phase.

2. Gouge and Microbreccia

Mineral compositional data for site 2 samples demonstrate that the material in the gouge zone does not correspond to the biotite-hornblende adamellite adjacent to the fault. Plagioclase porphyroclasts in the gouge range from albite ($Ab_{94.9-96.9}$) to more potassic compositions ($Ab_{74.6-83.5}$ $Or_{12.4-21.9}$) with low anorthite component ($<An_{4.5}$). In contrast, plagioclase in the adamellite is andesine ($An_{30.8-44.8}$). Likewise the composition of chlorite (derived from biotite) is systematically different. For the gouge chlorite, Al_2O_3 = 19.0-20.1 wt.%, MnO = 0.31-0.44 wt.%, Mg/(Mg + Fe) = 0.487-0.507. For the adamellite chlorite, Al_2O_3 = 21.3-22.3 wt.%, MnO = 0.13-0.25%, and Mg/(Mg + Fe) = 0.155-0.382. Other differences include the presence of hastingsite in the adamellite which is absent in the gouge and the presence of Th-rich allanite in the gouge which is absent in the adamellite. Although this may simply reflect sampling bias it may also be a consequence of the considerable displacement of rock units adjacent to this fault.

The mineralogy of gouge at site 9 also does not match well the juxtaposed rock units. The gneiss has been retrograded to greenschist grade and contains albite ($Ab_{80.0}Or_{16.0}$-$Ab_{98.5}Or_{0.8}$) as the only feldspar. As before, the Martinez Formation (SG-9b) consists dominately of sodic plagioclase ($Ab_{85.2}An_{13.0}$-$Ab_{99.1}$ $An_{0.5}Or_{0.4}$) and potassic alkali feldspar ($Or_{72.6}Ab_{26.8}$-$Or_{91.6}Ab_{8.4}$). In contrast the cataclasite has three types of feldspar: (1) a minor amount of sodic plagioclase ($Ab_{88.9}Or_{7.2}An_{3.9}$-$Ab_{96.3}Or_{2.3}An_{1.4}$), (2) some potassic alkali feldspar ($Or_{80.2}Ab_{19.5}$-$Or_{91.4}Ab_{8.4}$), and (3) a significant amount of calcic oligoclase-sodic andesine ($An_{27.6}Ab_{68.5}Or_{3.8}$-$An_{37.4}Ab_{59.6}Or_{3.0}$). The latter feldspar does not occur in either of the potential protoliths and is quite similar to the plagioclase of the Josephine Granodiorite which is exposed on the southside of the fault, one kilometer to the west.

Consistent with the right lateral movement, it is probable that this gouge was largely derived from this now displaced crystalline unit. As mentioned above this gouge contains minor amounts of laumontite (Table 2M), a mineral diagonistic of very low-grade metamorphism, specifically the laumontite zone of the zeolite facies (Liou, 1979). As andesine is not stable at this low-grade, it is evident that this mineral, as is much of the mineralogy of these cataclastic rocks, is relict from an earlier igneous (or metamorphic) history.

Gouge at site 5 is unusual in its high muscovite content in its ultrafine grained, moderately foliated matrix. Gouge at sites 12, 14 and 16 also have a matrix rich in foliated, very fine grained mica. The muscovite in SG-5 has a moderately low content of celadonite (the siliceous end-member K (Mg, Fe^{2+}) (Fe^{3+},Al) $Si_4O_{10}(OH)_2$ common in phengitic micas of low-temperature origin) which ranges from 11.6-14.2%. This differs from the composition of sericitic muscovite (alteration product of feldspar) common at sites 2, 6, 9, and 12 which have higher celadonite contents of 13.6-28.4%. Consistent with the high muscovite content, the matrix chlorite in SG-5 is also quite aluminous with Al_2O_3 ranging 22.7-23.8 wt.%. Chlorite in gouge at the other sites (sites 2, 6, 7, 8, 9, and 12) has generally lower Al_2O_3 (15.7-20.0%). Chlorite, as with sericite, is a dominant primary mineral of the gouge. This is evidenced by the abundance chloritization of biotite (Table 2E) and growth of new discrete crystals. The chlorite commonly similar to the pre-existing biotite in terms of Mg/(Mg + Fe) and Al. For example, the chlorite in the microbreccia at site 6, is generally only slightly Mg-richer than the biotite from which it was derived. Here the Mg/(Mg + Fe) of the chlorite and biotite are 0.448-0.479 and 0.429 respectively.

The microbreccia at site 6 also shows evidence of mixing of presumably different portions of the same adamellite having slight differences in composition. In SG-6, the plagioclase has the composition of $An_{10.8-14.4}$ in addition to traces of albite of retrograde origin. Yet thin through going brecciated zones (2-4 mm wide) contain plagioclase porphyroclasts that are systematically Ca-richer with a composition of $An_{15.6-17.6}$.

D. Petrochemistry

As an aid to establish the protolith for the cataclastic rocks and to ascertain the role of chemical mobility (e.g., leaching or enrichment) in its formation, we have analysed the cataclastic rocks and the juxtaposed rock units at several sites. Tabulated in Table 3, the comparison of cataclastic rocks and potential protolith(s) can be easily viewed in Figure 6.

The plotted element abundance pattern constitutes a compositional "fingerprint" for the rock units and inspection of Figure 6 shows: (1) the cataclasite of site 7 is more derived from the Martinez sedimentary breccia rather than the Josephine Granodiorite, (2) the cataclasite of site 8 is derived more from the Mendenhall Gneiss (modeled 85%) than from the Josephine Granodiorite, (3) the cataclasite at site 16 is derived more from the PЄ (?) gneiss at that locality than the biotite adamellite, (4) gouge at site 13 matches well the Josephine (?) Granodiorite that exist on both sides of the fault at, and (5) the gouge at site 9 does not clearly match either of the juxtaposed rock units at the locality. These conclusions are consistent with mineralogic comparisons made earlier. Note that the cataclasites at sites 7, 8, and 16 have not

Figure 6. Major and trace element compositions of cataclastic rocks and juxtaposed rock units along the San Gabriel Fault. All analyses have recast to volatile-free basis to preclude effects of variable hydration. The cataclastic material (solid line) is cataclasite for sites 7, 8, and 16 and gouge for sites 9 and 13. Note that (1) the cataclasite chemistry is approximated well by only one of the two juxtaposed lithologies indicating a preferential contribution of that unit to the formation of the cataclasized zone and (2) the strong enrichment of Lithium in the cataclasite of sites 7, 8, and 16 and some of the gouge at site 9 reflecting the major mobility of this trace element.

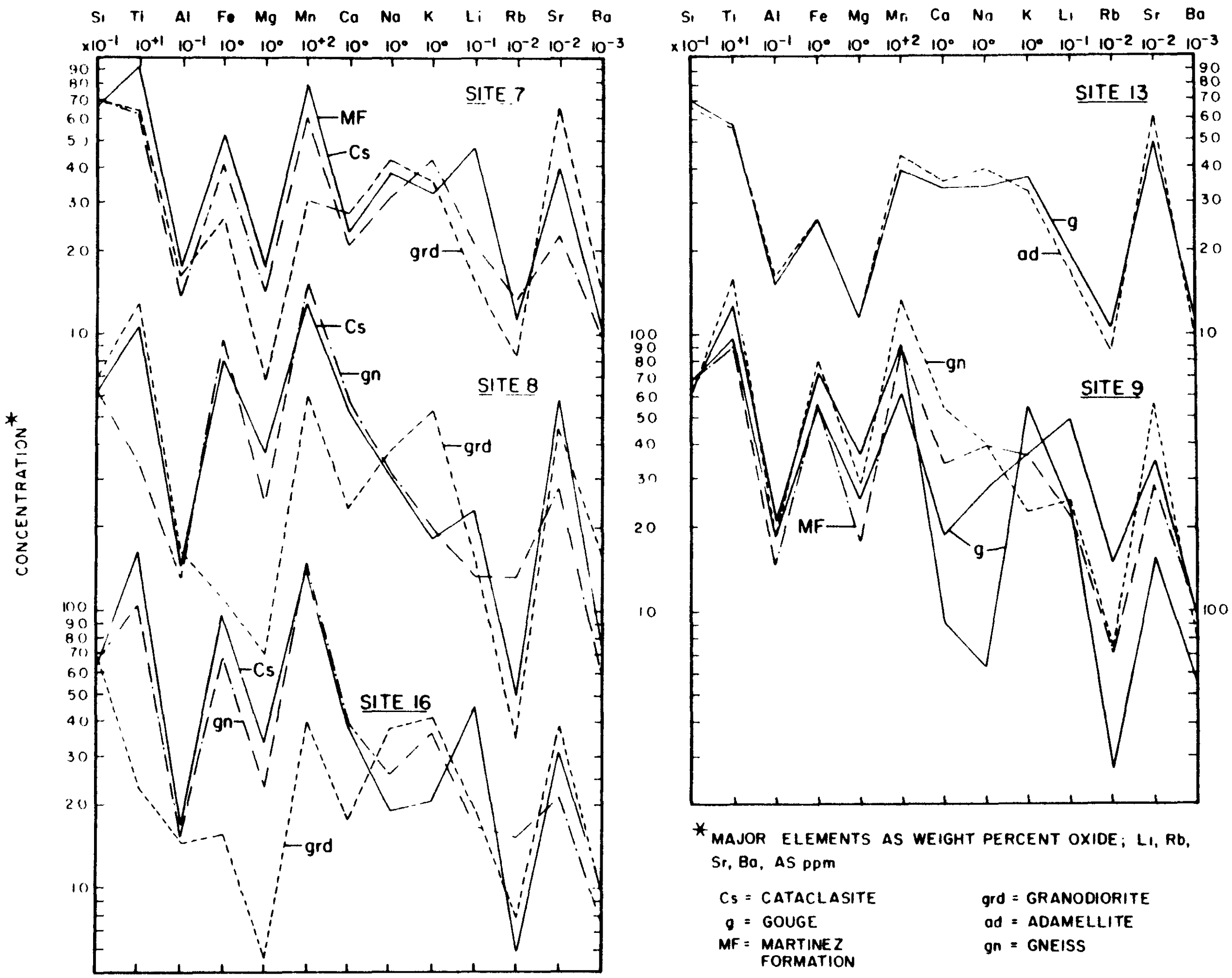
CONCENTRATION*
Si Ti Al Fe Mg Mn Ca Na K Li Rb Sr Ba
x10^-1 10^+1 10^-1 10° 10° 10^+2 10° 10° 10° 10^-1 10^-2 10^-2 10^-3
SITE 7
MF
Cs
grd
SITE 8
Cs
gn
grd
SITE 16
Cs
gn
grd
SITE 13
g
ad
SITE 9
gn
MF
g
* MAJOR ELEMENTS AS WEIGHT PERCENT OXIDE; Li, Rb, Sr, Ba, AS ppm
Cs = CATACLASITE
g = GOUGE
MF = MARTINEZ FORMATION
grd = GRANODIORITE
ad = ADAMELLITE
gn = GNEISS

formed preferentially from the massive granitic units at those localities. Although displacement history may be a factor, these relations suggest that a physically heterogeneous lithology, such as a more biotitic, foliated gneiss may be more easily milled-down on the fault surface that a massive, more leucocratic granitoid.

Chemical mobility can be addressed by noting elemental compositions of the cataclastic rock that are anomalous relative to the designated protolith. All of the cataclastic rocks show at least moderate hydration relative to their respective protoliths with an average of 1.85% added H_2O (range 0.40-3.87). To evaluate net changes for other compositional constituents, the analyses have also been calculated on a volatile-free basis (Table 3). In general, the major elements show no evidence of significant mobility. Moreover, the gouge at site 13 shows no evidence of mobility for any element. The cataclasites at sites 7, 8, and 16 show a moderate depletion in K and Rb and a moderate enrichment in Sr. The most dramatic change, however, is for Li which exhibits a marked enrichment, a 71 to 172% increase. Li is commonly concentrated in the micas but unlike the other alkali metals, it goes into the octahedral sites, a consequence of its small size. Its single charge makes it anomalous relative to the other divalent (Fe^{2+},Mg, Mn) trivalent (Fe^{3+}, Al^{3+}), and quadrivalent (Ti) octahedral cations and logically is less tightly bound. We suggest that during cataclasis and alteration, Li is far more easily mobilized and concentrated in any new micas that form (e.g. phengitic muscovite, chlorite, stilpnomelane, or biotite) preferentially in the cataclasized material.

Li was not found to be mobilized in the gouge along the San Andreas Fault (Anderson, et al., in press). This is consistent as that gouge, formed at higher level conditions, had minimal mineralogic changes during cataclasis.

E. Grain Size Distribution

1. Cataclasites

Histograms showing the grain-size distributions for the cataclasites (samples SG-7, SG-8 and SG-16A) are shown in Figure 7 and cumulative probability plots are shown in Figure 8. It should be stressed that these histograms and probability curves are based on frequency rather than weight percentages, and that approximately 84.8, 89.3 and 90.1 percent of samples SG-7, SG-8 and SG-16A respectively are finer than 0.0078 mm, the lower limit of optical measurement. Hence the size distribution data (Table 4, Figures 7 and 8) represents the porphyroclast portion of these rocks, which is 15.2, 10.7 and 9.9 volume % for SG-7, SG-8 and SG-16A, respectively.

Cumulative probability curves for SG-7 and SG-8 (Figure 8) plot as straight line segments on logarithmic normal probability paper. This suggests that logarithmic normal probability density functions might characterize each sample; however, the possibility of mixed stochastic distributions in the finer (matrix) portion cannot be ignored. Assuming a logarithmic normal distribution for each sample, the method of Cohen (1951) was used to estimate the mean and standard deviation of each singly truncated distribution shown in Figure 7. The calculations for SG-7 and SG-8 are virtually identical with mean values equal to 0.00012 mm (13ϕ)

Figure 7. Histograms showing frequency of grain sizes $\geq$ 0.0078 mm in diameter for samples SG-7 and SG-8 and schematic diagrams showing estimated original grain-size distribution (solid line) and present size distribution (dashed line) for each sample. Shaded parts of schematic diagrams represent measurable grains which existed in the original gouge and were not affected by later recrystallization. Unshaded parts of dashed distributions represent recrystallized matrix derived from finer-grained gouge. The letter "n" equals the number of measured grain daimeters.

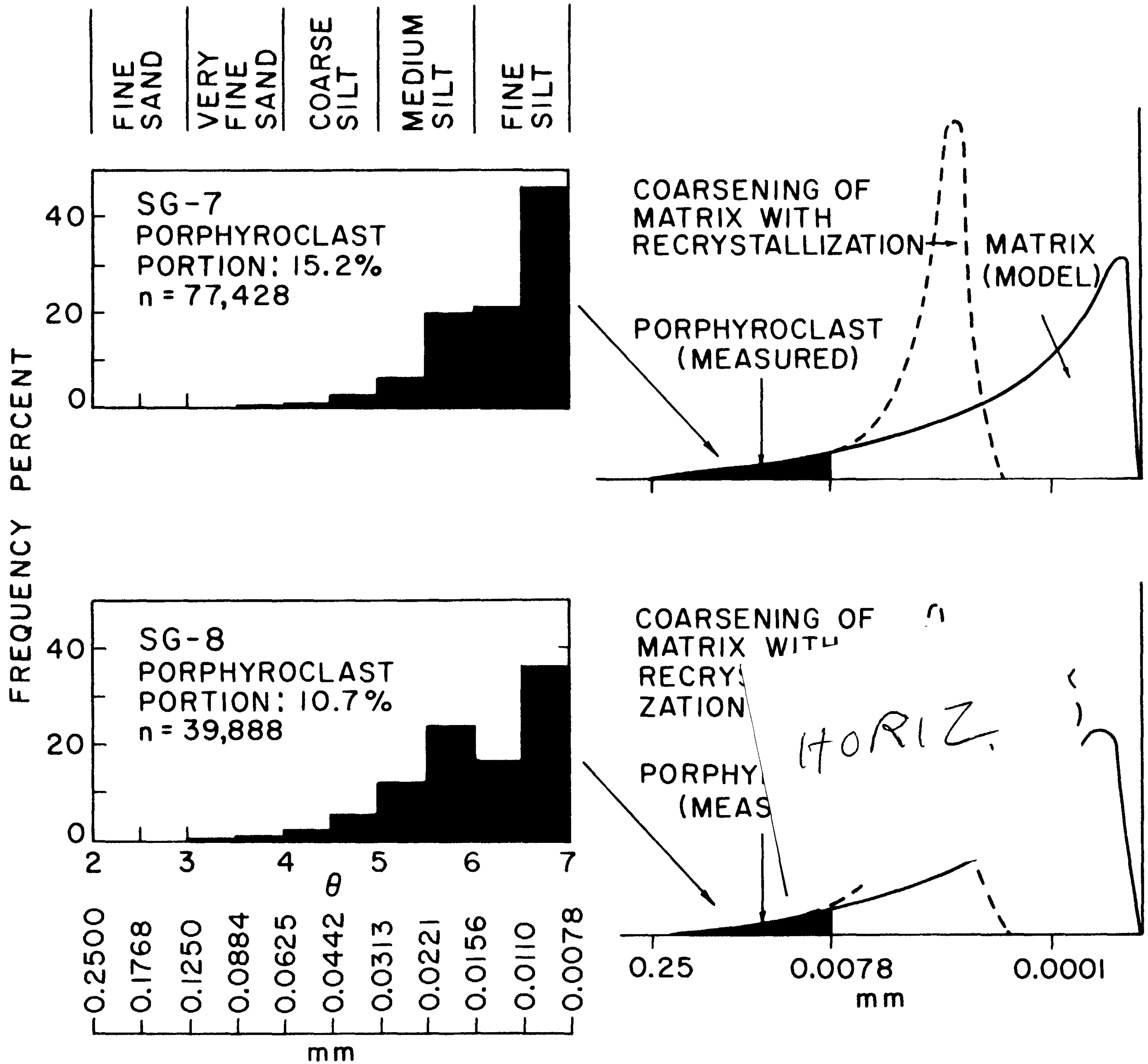
FINE SAND
VERY FINE SAND
COARSE SILT
MEDIUM SILT
FINE SILT
SG-7
PORPHYROCLAST
PORTION: 15.2%
n = 77,428
COARSENING OF MATRIX WITH RECRYSTALLIZATION
MATRIX (MODEL)
PORPHYROCLAST (MEASURED)
FREQUENCY PERCENT
40
20
0
SG-8
PORPHYROCLAST
PORTION: 10.7%
n = 39,888
COARSENING OF
MATRIX WIT
RECRY
ZATION
PORPHY
(MEAS
HORIZ.
2
3
4
5
6
7
θ
0.2500
0.1768
0.1250
0.0884
0.0625
0.0442
0.0313
0.0221
0.0156
0.0110
0.0078
mm
0.25
0.0078
0.0001
mm

Figure 8. Comparison of logarithmic normal cumulative probability plots for the coarse-grained (porphyroclast) fraction ($\geq$ 0.0078 mm diameter) of cataclasites versus gouge and microbreccia of the San Gabriel Fault Zone.

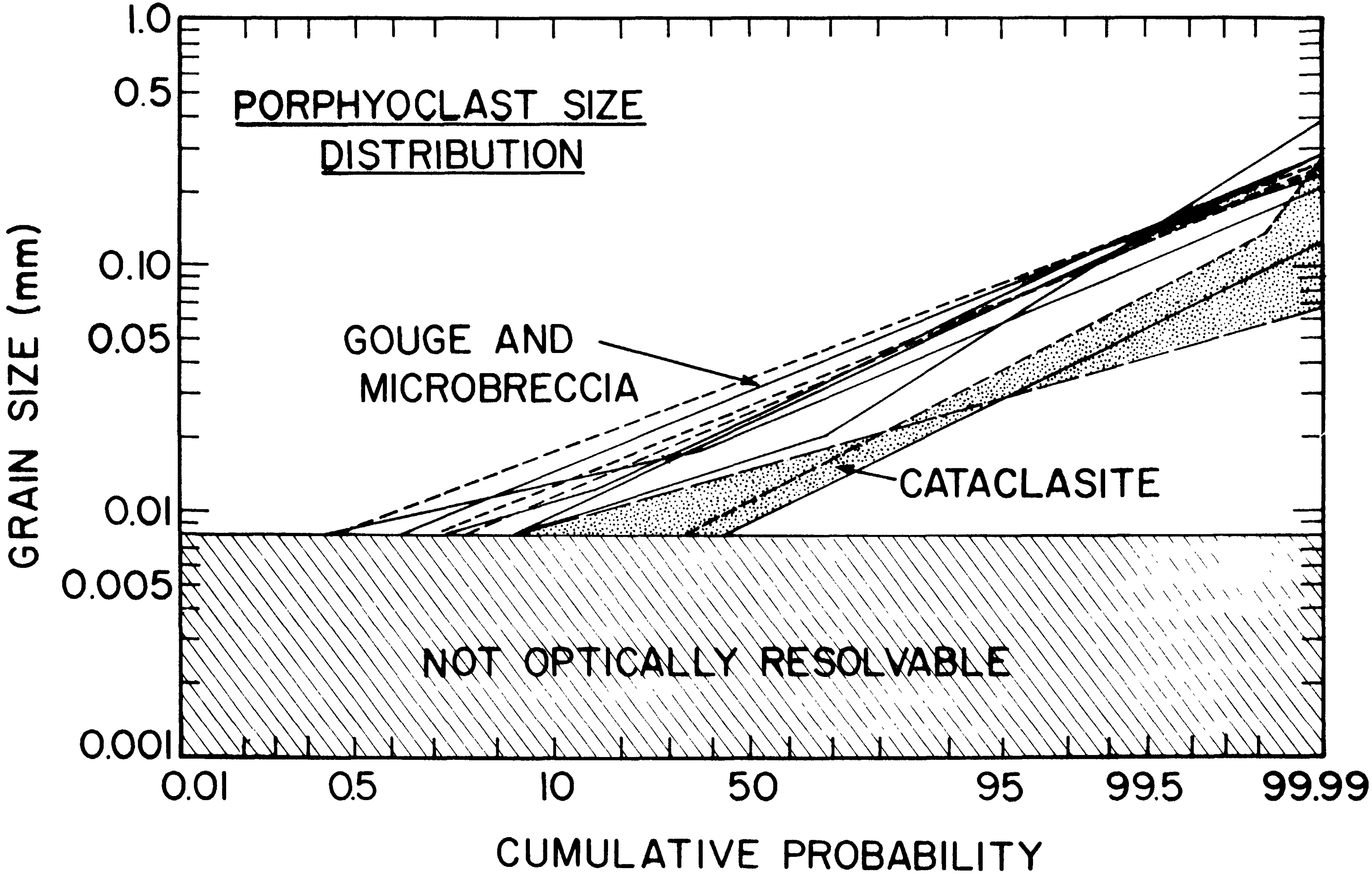
PORPHYOCLAST SIZE DISTRIBUTION
GOUGE AND MICROBRECCIA
CATACLASITE
NOT OPTICALLY RESOLVABLE
GRAIN SIZE (mm)
1.0
0.5
0.10
0.05
0.01
0.005
0.001
0.01
0.5
10
50
95
99.5
99.99
CUMULATIVE PROBABILITY

and standard deviation equal to about 0.63 ϕ units. These parameters are used in Figure 7 to schematically represent the initial (pre-recrystallization) particle size distribution of the cataclasite matrix in samples SG-7 and SG-8. It should be noted that there is no way to verify these estimates due to extensive recrystallization in both samples, and such estimates are meaningless should mixed grain-size distributions occur in these samples. These estimates suggest that the recrystallization has coarsened the matrix of the cataclasites as the smallest crystal size observed in the matrix of SG-7 is 0.0003 mm and the smallest in SG-8 is 0.0002 mm as viewed from S.E.M. photomicrographs (Plate 3). Likewise, the average grain size in the crystalline matrix is about 0.001 and 0.0003 mm for SG-7 and SG-8 respectively.

Although the porphyroclast portion of sample SG-16A plots according to a logarithmic normal distribution (Figure 8), the histogram for this sample (Figure 9) indicates that the total grain size distribution must be at least bimodal. The occurrence of bimodality or polymodality in sample SG-16 coupled with its truncated state make it impossible to calculate meaningful estimates for characteristic population parameters.

2. Microbreccia and Gouge

Histograms showing the measurable grain-size distributions for microbreccia and gouge samples (SG-2, SG-5, SG-6, SG-10A, SG-13A, SG-13B, SG-15A, and SG-18A) are presented in Figure 9 and corresponding logarithmic normal cumulative probability plots in Figure 8. The porphyroclast portion for each sample is indicated on the appropriate histogram. The total size distribution for each of these samples must be at least bimodal with one mode in the medium- to coarse-silt fraction and the other in the clay to

Figure 9. Histograms showing frequency of grain sizes > 0.0078 mm in diameter (porphyroclasts) for samples SG-2,5,6,10A,13A,13B,15A,18A,and 16A. The letter "n" equals the number of measured grain diameters.

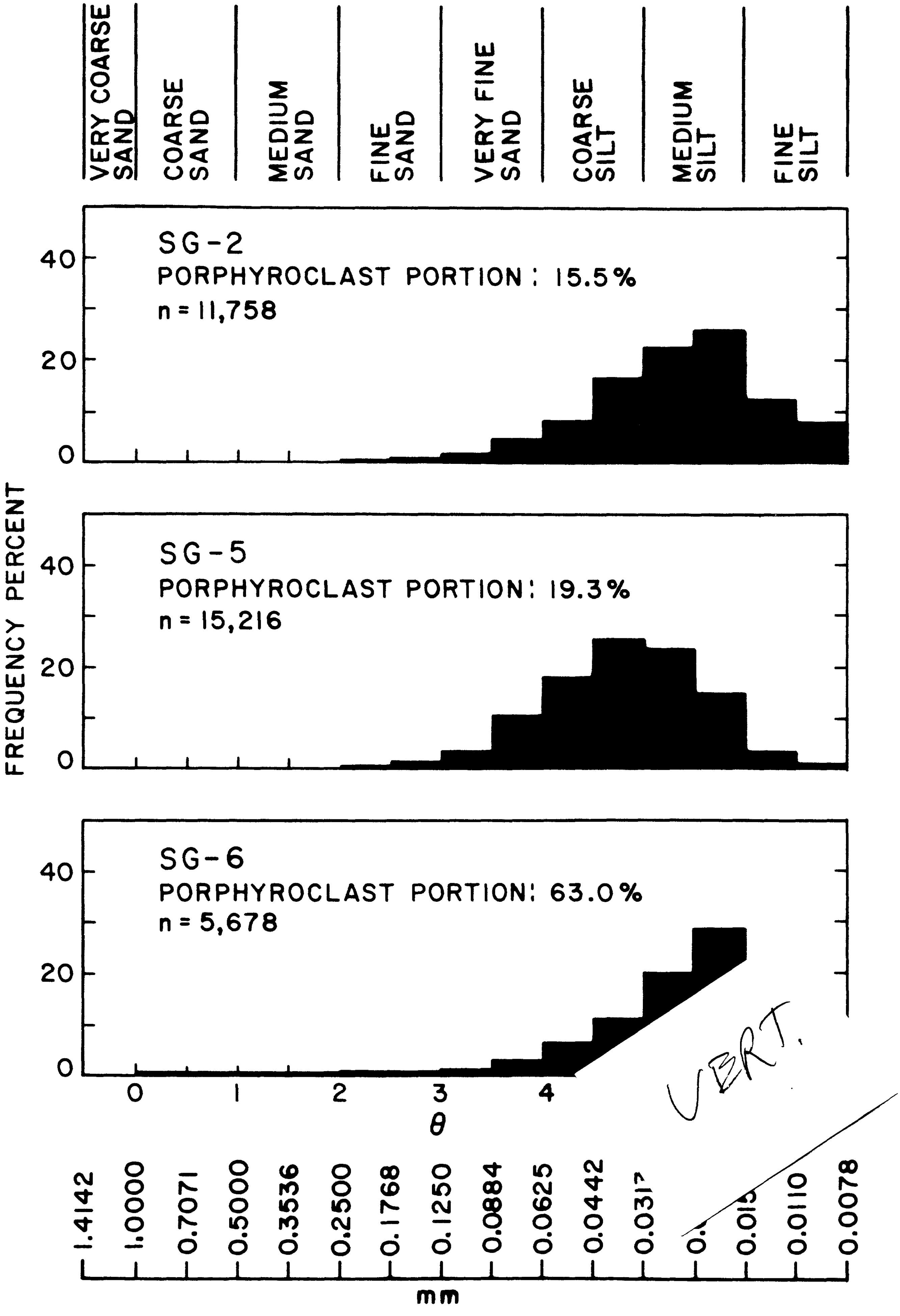
VERY COARSE SAND
COARSE SAND
MEDIUM SAND
FINE SAND
VERY FINE SAND
COARSE SILT
MEDIUM SILT
FINE SILT
FREQUENCY PERCENT
SG-2
PORPHYROCLAST PORTION: 15.5%
n = 11,758
SG-5
PORPHYROCLAST PORTION: 19.3%
n = 15,216
SG-6
PORPHYROCLAST PORTION: 63.0%
n = 5,678
0
20
40
0
1
2
3
4
θ
1.4142
1.0000
0.7071
0.5000
0.3536
0.2500
0.1768
0.1250
0.0884
0.0625
0.0442
0.0110
0.0078
mm
VERT.

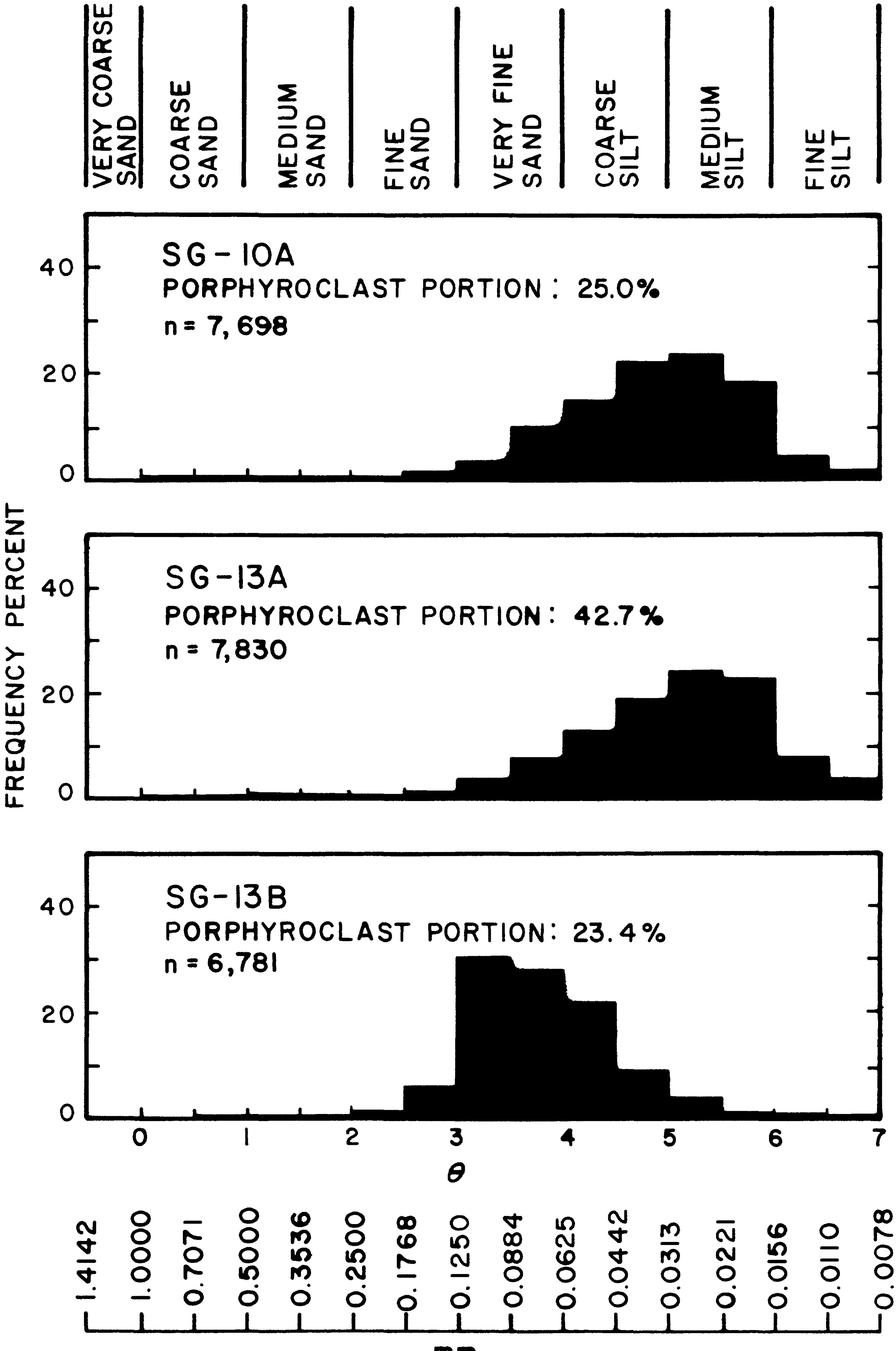
VERY COARSE SAND
COARSE SAND
MEDIUM SAND
FINE SAND
VERY FINE SAND
COARSE SILT
MEDIUM SILT
FINE SILT
SG-10A
PORPHYROCLAST PORTION: 25.0%
n = 7,698
SG-13A
PORPHYROCLAST PORTION: 42.7%
n = 7,830
SG-13B
PORPHYROCLAST PORTION: 23.4%
n = 6,781
FREQUENCY PERCENT
0
20
40
0 1 2 3 4 5 6 7
θ
1.4142 1.0000 0.7071 0.5000 0.3536 0.2500 0.1768 0.1250 0.0884 0.0625 0.0442 0.0313 0.0221 0.0156 0.0110 0.0078

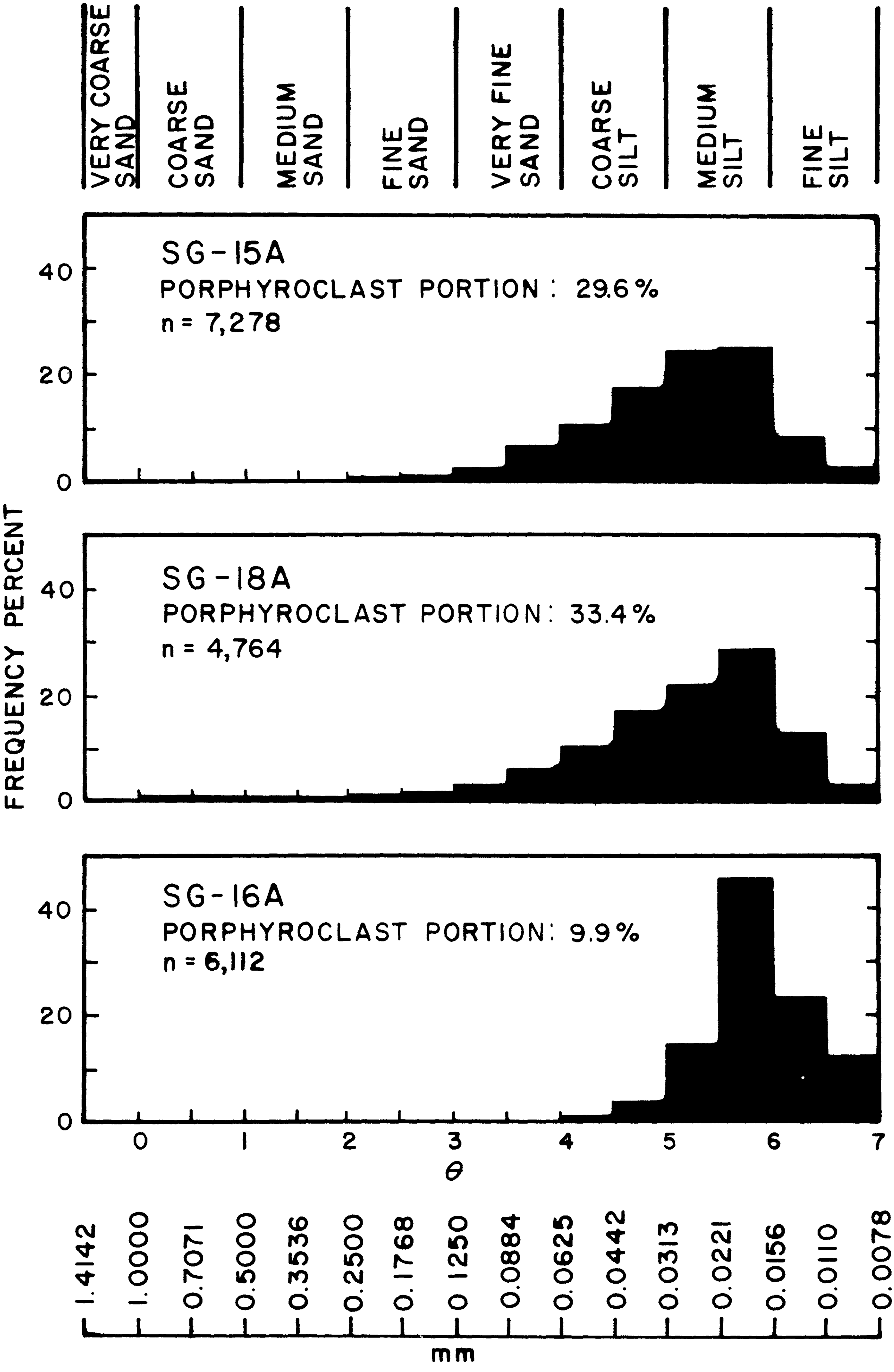

VERY COARSE SAND
COARSE SAND
MEDIUM SAND
FINE SAND
VERY FINE SAND
COARSE SILT
MEDIUM SILT
FINE SILT
SG-15A
PORPHYROCLAST PORTION: 29.6%
n = 7,278
SG-18A
PORPHYROCLAST PORTION: 33.4%
n = 4,764
SG-16A
PORPHYROCLAST PORTION: 9.9%
n = 6,112
FREQUENCY PERCENT
0
20
40
0 1 2 3 4 5 6 7
θ
1.4142 1.0000 0.7071 0.5000 0.3536 0.2500 0.1768 0.1250 0.0884 0.0625 0.0442 0.0313 0.0221 0.0156 0.0110 0.0078
mm

very-fine silt fraction (<0.0078 mm in diameter). S.E.M. photomicrography shows that the minimum grain size in the matrix portion of the microbreccia and gouge samples ranges from 0.00011 mm (SG-2) to 0.0011 (SG-13A and SG-13B). The minimum identifiable grain size for all samples except SG-13A and SG-13B is less than 0.0005 mm. The cumulative probability curves for the porphyroclast portion of these samples are nearly logarithmic normal; however, the change of slope in the finer grain sizes in samples SG-5, SG-6, SG-13B and SG-18A most likely represents mixing of at least two grain-size populations. It is interesting to note that the porphyroclast portion in the microbreccia and gouge samples range from 15.5 to 63.0% by volume and average 31.5%; whereas in the cataclasite samples, corresponding values range from 9.9 to 15.2% and average 11.9%.

3. Comparison with gouge of the San Andreas Fault

The principal conclusion that can be reached from the textural analyses carried out is that the cataclastic rocks from the San Gabriel Fault Zone are much finer grained than gouge samples from the present trace of the San Andreas Fault system in southern California (Anderson, et al., in press). It is difficult to make a direct comparison because the present values are in frequency percentages rather than weight percentages and the measured grains in this report only represent a part of the total grain-size distribution. Recrystallization of the volumetrically dominant matrix further complicates a direct comparison of these two sets of gouge data.

It is clear that very few grains coarser than fine sand (0.25 mm) were measured, and the vast majority of the grains observed in all samples except SG-6 are less than 0.0078 mm, i.e. very-fine silt or clay size. Such values contrast markedly with the gouge textures developed in the upper levels of the present trace of the San Andreas Fault (Anderson, et al., in press), where much of the gouge is silt-, sand-, granule-, and gravel-size with little very fine silt or clay. This reduction of grain size and increase in sorting (uniformity of grain size) most likely reflects increased confining pressure and/or increased displacement (Engelder, 1974; Aydin, 1977).

V. SUMMARY

In evaluation of cataclastic rocks within the San Andreas Fault System of southern California, the San Gabriel Fault, a deeply eroded late Oligocene to mid-Pliocene precursor to the San Andreas, was chosen for petrologic study as it should provide intra-fault material representative of deeper crustal levels. Cataclastic rocks along the present trace of the San Andreas in this area are exclusively a variety of fault gouge which is essentially a rock flour with a quartz, feldspar, biotite, chlorite, amphibole, epidote, and Fe-Ti oxide mineralogy representing the milled down equivalent of the original rock (Anderson and Osborne, 1979; Anderson et al., in press). Fault gouge along with breccia is likewise common along the San Gabriel Fault but only where the cataclasized zone is several tens of meters wide. At several localities, the cataclasized zone is extremely narrow (few centimeters) and the cataclastic rock type is cataclasite (Higgins, 1971), a dark, aphanitic, and highly comminuted and indurated rock. Conceivably, such narrowing of the cataclasized zone and intensity of cataclasis is what might be expected in the higher confining pressure of deeper crustal levels.

The cataclasite and gouge along the San Gabriel Fault is considerably finer grained than gouge along the San Andreas. The average grain diameter for the San Andreas gouge is 0.01 to 0.06 mm whereas for the San Gabriel cataclastic rocks it ranges from 0.0001 to 0.007 mm. Moreover, while the San Andreas gouge remains particulate to the smallest grain size, the ultrafine grain matrix of the San Gabriel cataclasite is recrystallized.

The cataclastic rocks along the San Gabriel Fault show more mineralogic changes than observed for gouge along the San Andreas Fault. At the expense of biotite, amphibole, and feldspar there is some growth of new chlorite, celadonitic (phengitic) muscovite, stilpnomelane or biotite, hematite, ferro-pseudo brookite laumontite, and zeolite. However, much of the mineralogy is still relict from the earlier igneous or metamorphic history of the protolith and porphyroclasts even in the most cataclasized material includes relict plagioclase (oligoclase to andesine), alkali feldspar, quartz, biotite, actinolite, allanite, and Fe-Ti oxides (ilmenite and magnetite). We have found no significant development of any clay minerals (illite, kaolinite, or montmorillonite). For most sites, the compositions of these minerals directly correspond to the mineral compositions in rock types on one or both sides of the fault.

Whole rock major and trace element chemistry coupled with mineral compositions show that mixing within the cataclasized zone is not uniform and that originally micaceous or foliated or physically more heterogeneous rock units may have a disproportionally larger contribution to the final make-up of the intrafault material. As previously found for the gouge along the San Andreas, chemical mobility is not a major factor in the formation of cataclastic rocks of the San Gabriel Fault. We see no major changes for Si, Ti, Al, Fe, Mg, Ca, Na, or Ba. There is moderate mobility of K, Rb, Sr and marked mobility of Li, a probable result of the alteration and formation of new mica minerals.

VI. ACKNOWLEDGEMENTS

Modal and x-ray diffraction studies were carried out by subcontract to Kent State University under the supervision of Professor Donald R. Palmer. Paul Adams, our research assistant, did all of the electron microprobe analyses and some of S.E.M. photomicroscopy. More S.E.M. work was done by Cindy Wiersma and David Crist. Whitney Moore did most of the whole rock chemical analyses. Grain size data was collected by Christine M. Farrens, Scott D. Katz, Cathy A. Kovacevich, Tanya Y. Lee, Anna M. Vasko. We are indebted to Sharon Wallace who masterfully typed this and preceding reports into their final form.

VII. REFERENCES CITED

Anderson, J. L. and R. H. Osborne (1979), Fabric, textural characteristics, mineralogy, and petrochemistry of intrafault material. In: J.F. Evernden (editor) summaries of technical reports 8, U.S. Geological Survey, 485-486.

Anderson, J. L., R. H. Osborne, and D. F. Palmer (in press), Petrogenesis of cataclastic rocks within the San Andreas Fault Zone of southern California, U.S.A.: Tectonophysics.

Albee, A. L. and Ray, L.(1970), Correction factors for electron probe microanalysis of silicates, oxides, carbonates, phosphates, and sulfates. In: Anal. Chem., 42, 1408-1414.

Aydin, Atilla (1977), Small faults formed as deformation bands in sandstone: In: U.S.G.S., Proceedings of Conference II, Experimental Studies of Rock Friction with Application to Earthquake Prediction, 617-653.

Bence, A. E. and Albee, A. L. (1968), Empiracle correction factors for the electron microanalysis of silicates and oxides. In: Jour. Geol., 76, 382-403.

Blatt, H. G. Middleton, and R. Murray (1972), Origin of sedimentary rocks. In: Prentice-Hall, 634.

Brace, W. F. (1972), Laboratory studies of stick-slip and their application to earthquakes. In: Tectonophysics, 14, 189-200.

Byerlee, J., Mjachkin, V., Summers, R., and Voevoda, O. (1978), Structures developed in fault gouge during stable sliding and stick-slip. In: Tectonophysics, 44, 161-171.

Carter, B. and L. T. Silver (1972), Structure and petrology of the San Gabriel Anorthosite-syenite body, In: California 24th Int. Geol. Congr. (Montreal) Section 2, 303-311.

Cohen, A. C., Jr., (1951), On estimating the mean and variance of singly truncated normal frequency distributions from the first three sample moments: In: Ann. Inst. Statist. Math., Tokyo, v. 3, 37-44.

Crowell, J. C., (1952), Probable large lateral displacement on San Gabriel fault, southern California: In: A.A.P.G. Bull 35, 2026-2035.

Crowell, J. C. (1954), Strike-slip displacement of the San Gabriel fault, southern California: In: Geology of Southern California, Calif. Div. Mines Bulletin 170, IV, 49-52.

Crowell J. C. (1962), Displacement along the San Andreas fault, California: In: G.S.A. Special Papers #71, 1-61.

Crowell, J. C. (1968), Movement histories of faults in the Transverse Ranges and speculations on the tectonic history of California: In: Proceedings on Conference on Geologic Problems of San Andreas Fault System, ed. R. L. Kovach and A. Nur., Stanford Univ. Pub., 323-341.

Crowell, J. C. (1973), Problems concerning the San Andreas fault system in southern California: In: Proceedings of the Conference on Tectonic Problems of the San Andreas Fault System, ed. W. R. Dickinson and A. Grantz, Stanford University Pub., 125-135.

Crowell, J. C. (1975), The San Gabriel fault and Ridge Basin, southern California: In: California Division of Mines and Geology Bulletin, 118, 208-219.

Crowell, J. C. (1975), The San Andreas fault in southern California: In: Cal. Div. of Mines and Geology Bulletin, 118, 7-26.

Crowell, J. C. (1979), The San Andreas fault system through time: Jour. Geol. Soc. Lond 136, 293-302.

Dibblee, T. W., Jr. (1968), Displacements on the San Andreas fault system in the San Gabriel, San Bernardino, and San Jacinto Mountains, southern California: In: Proceedings of Conference on Geologic Problems of San Andreas Fault System, ed. R. L. Kovach and A. Nur, Stanford Univ. Pub., 8, 260-278.

Dibblee, T. W., Jr. (1975), Late Quarternary uplift of the San Bernardino Mountains on the San Andreas and related faults: In: Cal. Div. of Mines and Geology Bulletin 118, 127-135.

Eaton, J. E. (1939), Ridge Basin, California: In: A.A.P.G. Bull. 23, 517-558.

Ehlig, P. L. (1971), Geologic Framework of the San Gabriel Mountains: California Division of Mines and Geology Bulletin, 196, 7-18.

Ehlig, P L. (1973), History, seismicity and engineering geology of the San Gabriel fault: In: Assoc. Engin. Geol., Special Pub., 247-251.

Ehlig, P. L. (1975), Basement rocks of the San Gabriel Mountains, south of the San Andreas fault, southern California: In: Cal. Div. of Mines and Geology Bulletin 118, 177-186.

Engelder, J. T. (1974), Cataclasis and the generation of fault gouge: In: Geological Society of America Bulletin 85, 1515-1522.

Engelder, T. (1977), Aspects of asperity--Surface interaction during frictional sliding: In: U.S.G.S. Proceedings of Conference II Experimental Studies of Rock Friction with Application to Earthquake Prediction, 117-137.

Galehouse, J. S. (1971), Point counting, In: Carver, R. E., ed., Procedures in sedimentary petrology. New York, Wiley-Interscience, 653.

Guidotti, C. V., J. T. Cheney, and S. Guggenheim (1976), Distribution of titanium between coexisting muscouite and biotite in pelitic schists from northwertern, Maine: In: Amer. Min 62, 438-448.

Higgins, M. W. (1971) Cataclastic rocks, In: U.S.G.S. Professional Paper 687, 97.

Hill, M. L. (1930), Structure of the San Gabriel Mountains north of Los Angeles, California: Univ. Calif. Pub. Geol. Scil, 19, 137-170.

Hsu, K. J. (1955), Granulites and mylonites of the region about Cucamonga and San Antonio Canyons, San Gabriel Mountains, California: In: Univ. Calif. Pub. Geol. Sci. 30, 223-351.

Jahns, R. H. (1973), Tectonic evolution of the Transverse Ranges Province as related to the San Andreas fault system: In: Proceedings of the Conference on Tectonic Problems of the San Andreas Fault System, ed. W.R. Dickinson and A. Grantz, Stanford Univ. Pub. 11, 149-170F.

Kew, W. S. W. (1924), Geology and oil resources of part of Los Angeles and Ventura Counties, California: In: U.S.G.S. Bull. 753, 1-197.

Liou, John, G. (1979) Zeolite facies metamorphism of basaltic rocks from the East Taiwan Ophiolite: Am. Min. 64, 1-14.

Logan, J. M. (1977), Creep, stable sliding, and premonitory slip, In: U.S.G.S. proceedings of Conference II, Experimental Studies of Rock Friction with Application to Earthquake Prediction, 205-237.

Logan, J. M. (1978), Laboratory and field investigations of fault gouge. In: J. F. Evernden (editor), Summaries of Technical Reports 6, U.S. Geological Survey 370-373.

Logan, J. M. (1978), Laboratory and field investigations of fault gouge. In: J. F. Evernden (editor), Summaries of Technical Reports 7, U.S. Geological Survey, 492-494.

Logan, J. M. and M. Friedman (1977), Mechanical properties of rocks affecting earthquake prediction and control: In: Summary of Tech. Reports III, U.S.G.S. National Earthquake Hazards Reduction Program, 140-142.

Miller, W. S. (1934), Geology of the Western San Gabriel Mountains of California: In: Univ. Calif. Pub. Math. and Phys. Sci., 1, 1-114.

Morton, D. M. (1975), Synopsis of the geology of the eastern San Gabriel Mountains, southern California: In: California Division of Mines and Geology Bulletin, 118, 170-176.

Morton, D. M. and A. K. Baird (1971), Tectonic setting of the San Gabriel Mountains: In: Cal. Div. of Mines and Geology Bulletin, 196, 2-6.

Nason, R. D. (1972), Propagation of fault creep events, In: NOAA Technical Report ERL 236-ESL 21.

Nason, R. D. (1973), Fault creep and earthquakes on the San Andreas fault. In: R. L. Kovach and A. Nur (editor), Proceedings of the Conference on Tectonic Problems of the San Andreas Fault System, Stanford Univ. Pub., 13 275-285.

Oakeshott, G. B. (1958), Geology and Mineral Deposits of San Fernando Quadrangle, Los Angeles County, California: In: Cal. Div. Mines Bull. 172, 147.

Oakeshott, G. B. (1971), Geology of the epicentral area: In: Cal. Div. of Mines and Geology Bulletin 196, 19-30.

Scholz, C., P. Molnar, and T. L. Johnson (1962), Detailed studies of frictional sliding of granite and implications for the earthquake mechanism: In: Jour. Geophys. Research, b 77, 6392-6406.

Stesky, R. M. and W. F. Brace (1973), Estimation of frictional stress on the San Andreas fault from laboratory measurements: In: R. L. Kovach and A. Nur, eds., Proceedings of the Conference on Tectonic Problems of the San Andreas Fault System, Stanford Univ. Press, 206-214

Wang, C. Y. (1977), Experimental investigation of mechanical properties of clay gouge and cataclastics along the San Andreas fault: In: Summary of Tech. Reports III, U.S.G.S. National Earthquake Hazards Reduction Program, 28-34.

Weber, F. H., Jr. (1977), Investigation of the northwestern portion of the San Gabriel fault Zone, Los Angeles and Ventura Counties, with regard to character and regency of movement: In: U.S.G.S., Summaries of Technical Reports, Vol. IV. Submitted to National Earthquake Hazards Reduction Program, 25-26.

Wu, F. T., L. Blatter, and H. Robertson, (1975), Clay gouges in the San Andreas fault system and their possible implications: In: Pure and Applied Geophysics, v 113, 87-95.

Wu, F. T. (1977), Mineralogy and physical nature of clay gouge: In: U.S.G.S. Proceedings of Conference II Experimental Studies of Rock Friction with Application to Earthquake Prediction, 389-445.

List of Tables

Table 1

SG SAMPLES	1pgr1 $\bar{X}$	1pgrd $\bar{X}$	2pgr $\bar{X}$	2 $\bar{X}$	3A $\bar{X}$	3B $\bar{X}$	3C $\bar{X}$	3D $\bar{X}$	3pbs $\bar{X}$
Plagioclase	30.2	60.8	27.8	28.6	32.5	48.0	43.3	41.4	30.7
K-Feldspar	33.3	0.8	28.0	12.8	--	0.5	1.4	0.1	--
Quartz	25.3	22.1	28.6	12.7	2.6	16.8	13.4	14.5	11.2
Chlorite & Biotite	2.9	6.1	1.6	2.1	0.2	10.5	7.9	18.2	6.3
Hornblende	1.7	5.1	1.4	0.9	56.5	13.4	13.7	13.3	41.6
Hem/lim/mag. Opaques	1.7	0.3	0.1	0.2	3.0	4.2	13.1	7.3	1.8
Epidote	2.2	3.8	1.6	8.0	2.5	2.7	2.0	3.3	6.0
Calcite	--	--	--	--	--	--	--	--	--
Sphene	0.1	0.1	0.1	T	0.1	0.2	T	T	0.2
Ground Mass	0.7	--	2.5	32.8	1.3	3.0	5.0	--	2.1
Muscovite	0.9	0.5	1.7	0.1	--	0.1	--	--	0.1
Porosity	0.8	--	6.4	1.8	1.3	0.6	0.2	1.7	--
Apatite	--	--	--	--	--	0.1	--	0.1	--
Zircon	--	--	--	--	--	--	--	0.1	--
Total Points	3005	3008	3005	3011	3014	3006	3003	3015	3014
Total %	100.0	100.0	100.0	100.0	100.0	100.0	100.0	100.0	100.0

MODAL ANALYSES OF CATACLASTIC ROCKS FROM THE SAN GABRIEL FAULT ZONE

Table 1 (continued)

4pa $\bar{X}$	4pgr $\bar{X}$	5 $\bar{X}$	6 $\bar{X}$	7pb $\bar{X}$	7 $\bar{X}$	7pgr $\bar{X}$	8a $\bar{X}$	8b $\bar{X}$	8pgh $\bar{X}$	8pgr $\bar{X}$
42.8	44.5	2.2	22.1	27.4	23.7	38.1	33.5	33.5	31.7	48.3
--	--	0.4	49.7	20.7	8.3	10.6	4.8	0.4	--	8.4
6.9	52.3	19.9	25.6	24.7	13.8	6.3	12.4	11.8	29.3	28.9
0.5	0.4	3.9	0.3	2.1	0.7	0.6	2.6	11.0	18.4	8.4
47.8	0.7	2.3	0.1	--	0.1	--	1.8	10.3	--	0.2
1.1	0.6	6.8	1.0	2.4	3.2	1.0	2.8	4.1	2.6	0.6
0.6	0.6	31.5	0.2	1.5	6.1	5.8	1.8	2.3	4.5	0.2
--	--	--	0.4	0.6	0.6	--	6.7	1.5	3.6	--
0.1	0.1	0.2	--	0.1	0.4	0.4	0.2	0.1	--	0.1
--	--	30.2	--	15.1	43.5	36.4	29.8	24.8	--	4.8
--	0.4	--	0.3	5.1	--	0.8	3.6	0.1	8.2	0.1
--	0.4	2.6	--	0.1	--	--	--	0.1	0.5	--
0.2	--	--	--	0.2	--	--	--	--	1.2	--
--	--	--	--	--	--	--	--	--	--	--
3012	3004	3000	3011	3006	3002	3000	3002	3202	3077	3015
100.0	100.0	100.0	100.0	100.0	100.0	100.0	100.0	100.0	100.0	100.0

Table 1 (continued)

SG SAMPLES	9b	9c	10a	10b	10d	116	12	13a	13ap	13bp
Plagioclase	20.1	43.7	22.3	18.7	2.4	20.2	6.5	30.1	34.1	10.5
K-Feldspar	24.3	--	28.7	0.3	23.1	26.4	--	23.5	24.9	--
Quartz	27.7	20.5	28.5	17.2	23.6	28.2	14.9	28.4	26.6	5.3
Chlorite	0.5	0.3	--	1.2	--	1.2	0.7	11.3	8.9	0.1
Biotite	--	6.5	--	--	--	--	0.1	1.5	0.2	--
Hornblende-Actinolite	--	0.1	--	--	--	0.1	--	--	--	51.6
Hem/lim/mag. Opaques	0.1	1.8	--	0.2	--	0.1	0.1	0.1	0.1	2.1
Epidote	--	0.1	--	--	--	--	--	--	--	--
Calcite	14.2	0.1	16.3	1.1	45.2	6.4	8.1	0.1	2.0	4.5
Sphene	--	--	--	--	--	--	--	--	--	--
Ground Mass	11.0	25.4	--	26.8	0.1	16.8	68.6	4.7	1.8	25.3
Muscovite-Sericite	--	0.2	4.2	32.4	5.1	0.2	--	--	1.3	--
Porosity	2.1	1.3	--	2.1	0.5	0.4	1.0	0.3	0.1	0.6
Apatite	--	--	--	--	--	--	--	--	--	--
Zircon	--	--	--	--	--	--	--	--	--	--
Total Points	3212	3100	3002	3009	3150	3042	3122	3011	3207	3015
Total %	100.0	100.0	100.0	100.0	100.0	100.0	100.0	100.0	100.0	100.0

Table 1 (continued)

SG SAMPLES	14	15a	15mp	16b	16c	16d	16e	17	18
Plagioclase	36.4	10.3	50.1	27.1	6.7	6.5	36.8	3.2	16.3
K-Feldspar	21.8	--	--	--	--	10.2	17.0	--	0.2
Quartz	22.1	25.8	15.5	17.2	17.2	36.0	35.2	4.2	21.7
Chlorite	10.3	13.7	14.7	--	--	24.0	6.6	--	9.0
Biotite	0.4	--	0.1	--	0.1	--	0.6	--	--
Hornblende-Actinolite	--	0.1	12.6	0.7	--	1.0	--	--	--
Hem/lim/mag. Opaques	0.1	1.5	0.2	1.5	--	0.9	--	--	3.3
Epidote	--	--	--	--	--	--	--	--	--
Calcite	0.5	0.4	0.1	1.1	10.1	17.9	0.2	0.8	1.7
Sphene	--	--	--	--	--	--	--	--	--
Ground Mass	8.0	46.3	5.9	52.6	45.5	2.9	2.3	25.5	12.2
Muscovite-Sericite	--	0.8	0.1	--	20.1	--	0.1	66.3	34.5
Porosity	0.3	1.1	0.7	0.3	0.3	0.6	1.2	--	1.1
Apatite	--	--	--	--	--	--	--	--	--
Zircon	0.1	--	--	--	--	--	--	--	--
Total Points	3310	3021	3501	3002	3025	3138	3592	3340	3305
Total %	100.0	100.0	100.0	100.0	100.0	100.0	100.0	100.0	100.0

TABLE 2A. Analyses of Plagioclase from the San Gabriel Fault Zone

Sample					SG8-pgn						
Specimen	A-1	A-2	A-3	A-4	B-1	B-2	B-3	D	D-2	4	F
SiO_2	68.73	61.32	61.18	66.90	60.39	60.46	66.13	68.00	61.28	64.65	68.17
TiO_2	0.00	0.01	0.05	0.03	0.02	0.001	0.11	0.03	0.06	0.03	0.00
Al_2O_3	19.96	24.40	24.45	20.85	24.58	25.04	19.94	20.37	23.02	21.13	20.50
FeO	0.05	0.12	0.05	0.03	0.14	0.16	2.85	0.09	0.40	0.05	0.02
MgO	0.00	0.00	0.00	0.00	0.00	0.01	0.58	0.00	0.11	0.000	0.00
BaO	0.00	0.00	0.15	0.13	0.000	0.23	0.037	0.000	0.00	0.58	0.00
CaO	1.85	6.40	6.44	2.03	6.53	6.90	1.04	2.28	4.61	0.74	0.59
Na_2O	10.87	8.49	7.71	11.48	8.60	8.20	10.04	10.01	8.60	9.27	11.44
K_2O	0.07	0.15	0.81	0.14	0.15	0.16	0.77	0.07	0.27	2.18	0.08
TOTAL	101.53	100.90	100.83	101.59	100.40	101.16	101.49	100.84	98.34	98.42	100.80
					Formula Based on 8 Oxygens						
Si	2.966	2.709	2.710	2.906	2.687	2.674	2.905	2.952	2.767	2.907	2.958
Ti	0.000	0.000	0.002	0.001	0.001	0.000	0.004	0.001	0.002	0.001	0.000
Al	1.016	1.271	1.277	1.068	1.289	1.306	1.033	1.043	1.225	1.120	1.049
Fe	0.002	0.004	0.002	0.001	0.005	0.006	0.105	0.003	0.015	0.002	0.001
Mg	0.000	0.000	0.000	0.000	0.000	0.000	0.038	0.000	0.007	0.000	0.000
Ba	0.000	0.000	0.003	0.002	0.000	0.004	0.001	0.000	0.000	0.010	0.000
Ca	0.086	0.303	0.306	0.095	0.312	0.327	0.049	0.106	0.223	0.036	0.027
Na	0.910	0.727	0.662	0.967	0.742	0.703	0.855	0.843	0.753	0.791	0.963
K	0.004	0.008	0.046	0.008	0.008	0.009	0.043	0.004	0.015	0.125	0.004
An	8.57	29.17	30.16	8.84	29.33	31.47	5.18	11.11	22.60	3.74	2.74
Ab	91.03	70.02	65.35	90.42	69.87	67.67	90.25	88.47	75.96	83.13	96.82
Or	0.40	0.81	4.49	0.74	0.80	0.87	4.57	0.43	1.54	13.13	0.44
Remarks[1]	F,E	F	F	F	C	F	F	C	C	C,S	C,E,CC

[1] M= matrix, C= coarse, F= fine grained, S= sericitized, brecciated fragment, Ph= phenocryst
P= porphyroclast, E= with epidote, CC=with calcite, B= brecciated

(Analyses of Plagioclase continued.)

Sample	SG8-pgr						SG8-2		
Specimen	A-2	B	C-cor	C-Rim	H-cor	H-Rim	A-1	A-2	A-3
SiO_2	63.41	62.62	62.32	62.74	63.49	62.16	59.09	60.72	67.09
TiO_2	0.02	0.08	0.00	0.00	0.00	0.05	0.08	0.00	0.01
Al_2O_3	23.68	23.77	24.01	23.35	22.99	23.53	24.34	24.86	20.30
FeO	0.17	0.23	0.02	0.11	0.03	0.10	2.19	0.17	0.00
MgO	0.00	0.00	0.00	0.00	0.01	0.00	0.76	0.00	0.00
BaO	0.04	0.00	0.16	0.01	0.00	0.00	0.06	0.00	0.05
CaO	5.13	5.12	5.59	5.08	4.77	5.45	6.20	6.72	1.45
Na_2O	9.04	8.99	8.71	9.04	9.57	9.04	6.69	8.49	11.48
K_2O	0.19	0.31	0.31	0.22	0.15	0.19	0.86	0.07	0.07
TOTAL	101.68	101.11	101.13	100.55	100.99	100.53	100.23	101.04	100.45
			Formula Based on 8 Oxygens						
Si	2.768	2.755	2.742	2.770	2.789	2.751	2.658	2.683	2.936
Ti	0.001	0.003	0.000	0.000	0.000	0.002	0.003	0.000	0.000
Al	1.219	1.233	1.246	1.215	1.190	1.228	1.290	1.295	1.047
Fe	0.006	0.009	0.001	0.004	0.001	0.004	0.082	0.006	0.000
Mg	0.000	0.000	0.000	0.000	0.000	0.000	0.051	0.000	0.000
Ba	0.001	0.000	0.003	0.000	0.000	0.000	0.001	0.000	0.001
Ca	0.240	0.241	0.264	0.240	0.224	0.259	0.299	0.318	0.068
Na	0.765	0.767	0.744	0.774	0.815	0.776	0.583	0.728	0.974
K	0.011	0.017	0.017	0.012	0.008	0.011	0.049	0.024	0.004
An	23.62	23.53	25.74	23.42	21.41	24.75	32.08	30.31	6.50
Ab	75.34	74.80	72.58	75.38	77.79	74.22	62.62	69.29	93.12
Or	1.04	1.68	1.68	1.20	0.80	1.03	5.30	0.39	0.38
Remarks	B,M	B,M	Ph Core	Ph Rim	Ph Core	Ph Rim	M	M	P

(Analyses of Plagioclase continued)

Sample				SG8-2						SG8-A
Specimen	A-4	B-1	B-2	C-1	C-2	C-3	2-2	4	4-1	A-1
SiO_2	60.39	61.69	68.25	62.92	59.18	65.77	61.11	65.78	64.54	58.41
TiO_2	0.04	0.17	0.01	0.10	0.00	0.00	0.03	0.03	0.00	0.01
Al_2O_3	24.58	23.67	20.56	22.15	25.30	21.72	24.37	20.79	20.78	24.74
FeO	0.14	0.16	0.17	0.71	0.66	0.02	0.25	0.16	0.08	0.34
MgO	0.00	0.04	0.00	0.25	0.13	0.000	0.02	0.00	0.000	0.00
BaO	0.04	0.03	0.00	0.11	0.30	0.05	0.03	0.00	0.00	0.00
CaO	6.67	4.91	1.50	2.76	5.61	3.24	6.01	1.70	2.51	7.78
Na_2O	8.33	8.19	11.25	9.28	7.96	10.01	8.10	10.97	10.55	6.81
K_2O	0.07	1.02	0.13	0.73	1.33	0.10	0.24	0.63	0.09	0.08
TOTAL	100.57	99.87	101.88	98.99	100.47	100.92	100.17	99.57	98.54	98.22
					Formula Based on 8 Oxygens					
Si	2.681	2.753	2.942	2.821	2.652	2.871	2.716	2.907	2.887	2.658
Ti	0.001	0.006	0.000	0.003	0.000	0.000	0.001	0.001	0.000	0.000
Al	1.303	1.245	1.045	1.171	1.337	1.118	1.277	1.083	1.096	1.326
Fe	0.005	0.006	0.006	0.027	0.025	0.001	0.009	0.006	0.003	0.013
Mg	0.000	0.002	0.000	0.016	0.009	0.000	0.001	0.000	0.000	0.000
Ba	0.001	0.001	0.000	0.002	0.005	0.001	0.001	0.000	0.000	0.000
Ca	0.317	0.235	0.069	0.132	0.269	0.152	0.286	0.081	0.120	0.379
Na	0.717	0.708	0.941	0.807	0.692	0.848	0.698	0.941	0.915	0.601
K	0.004	0.058	0.007	0.042	0.076	0.006	0.014	0.007	0.005	0.005
An	30.57	23.46	6.79	13.50	25.97	15.09	28.67	7.84	11.54	38.51
Ab	69.07	70.73	92.49	82.23	66.72	84.33	69.96	91.46	87.97	61.02
Or	0.37	5.81	0.72	4.27	7.31	0.58	1.37	0.71	0.48	0.47
Remarks	M	M	M	M	M	P	M	M	P,C	P

(Analyses of Plagioclase continued)

Sample			SG-7		
Specimen	08-2	01-2	08-1	C-2	C-2-2
SiO_2	65.18	65.15	66.53	65.53	66.73
TiO_2	.02	.06	.00	.00	.00
Al_2O_3	24.91	22.94	23.72	19.45	20.42
FeO	.33	.29	.16	.40	1.29
MgO	.14	.11	.05	.06	.50
BaO	.06	.11	.09	.02	.03
CaO	1.28	1.10	1.18	.21	.21
Na_2O	9.80	10.16	10.98	11.69	11.43
K_2O	1.93	1.30	1.13	.24	.17
TOTAL	103.67	101.22	103.83	97.59	100.77
Si	2.788	2.845	2.833	2.951	2.920
Ti	.001	.002	.000	.000	.000
Al	1.256	1.181	1.191	1.033	1.053
Fe	.012	.011	.006	.016	.047
Mg	.009	.007	.003	.004	.033
Ba	.001	.002	.002	.000	.001
Ca	.059	.052	.054	.010	.010
Na	.813	.861	.907	1.021	.970
K	.106	.072	.061	.014	.010
An	6.02	5.25	5.28	0.96	1.00
Ab	83.18	87.41	88.73	97.69	98.03
Or	10.80	7.34	5.99	1.35	0.97
Remarks	P	P	P	P	P

(Analyses of Plagioclase continued)

Sample	SG8-A			SG-7		SG7-PB				
Specimen	A-2	B-1	D	C-1	1-1	A-1	A-2	B-1	B-2	B-4
SiO_2	59.03	41.46	59.31	66.70	61.91	66.29	67.08	66.66	69.39	67.78
TiO_2	0.09	0.00	0.00	0.00	0.06	0.01	0.00	0.00	0.00	0.02
Al_2O_3	24.41	21.90	24.41	19.21	22.85	21.41	20.44	19.89	19.97	20.46
FeO	0.12	0.60	0.19	0.38	0.68	0.67	0.22	0.69	0.06	0.46
MgO	0.00	0.21	0.00	0.02	0.32	0.20	0.018	0.20	0.00	0.15
BaO	0.00	0.04	0.04	0.00	0.00	0.00	0.03	0.07	0.00	0.05
CaO	7.52	4.39	7.05	0.09	1.02	0.13	0.38	0.54	0.27	0.41
Na_2O	6.99	7.82	7.18	11.93	8.46	10.53	11.59	10.63	12.13	10.19
K_2O	98.23	96.82	98.34	98.45	97.61	100.76	100.10	99.55	101.91	99.93
TOTAL										
				Formula Based on 8 Oxygens						
Si	2.680	2.809	2.687	2.973	2.813	2.904	2.942	2.949	2.980	2.964
Ti	0.003	0.000	0.000	0.000	0.002	0.000	0.000	0.000	0.000	0.001
Al	1.307	1.180	1.304	1.010	1.224	1.106	1.057	1.038	1.011	1.055
Fe	0.005	0.023	0.007	0.014	0.026	0.025	0.008	0.0256	0.002	0.017
Mg	0.000	0.014	0.000	0.001	0.022	0.013	0.001	0.013	0.000	0.010
Ba	0.000	0.001	0.001	0.000	0.000	0.000	0.000	0.001	0.000	0.001
Ca	0.366	0.215	0.342	0.004	0.050	0.006	0.018	0.026	0.012	0.019
Na	0.615	0.693	0.631	1.031	0.746	0.894	0.986	0.912	1.010	0.864
K	0.003	0.024	0.010	0.007	0.134	0.085	0.020	0.049	0.005	0.023
An	37.16	23.04	34.79	0.40	5.36	0.62	1.73	2.59	1.21	2.11
Ab	62.48	74.40	64.15	98.92	80.28	90.76	96.35	92.41	98.28	95.31
Or	0.35	2.56	1.06	0.68	14.37	8.61	1.93	5.00	0.52	2.57
Remarks	P	P	P	P	P	B	B	B	B	M

(Analyses of Plagioclase continued)

Sample	SG7-PB								SG7-2	
Specimen	B-5	C-1	C-2	1-1	1-2	$2_{(1)}$	$2_{(2)}$	4-1	A	D
SiO_2	68.54	65.69	63.87	67.13	68.37	67.41	68.17	69.20	63.45	64.39
TiO_2	0.04	0.08	0.00	0.00	0.08	0.04	0.04	0.04	0.06	0.02
Al_2O_3	20.48	22.47	22.32	21.74	20.48	20.54	21.26	20.30	23.37	22.57
FeO	0.15	0.15	0.30	0.19	0.20	0.11	0.08	0.07	0.13	0.36
MgO	0.00	0.00	0.07	0.01	0.08	0.00	0.06	0.00	0.02	0.12
BaO	0.02	0.01	0.36	0.01	0.04	0.25	0.04	0.12	0.07	0.23
CaO	0.37	2.13	0.73	0.54	0.36	0.88	0.36	0.46	3.55	0.50
Na_2O	11.24	10.25	7.04	10.64	11.79	8.84	11.37	11.44	8.76	8.88
K_2O	0.54	0.70	4.86	1.02	0.58	4.25	0.67	0.08	0.81	2.24
TOTAL	101.37	101.48	99.54	101.29	101.97	102.31	102.06	101.70	100.21	99.30
				Formula Based on 8 Oxygens						
Si	29.03	2.857	2.864	2.912	2.950	2.938	2.933	2.976	2.801	2.864
Ti	0.001	0.003	0.000	0.000	0.003	0.001	0.001	0.001	0.002	0.001
Al	1.044	1.153	1.180	1.112	1.042	1.056	1.078	1.029	1.216	1.184
Fe	0.006	0.006	0.011	0.007	0.007	0.004	0.003	0.002	0.005	0.013
Mg	0.000	0.000	0.005	0.000	0.005	0.000	0.004	0.000	0.001	0.008
Ba	0.000	0.000	0.006	0.000	0.001	0.004	0.001	0.002	0.001	0.004
Ca	0.017	0.099	0.035	0.025	0.017	0.041	0.017	0.021	0.168	0.024
Na	0.943	0.865	0.612	0.895	0.986	0.747	0.948	0.954	0.750	0.766
K	0.030	0.039	0.278	0.057	0.032	0.236	0.037	0.004	0.046	0.127
An	1.71	9.90	3.81	2.58	1.62	4.01	1.67	2.18	17.44	2.58
Ab	95.29	86.23	66.15	91.63	95.32	72.92	94.64	97.39	77.82	83.54
Or	3.00	3.87	30.04	5.79	3.06	23.07	3.69	0.43	4.75	13.88
Remarks	B	B,F	B,F	B	B	B	B	M	P	M

(Analyses of Plagioclase continued)

Sample				SG7-PGR				SG-6	
Specimen	D	K	D	F	B	A	A	E-Rim	E-Core
SiO_2	65.21	61.27	61.81	62.34	62.35	62.39	62.37	68.41	67.47
TiO_2	0.00	0.00	0.00	0.01	0.03	0.05	0.00	0.00	0.07
Al_2O_3	22.50	23.34	23.59	24.33	23.83	24.18	24.06	19.99	19.33
FeO	0.06	0.13	0.08	0.14	0.13	0.08	0.08	0.06	0.31
MgO	0.00	0.00	0.00	0.00	0.00	0.00	0.00	0.00	0.00
BaO	0.00	0.00	0.06	0.00	0.03	0.02	0.01	0.11	0.04
CaO	2.86	4.96	4.95	5.11	5.09	5.06	5.20	0.37	0.27
Na_2O	9.12	8.67	8.64	8.26	8.41	8.42	8.44	11.81	11.67
K_2O	0.33	0.43	0.43	0.31	0.36	0.27	0.42	0.14	0.08
TOTAL	100.08	98.8	99.55	100.49	100.21	100.47	100.58	100.89	99.24
Si	2.860	2.755	2.757	2.748	2.759	2.752	2.751	2.971	2.981
Ti	0.000	0.000	0.000	0.000	0.001	0.002	0.000	0.000	0.002
Al	1.164	1.237	1.240	1.265	1.243	1.257	1.251	1.023	1.007
Fe	0.002	0.005	0.003	0.005	0.005	0.003	0.003	0.002	0.011
Mg	0.000	0.000	0.000	0.000	0.000	0.000	0.000	0.000	0.000
Ba	0.000	0.000	0.001	0.000	0.000	0.000	0.000	0.002	0.001
Ca	0.134	0.239	0.237	0.241	0.241	0.239	0.246	0.017	0.013
Na	0.776	0.756	0.747	0.706	0.721	0.720	0.722	0.995	0.100
K	0.018	0.025	0.024	0.017	0.020	0.015	0.024	0.008	0.005
An	14.48	23.45	23.47	25.01	24.54	24.55	24.78	1.70	1.25
Ab	83.55	74.11	74.11	73.19	73.41	73.89	72.83	97.53	98.29
Or	1.97	2.44	2.43	1.81	2.05	1.56	2.39	0.77	0.46
Remarks	B	C	B	B	B	B	B	C	C

(Analyses of Plagioclase continued)

Sample					SG-6					SG-5
Specimen	C-Rim	I	C-Rim2	C-Core	L	K-2	K-1	A-1	A-2	A
SiO_2	63.12	65.57	65.92	64.89	64.41	63.17	64.16	64.74	64.72	61.65
TiO_2	0.00	0.00	0.05	0.00	0.00	0.00	0.00	0.00	0.05	0.03
Al_2O_3	21.60	22.57	21.04	21.68	21.70	22.92	22.35	22.79	22.35	24.71
FeO	0.07	0.07	0.06	0.13	0.09	0.11	0.19	0.04	0.09	0.04
MgO	0.00	0.00	0.00	0.00	0.00	0.00	0.00	0.00	0.00	0.00
BaO	0.15	0.01	0.10	0.07	0.00	0.00	0.00	0.00	0.00	0.08
CaO	2.95	3.00	2.64	2.30	2.17	3.87	3.61	3.67	3.49	5.16
Na_2O	9.54	10.49	9.83	9.16	9.81	9.87	9.82	10.16	10.33	7.97
K_2O	0.21	0.25	0.10	1.48	0.25	0.20	0.20	0.19	0.16	1.37
TOTAL	97.62	101.95	99.73	99.72	98.42	100.14	100.33	101.59	101.18	101.01
Si	2.851	2.841	2.905	2.875	2.874	2.795	2.828	2.819	2.831	2.722
Ti	0.000	0.000	0.002	0.000	0.000	0.000	0.000	0.000	0.002	0.001
Al	1.150	1.153	1.093	1.133	1.142	1.196	1.161	1.170	1.153	1.287
Fe	0.003	0.003	0.002	0.005	0.003	0.004	0.007	0.001	0.003	0.001
Mg	0.000	0.000	0.000	0.000	0.000	0.000	0.000	0.000	0.000	0.000
Ba	0.003	0.000	0.002	0.001	0.000	0.000	0.000	0.000	0.000	0.001
Ca	0.143	0.139	0.125	0.109	0.104	0.184	0.170	0.171	0.163	0.244
Na	0.835	0.881	0.840	0.787	0.849	0.847	0.839	0.858	0.876	0.682
K	0.012	0.014	0.006	0.084	0.014	0.011	0.011	0.011	0.009	0.077
An	14.41	13.46	12.85	11.15	10.75	17.63	16.67	16.45	15.59	24.32
Ab	84.39	85.21	86.55	80.32	87.81	81.30	82.21	82.53	83.55	67.98
Or	1.20	1.33	0.60	8.54	1.44	1.07	1.12	1.02	0.86	7.70
Remarks	C-Rim	C	C-Rim	C-Core,S	C	B	B	B	B	P

(Analyses of Plagioclase continued)

Sample	SG-5					SG-2					
Specimen	C-1	G-1	C-3	C-2	D	B-1	B-2	D-2	C	I	A-2
SiO_2	61.94	61.31	60.31	61.87	60.97	67.39	67.44	65.43	67.89	68.05	66.98
TiO_2	0.06	0.01	0.00	0.00	0.07	0.00	0.00	0.03	0.00	0.00	0.00
Al_2O_3	24.43	23.71	24.46	24.41	24.04	20.39	20.70	20.61	20.41	20.34	19.98
FeO	0.00	0.08	0.00	0.01	0.01	0.03	0.01	0.06	0.08	0.03	0.06
MgO	0.00	0.00	0.00	0.00	0.00	0.00	0.00	0.00	0.00	0.00	0.00
BaO	0.04	0.04	0.06	0.00	0.00	0.03	0.15	0.14	0.00	0.00	0.12
CaO	5.20	5.03	5.42	5.64	5.66	0.55	0.85	0.72	0.83	0.88	0.85
Na_2O	8.88	7.82	8.58	8.73	7.09	10.50	11.05	8.47	11.12	11.26	9.48
K_2O	0.06	0.97	0.23	0.06	1.91	0.09	0.19	3.78	0.14	0.14	0.14
TOTAL	100.62	98.99	99.06	100.73	99.75	98.98	100.39	99.24	100.48	100.70	99.61
Si	2.733	2.752	2.708	2.727	2.731	2.967	2.943	2.927	2.956	2.958	2.963
Ti	0.001	0.000	0.000	0.000	0.002	0.000	0.000	0.001	0.000	0.000	0.000
Al	1.271	1.255	1.295	1.269	1.270	1.058	1.065	1.087	1.048	1.043	1.042
Fe	0.000	0.003	0.000	0.000	0.001	0.001	0.000	0.002	0.003	0.001	0.002
Mg	0.000	0.000	0.000	0.000	0.000	0.000	0.000	0.000	0.000	0.000	0.000
Ba	0.001	0.001	0.001	0.000	0.000	0.001	0.003	0.002	0.000	0.000	0.002
Ca	0.246	0.242	0.261	0.267	0.272	0.026	0.040	0.035	0.039	0.041	0.040
Na	0.760	0.631	0.747	0.747	0.616	0.897	0.935	0.735	0.939	0.949	0.813
K	0.005	0.056	0.013	0.003	0.109	0.005	0.011	0.216	0.008	0.008	0.121
An	24.36	24.71	25.55	26.23	27.27	2.81	4.02	3.50	3.91	4.08	4.12
Ab	75.30	69.59	73.14	73.47	61.79	96.66	94.91	74.59	95.28	95.12	83.47
Or	0.34	5.70	1.31	0.30	10.94	0.53	1.08	2.91	0.81	0.80	12.41
Remarks	P	P,F	M	M	P	P	P	P	P	P	P

(Analyses of Plagioclase continued)

Sample	SG-2	SG2-PGR						
Specimen	A-1	E-1	F	E-2	E-2-Rim	C-Core	B	C-Rim
SiO_2	65.08	57.22	56.87	57.84	57.31	58.91	60.75	60.74
TiO_2	0.00	0.00	0.00	0.00	0.05	0.05	0.00	0.10
Al_2O_3	21.20	27.55	27.45	27.65	26.73	26.63	25.07	24.83
FeO	0.33	0.06	0.03	0.09	0.13	0.10	0.10	0.07
MgO	0.21	0.01	0.01	0.00	0.00	0.00	0.00	0.01
BaO	0.03	0.03	0.03	0.03	0.14	0.10	0.04	0.08
CaO	0.89	9.39	9.42	9.06	8.68	8.03	6.53	6.50
Na_2O	9.86	6.35	6.52	6.70	6.58	7.25	7.91	8.04
K_2O	1.10	0.09	0.08	0.13	0.07	0.11	0.10	0.07
TOTAL	98.70	100.69	100.42	101.49	99.68	101.18	100.50	100.43
Si	2.901	2.550	2.544	2.557	2.579	2.607	2.690	2.695
Ti	0.000	0.000	0.000	0.000	0.002	0.002	0.000	0.003
Al	1.114	1.448	1.448	1.441	1.418	1.390	1.309	1.299
Fe	0.012	0.002	0.001	0.003	0.005	0.004	0.004	0.002
Mg	0.014	0.000	0.001	0.000	0.000	0.000	0.000	0.001
Ba	0.001	0.001	0.001	0.001	0.002	0.002	0.001	0.001
Ca	0.043	0.449	0.452	0.429	0.418	0.381	0.310	0.309
Na	0.852	0.549	0.566	0.574	0.574	0.622	0.679	0.692
K	0.063	0.005	0.004	0.007	0.004	0.006	0.005	0.004
An	4.46	44.75	44.21	42.49	41.97	37.75	31.18	30.75
Ab	88.98	54.77	55.38	56.81	57.62	61.64	68.28	68.87
Or	6.56	0.49	0.42	0.71	0.41	0.61	0.54	0.39
Remarks	P	C	F	C-Core	C-Rim	C-Core	C	C-Rim

(Analyses of Plagioclase continued)

Sample	SG-9C										
Specimen	C-1	A-1	A-2	B-1	D-1	C-3	F-2	D-3	B-3	B-2	C-2
SiO_2	69.67	69.51	68.65	69.52	69.45	69.82	69.32	69.74	69.93	69.64	68.70
TiO_2	.05	.10	.04	.00	.06	.05	.04	.05	.08	.01	.00
Al_2O_3	19.45	19.84	19.21	19.91	20.22	19.94	19.97	20.22	20.25	19.96	19.91
FeO	.03	.00	.02	.10	.07	.03	.13	.04	.01	.17	.04
MgO	.00	.00	.00	.00	.00	.00	.00	.00	.00	.00	.00
BaO	.00	.00	.09	.00	.03	.00	.04	.02	.01	.15	.05
CaO	.14	.20	.20	.22	.20	.26	.29	.32	.26	.31	.24
Na_2O	11.53	11.29	9.67	11.54	9.99	11.05	10.65	11.78	11.05	11.52	10.15
K_2O	.14	.09	1.49	.17	.35	.12	1.09	.09	.13	.17	.24
TOTAL	101.01	101.03	99.35	101.46	100.37	101.29	101.53	102.27	101.72	101.92	99.32
Si	3.010	3.001	3.020	2.992	3.006	3.003	2.991	2.982	2.995	2.989	3.005
Ti	.002	.003	.001		.002	.002	.001	.002	.003	.000	
Al	.991	1.010	.996	1.011	1.032	1.011	1.016	1.019	1.023	1.010	1.027
Fe	.001		.001	.004	.003	.001	.005	.001	.000	.006	.001
Mg				.000							
Ba			.001			.000	.001	.000	.000	.003	.001
Ca	.007	.009	.009	.010	.009	.012	.013	.015	.012	.014	.011
Na	.966	.945	.825	.963	.839	.922	.891	.977	.918	.959	.861
K	.008	.005	.084	.009	.020	.006	.060	.005	.007	.010	.013
An	.669	.984	1.008	1.027	1.085	1.295	1.387	1.473	1.267	1.468	1.263
Ab	98.545	98.523	89.884	98.038	96.665	98.020	92.391	98.015	97.956	97.564	97.254
Or	.786	.493	9.108	.935	2.250	.686	6.223	.512	.777	.967	1.483
Remarks	F,B	C,S	C,S	C	F	C	C	F,B	C	F,S	F,B

(Analyses of Plagioclase continued)

Sample	SG-9C		SG-9B								
Specimen	E-1	J	A-1	B-2	E-1	B-1	C	H	F	A-2A	B-3
SiO_2	68.35	67.88	68.94	67.91	66.64	66.99	68.90	67.65	64.56	67.88	66.89
TiO_2	.00	.01	.01	.00	.00	.06	.04	.00	.00	.05	.00
Al_2O_3	20.59	20.98	19.46	19.37	19.96	19.91	19.93	20.31	21.45	20.53	20.43
FeO	.06	.15	.01	.04	.26	.04	.09	.08	.29	.10	.10
MgO	.00	.02	.00	.00	.08	.00	.00	.00	.10	.00	.00
BaO	.08	.05	.00	.00	.05	.11	.00	.00	.00	.01	.03
CaO	.60	.76	.10	.13	.11	.25	.38	.36	.86	.95	1.28
Na_2O	8.02	9.63	11.67	11.28	9.45	11.09	11.12	8.94	8.91	10.21	10.29
K_2O	.99	1.63	.07	.09	.67	.12	.10	.33	1.51	.15	.19
TOTAL	98.69	101.11	100.26	98.82	97.21	98.58	100.57	97.67	97.68	99.87	99.20
Si	3.000	2.948	3.001	2.997	2.984	2.971	2.989	2.998	2.902	2.965	2.949
Ti		.000	.000			.002	.001			.002	
Al	1.065	1.074	.999	1.008	1.054	1.041	1.020	1.061	1.367	1.057	1.062
Fe	.002	.005	.000	.002	.010	.002	.003	.003	.011	.004	.004
Mg		.001			.005				.007		
Ba	.001	.001			.001	.002	.000			.000	.001
Ca	.028	.035	.005	.006	.005	.012	.018	.017	.041	.044	.060
Na	.682	.811	.985	.966	.821	.954	.936	.768	.777	.865	.879
K	.055	.090	.004	.005	.038	.007	.006	.018	.087	.009	.010
An	3.709	3.768	.467	.608	.610	1.238	1.847	2.112	4.579	4.841	6.356
Ab	89.085	86.608	99.152	98.869	94.994	98.062	97.558	95.597	85.855	94.230	92.546
Or	7.205	9.624	.381	.523	4.396	.700	.595	2.292	9.566	.928	1.098
Remarks	C	C,S	C,S	C	C,B,S	C,S	C	C	C,S	C,S	C

(Analyses of Plagioclase continued)

Sample	SG-9B				SG-9A1				
Specimen	D	B-1	I	B-2	J-1	A-1	E	A-2	B-3
SiO_2	65.37	68.29	65.47	60.91	60.03	61.75	60.06	61.42	57.69
TiO_2	.00	.03	.00	.00	.00	.00	.00	.07	.08
Al_2O_3	21.78	19.18	21.14	24.28	24.21	25.54	25.24	25.04	24.68
FeO	.09	.05	.72	.20	.39	.30	.30	.30	.34
MgO	.00	.00	.34	.06	.14	.00	.00	.00	.02
BaO	.00	.00	.00	.00	.06	.01	.09	.00	.10
CaO	2.53	.28	.75	6.06	5.69	6.74	6.84	7.05	7.64
Na_2O	9.12	10.29	9.68	8.18	7.80	7.82	7.70	7.83	6.73
K_2O	.29	.37	1.20	.47	.66	.60	.58	.45	.52
TOTAL	99.17	98.50	99.31	100.17	98.98	102.77	100.81	102.16	97.79
Si	2.888	3.017	2.903	2.711	2.705	2.683	2.666	2.688	2.646
Ti		.001						.002	.003
Al	1.135	.999	1.105	1.274	1.286	1.308	1.321	1.292	1.335
Fe	.003	.002	.027	.008	.015	.011	.011	.011	.013
Mg		.000	.022	.004	.010				.001
Ba				.008	.001	.000	.001		.002
Ca	.120	.013	.036	.289	.275	.314	.325	.331	.376
Na	.782	.882	.833	.706	.681	.659	.663	.665	.598
K	.017	.021	.068	.027	.038	.033	.033	.025	.030
An	13.031	1.444	3.829	28.284	27.636	31.176	31.859	32.412	37.404
Ab	85.165	96.262	88.930	69.103	68.545	65.517	64.917	65.142	59.580
Or	1.084	2.294	7.241	2.613	3.819	3.307	3.224	2.446	3.016
Remarks	C,S	P,C	P,C	P,C	P,C	P,F	P,F	P,C	P,F

(Analyses of Plagioclase continued)

Sample					SG-12A				
Specimen	B-2	D	B-2A	B-2B	C-2	C-1	D-1	A	B
SiO_2	68.79	68.37	68.68	68.56	68.52	68.21	67.81	67.96	68.71
TiO_2	.00	.05	.00	.04	.02	.04	.11	.01	.00
Al_2O_3	20.03	20.22	19.93	20.12	19.48	19.63	20.88	20.07	19.76
FeO	.12	.10	.09	.11	.16	.10	.36	.06	.06
MgO	.01	.01	.00	.00	.07	.02	.42	.00	.00
BaO	.04	.02	.04	.00	.16	.02	.11	.00	.00
CaO	.33	.66	.68	.72	.77	.64	.51	.69	.70
Na_2O	12.19	12.58	12.61	12.72	12.79	10.71	10.57	11.44	10.73
K_2O	.67	.21	.20	.21	.19	.25	.73	.29	.33
TOTAL	102.18	102.21	102.24	102.47	102.16	99.63	101.48	100.52	100.28
Si	2.963	2.946	2.957	2.948	2.961	2.990	2.936	2.963	2.991
Ti		.002		.001	.001	.001	.004	.000	
Al	1.017	1.027	1.012	1.020	.992	1.015	1.066	1.032	1.014
Fe	.004	.003	.003	.004	.006	.004	.013	.002	.002
Mg	.001	.001			.004	.001	.027		
Ba	.001	.000	.001		.003	.000	.002		
Ca	.015	.031	.031	.033	.036	.030	.024	.032	.032
Na	1.018	1.051	1.053	1.061	1.072	.911	.887	.967	.906
K	.037	.012	.011	.011	.011	.014	.040	.016	.018
An	1.408	2.801	2.869	2.998	3.188	3.143	2.497	3.162	3.391
Ab	95.136	96.123	96.111	95.986	95.872	95.367	93.262	95.248	94.723
Or	3.456	1.077	1.020	1.015	.939	1.490	4.241	1.590	1.887
Remarks	P,C	C,B	P,F	P,F	P,C,B	P,CB	C,B	P,C	P,C

TABLE 2B. Analyses of Alkali Feldspar From the San Gabriel Fault Zone

Sample		SG8-PGR			SG8-2		SG8A	SG7-PB		
Specimen	A	E[1,2]	F[1]	E	4	A	1[2]	3[1]	B	A-1
SiO_2	64.82	64.97	65.03	64.92	65.22	64.65	63.00	65.15	65.85	65.89
TiO_2	.00	.00	.00	.00	.02	.01	.00	.09	.00	.05
Al_2O_3	18.36	18.51	18.50	18.42	19.56	17.94	17.83	18.60	18.80	18.50
FeO	.00	.03	.03	.01	.05	.22	.07	.15	.07	.09
MgO	.00	.00	.00	.00	.00	.01	.00	.00	.02	.00
BaO	.79	.52	.72	.46	.71	.53	.33	.21	.01	.02
CaO	.00	.00	.01	.08	.29	.01	.00	.19	.00	.22
Na_2O	.87	1.26	1.29	.72	6.51	.10	.07	2.57	1.06	2.30
K_2O	15.27	14.54	14.86	15.83	6.53	16.56	15.71	13.74	15.60	13.93
TOTAL	100.11	99.83	100.46	100.44	98.89	100.03	97.00	100.68	101.40	101.00
					Formula Based on 8 Oxygens					
Si	2.997	2.997	2.993	2.994	2.962	3.005	3.003	2.981	2.993	2.996
Ti	.000	.000	.000	.000	.001	.000	.000	.003	.000	.002
Al	1.001	1.007	1.004	1.002	1.047	.983	1.002	1.003	1.007	.992
Fe	.000	.000	.001	.000	.002	.009	.003	.006	.002	.004
Mg	.000	.000	.000	.000	.000	.000	.000	.000	.001	.000
Ba	.014	.009	.013	.008	.012	.010	.006	.004	.0002	.0004
Ca	.000	.000	.001	.004	.014	.000	.000	.009	.000	.011
Na	.078	.112	.115	.065	.573	.009	.006	.227	.093	.203
K	.901	.856	.873	.931	.378	.982	.955	.802	.904	.808
Or	90.74	87.62	87.13	92.36	38.69	98.10	98.76	76.97	90.65	79.03
Ab	7.85	11.46	11.48	6.45	58.65	.90	.62	21.79	9.33	19.86
An	.00	.00	.10	.40	1.43	.00	.00	.86	.00	1.08
Cn	1.41	.92	1.30	.79	1.23	1.00	.62	.38	.02	.04
Remarks[3]	B,F	Ph	Ph	Ph	P	P,F	P	B	B,F	B

[1] Integrated analyses of perthetic grain
[2] Excess molecular SiO_2 between 2.0-5.0 percent
[3] B = Brecciated, Ph= phenocrysts, P= porphyroclast, F= fine grained, C= coarse grained

(Analyses of Alkali Feldspar continued)

Sample	SG7-PB		SG7		SG7-PGR	SG-6	
Specimen	A-2	B-1	C-1	1	C[1]	E	F[1]
SiO_2	64.64	65.33	64.54	65.09	64.30	65.06	63.69
TiO_2	.00	.01	.00	.00	0.06	0.02	.00
Al_2O_3	19.08	18.28	18.34	18.33	18.27	18.32	17.96
FeO	.08	.10	.11	.11	0.04	0.01	0.10
MgO	.00	.00	.00	.00	.00	.00	.00
BaO	1.24	.39	.20	.29	0.25	0.16	0.24
CaO	.16	.00	.51	.01	0.01	.00	.00
Na_2O	1.18	.82	1.63	2.03	0.81	0.95	0.98
K_2O	14.78	15.43	13.90	14.34	15.27	15.26	14.91
TOTAL	101.16	100.35	99.22	100.20	99.00	99.78	97.85
			Formula Based on 8 Oxygens				
Si	2.967	3.006	2.990	2.994	2.998	3.004	0.090
Ti	.000	.0002	.000	.000	0.002	0.001	.000
Al	1.032	.992	1.002	.994	1.004	0.997	0.998
Fe	.003	.004	.004	.004	0.002	.000	0.004
Mg	.000	.000	.000	.000	.000	.000	.000
Ba	.022	.007	.004	.005	0.005	0.003	0.004
Ca	.008	.000	.025	.001	0.001	.000	.000
Na	.105	.073	.146	.181	0.073	0.085	0.090
K	.865	.906	.822	.841	0.909	0.899	0.896
Or	86.50	91.89	82.45	81.81	92.00	91.08	90.51
Ab	10.50	7.40	14.64	17.61	7.39	8.61	9.09
An	.80	0.00	2.51	.10	.10	.00	.00
Cn	2.20	.71	.40	.49	.51	.30	.40
Remarks	B,F	P	P	P,C	C	C	C

(Analyses of Alkali Feldspar continued)

Sample	SG-6		SG-2		SG-9A1		
Specimen	G[1]	F-2	A[1]	B	H	C	A
SiO_2	64.16	64.28	63.38	63.66	64.44	65.01	65.62
TiO_2	.00	.00	.00	0.12	.00	.01	.01
Al_2O_3	18.04	17.95	18.84	18.74	18.16	18.29	19.46
FeO	0.03	.00	0.16	0.09	.22	.27	.21
MgO	.00	0.01	0.04	.00	.05	.01	.00
BaO	0.19	0.04	0.30	0.39	.46	.57	.83
CaO	0.01	0.03	0.32	.00	.03	.01	.01
Na_2O	1.63	1.70	2.83	0.27	.90	1.30	1.46
K_2O	14.29	14.02	11.86	16.04	14.93	14.23	14.27
TOTAL	98.35	98.03	97.74	99.31	99.17	99.69	101.87
Si	3.001	3.008	2.964	2.975	3.000	3.003	2.971
Ti	.000	.000	.000	0.004		.000	.000
Al	0.995	.990	1.039	1.033	.997	.996	1.039
Fe	0.001	.000	0.006	0.003	.008	.010	.008
Mg	.000	.001	0.003	.000	.004	.000	
Ba	0.003	0.001	0.006	0.007	.008	.010	.015
Ca	.000	0.001	0.016	.000	.001	.001	.000
Na	0.148	0.154	0.257	0.025	.081	.116	.128
K	0.853	0.837	0.708	0.957	.887	.839	.824
Or	84.96	84.29	71.63	96.76	90.79	86.85	85.21
Ab	14.74	15.51	26.04	2.53	8.29	12.01	13.24
An	.00	.10	1.62	.00	.10	.10	.00
Cn	.30	.10	.61	.71	.82	1.04	1.55
Remarks	C	C	P,F	P,F	P,C	P,F	P,C

(Analyses of Alkali Feldspar continued)

Sample	SG-9A1		SG-12A				SG-9C		
Specimen	D	G	B-1	D	I	B-2	D-2	F-1	H
SiO_2	64.95	64.93	65.14	65.73	67.980	67.68	64.99	68.60	66.031
TiO_2	.06	.01	.04	.00	.08	.00	.07	.00	.00
Al_2O_3	18.29	19.00	18.25	18.90	19.46	19.35	22.28	20.02	22.26
FeO	.05	.12	.09	.10	.88	.12	.14	.04	.20
MgO	.00	.00	.00	.08	.52	.00	.00	.00	.09
BaO	.46	1.03	.08	.14	.03	.03	.15	.00	.00
CaO	.06	.04	.45	.28	.18	.67	1.56	.35	.80
Na_2O	1.56	2.09	5.11	5.04	8.96	10.96	8.63	9.86	8.75
K_2O	14.30	13.08	9.70	9.42	2.30	1.97	1.96	2.12	2.65
TOTAL	99.72	100.31	98.86	99.69	100.39	100.78	99.79	100.99	100.78
Si	3.001	2.979	2.990	2.982	2.984	2.970	2.875	2.984	2.890
Ti	.002	.000	.001		.003		.002		
Al	.996	1.028	.988	1.011	1.007	1.001	1.162	1.027	1.149
Fe	.002	.004	.003	.004	.032	.005	.005	.001	.007
Mg				.005	.034				.006
Ba	.008	.019	.001	.003	.001	.000	.003		
Ca	.003	.002	.022	.014	.008	.032	.074	.016	.038
Na	.140	.186	.455	.444	.763	.932	.740	.832	.743
K	.843	.766	.568	.546	.129	.110	.111	.117	.148
Or	84.81	78.73	54.30	54.22	14.32	10.24	11.96	12.16	15.95
Ab	14.08	19.12	43.50	44.09	84.68	86.78	79.74	86.15	80.00
An	.30	.21	2.10	1.39	.89	2.98	7.97	1.69	4.05
Cn	.80	1.95	.10	.30	.11	.00	.32	.00	.00
Remarks	P,C	P,C	P,F	P,C,B	P,C,S	P,F	F,B	C,B	C,B

(Analyses of Alkali Feldspar continued)

Sample			SG-9B		
Specimen	E[1]	A[1]	D[1]	G[1]	G-2[1]
SiO_2	65.06	64.38	64.14	65.95	65.83
TiO_2	.00	.01	.04	.00	.06
Al_2O_3	18.36	18.29	18.51	18.70	19.11
FeO	.06	.04	.06	.08	.32
MgO	.02	.00	.00	.00	.00
BaO	.23	.00	.35	.14	.16
CaO	.00	.00	.00	.38	.12
Na_2O	.96	.93	.98	3.01	3.13
K_2O	15.91	15.29	15.81	13.34	12.89
TOTAL	100.61	98.939	99.89	101.59	101.62
Si	2.994	2.998	2.979	2.982	2.972
Ti		.000	.001		.002
Al	.996	1.004	1.014	.997	1.017
Fe	.002	.001	.002	.003	.012
Mg	.001				
Ba	.004		.006	.003	.003
Ca				.018	.006
Na	.086	.084	.089	.264	.274
K	.934	.909	.937	.769	.743
Or	91.21	91.50	90.79	72.96	72.42
Ab	8.40	8.50	8.62	25.05	26.71
An	.00	.00	.00	1.71	.58
Cn	.39	.00	.58	.28	.29
Remarks	C	C	C	C	C

TABLE 2C. Analyses of Muscovite From the San Gabriel Fault Zone

Sample	SG8-PGR		SG-6		SG-5		
Specimen	F	D	F	I	F-1	B-1	G-2
SiO_2	46.11	46.23	46.84	44.78	46.44	45.67	44.84
Al_2O_3	28.59	29.92	29.77	30.45	33.14	34.54	33.57
FeO[1]	5.65	5.11	4.75	5.52	2.67	2.56	2.58
MgO	1.85	1.54	1.57	1.37	1.17	.67	.74
MnO	.04	.03	.05	.04	.00	.00	.02
ZnO	.15	.00	.03	.00	.07	.04	.00
TiO_2	.55	.31	.26	.47	.29	.39	.19
CaO	.01	.00	.00	.00	.00	.00	.03
Na_2O	.16	.17	.15	.25	.52	.87	.70
K_2O	10.65	11.10	11.29	11.43	10.48	9.91	9.58
F	.21	.42	.25	.00	.24	.22	.08
Cl	.01	.01	.00	.01	.00	.01	.02
TOTAL	93.98	94.84	94.96	94.32	95.02	94.88	92.35
	Formula Based on 6 Oct. + Tet. Cations						
Si	3.149	3.140	3.175	3.062	3.104	3.050	3.063
Al^{IV}	.851	.860	.825	.938	.896	.950	.937
Al^{VI}	1.451	1.536	1.554	1.518	1.716	1.769	1.766
Fe	.323	.290	.269	.316	.149	.143	.147
Mg	.189	.156	.159	.140	.117	.066	.001
Mn	.002	.002	.003	.003	.000	.000	.001
Zn	.008	.000	.001	.000	.004	.002	.000
Ti	.028	.016	.013	.024	.015	.019	.010
Ca	.001	.000	.000	.000	.000	.000	.002
Na	.021	.022	.019	.033	.068	.112	.092
K	.928	.962	.976	.998	.893	.844	.835
F	.046	.090	.053	.000	.051	.045	.018
Cl	.001	.001	.000	.001	.000	.002	.002
Mg/Mg+Fe	.369	.349	.371	.307	.440	.317	.338
%Mu[2]	70.5	74.6	75.8	72.6	79.0	77.3	79.1
Pq	2.1	2.2	1.9	3.3	6.8	11.2	9.2
Cel	27.5	23.2	22.3	24.1	14.2	11.6	11.7
Remarks[3]	Ser.	Ser.	Ser.	Ser.	M,Fo	M,Fo	M,Fo

1 All Fe analysed as FeO
2 Mole percent muscovite, paragonite, and celadonite
3 Ser. = sericite inclusion in feldspar, M = matrix, Fo = foliated

(Analyses of Muscovite continued)

Sample	SG-5		SG2-PGR			SG-9B	
Specimen	H-2	H-1	A	B	C	J	J-2
SiO_2	46.48	45.00	45.46	44.31	45.60	46.88	46.34
Al_2O_3	34.00	33.98	32.50	31.67	32.71	31.30	29.67
FeO	2.81	2.69	3.16	4.57	3.60	4.38	5.68
MgO	.08	.73	.77	1.14	.90	1.51	1.83
MnO	.01	.00	.01	.00	.01	.05	.02
ZnO	.03	.09	.11	.16	.00	.00	.08
TiO_2	.18	.31	.16	.48	.24	.27	.08
CaO	.00	.00	.00	.00	.00	.00	.00
Na_2O	.82	.80	.36	.32	.31	.10	.06
K_2O	9.89	10.08	10.98	10.57	10.89	11.38	10.87
F	.16	.03	.14	.00	.04	.36	.53
Cl	.00	.02	.01	.01	.01	.01	.01
TOTAL	94.46	93.73	93.66	93.23	94.31	96.08	94.95
Formula Units per 6 Oct. + Tet. Cations							
Si	3.091	3.044	3.108	3.033	3.084	3.127	3.126
Al^{IV}	.909	.956	.967	.892	.016	.873	.874
Al^{VI}	1.757	1.75	1.589	1.728	1.693	1.589	1.486
Fe	.156	.152	.181	.262	.204	.244	.321
Mg	.076	.073	.078	.116	.090	.151	.184
Mn	.000	.000	.000	.000	.000	.003	.001
Zn	.002	.004	.005	.008	.000		.004
Ti	.009	.016	.008	.025	.012	.014	.004
Ca	.000	.000	.000	.000	.000		
Na	.106	.105	.048	.042	.040	.013	.008
K	.839	.870	.957	.923	.940	.968	.936
F	.034	.006	.031	.001	.008	.076	.114
Cl	.000	.003	.001	.001	.001	.001	.001
Mg/Mg+Fe	.328	.325	.307	.301	.307	.381	.365
%Mu	77.2	77.0	74.7	82.2	80.6	78.2	73.5
Pg	10.6	10.5	4.8	4.2	4.0	1.3	0.8
Cel	12.2	12.5	20.6	13.6	15.4	20.6	25.7
Remarks	M,Fo	M,Fo	Ser.	M	Ser.	Ser.	Ser

(Analyses of Muscovite continued)

Sample Specimen	SG-12A F
SiO_2	48.49
Al_2O_3	29.19
FeO^1	3.42
MgO	1.84
MnO	.02
ZnO	.03
TiO_2	.05
CaO	1.51
Na_2O	.05
K_2O	10.58
F	.44
Cl	.00
TOTAL	95.44
Si	3.284
Al^{IV}	.716
Al^{VI}	1.615
Fe	.194
Mg	.186
Mn	.001
Zn	.001
Ti	.003
Ca	.110
Na	.007
K	.914
F	.095
Cl	.000
Mg/Mg+Fe	.490
$\%Mu^2$	70.9
Pg	0.7
Cel	28.4
Remarks	Ser,C

TABLE 2D. Analyses of Biotite From the San Gabriel Fault Zone

Sample			SG8-PGN					SG8-PGR		
Specimen	A(1)	A(2)	B(1)	B(2)	I	E	F	F2	F3	X
SiO_2	35.71	35.35	34.51	35.09	35.31	35.79	35.97	36.00	35.93	35.53
Al_2O_3	16.66	16.50	16.07	16.06	16.72	16.21	15.97	16.32	15.89	15.98
FeO[1]	21.18	21.38	23.23	22.75	21.67	21.09	20.65	20.34	20.83	21.19
MgO	9.58	9.53	10.17	10.95	9.60	9.49	9.95	9.95	9.64	9.36
MnO	.29	.25	.27	.20	.33	.77	.71	.84	.73	.71
ZnO	.17	.03	.17	.00	.00	.01	.05	.03	.00	.00
TiO_2	2.06	2.15	1.83	1.82	1.91	3.13	3.44	2.89	3.27	3.04
CaO	.06	.78	.13	.08	.03	.04	.00	.06	.00	.02
Na_2O	.05	.29	.04	.06	.11	.09	.15	.09	.06	.06
K	8.68	9.71	7.82	7.50	9.43	9.40	9.70	9.20	9.83	9.54
F	.18	.00	.00	.18	.10	.17	.75	.74	.63	.36
Cl	.07	.08	.07	.08	.10	.02	.01	.01	.01	.02
TOTAL	94.69	96.05	94.31	94.77	95.31	96.21	97.35	96.47	96.82	95.81
					Formula Based on 7 Octahedral + Tetbahedral Cations					
Si	2.800	2.788	2.690	2.701	2.772	2.793	2.794	2.800	2.809	2.797
Al^{iv}	1.200	1.212	1.310	1.299	1.228	1.207	1.206	1.200	1.191	1.203
Al^{vi}	.340	.322	.168	.159	.319	.284	.256	.296	.273	.279
Fe	1.389	1.411	1.515	1.465	1.423	1.376	1.341	1.324	1.362	1.395
Mg	1.120	1.121	1.183	1.257	1.124	1.104	1.152	1.154	1.124	1.098
Mn	.019	.017	.018	.013	.022	.051	.047	.055	.049	.047
Zn	.010	.002	.010	.000	.000	.001	.003	.002	.000	.000
Ti	.122	.127	.107	.106	.113	.184	.201	.169	.192	.180
Ca	.005	.066	.010	.007	.002	.003	.000	.005	.000	.002
Na	.007	.044	.005	.009	.016	.013	.022	.013	.009	.009
K	.869	.977	.778	.736	.944	.936	.962	.913	.980	.958
F	.044	.000	.000	.043	.025	.041	.185	.182	.154	.091
Cl	.010	.011	.009	.010	.013	.002	.002	.001	.001	.003
Mg/Mg+Fe	.446	.443	.438	.462	.441	.445	.462	.466	.452	.441
Charge	22.27	22.518	21.88	21.830	22.281	22.399	22.435	22.370	22.456	22.407
Remarks[2]	F	F	F	F	F	C	C	Ch	I	C

[1] All Fe as FeO

[2] F=fine grained, C= coarse grained, Ch= in contact with chlorite,
I=inclusion in another mineral, D= deformed, M= matrix, Int= interstitial magmatic

(Analyses of Biotite continued)

Sample	SG8-PGR							SG8-2	
Specimen	Y	A1*	A2*	B1*	B2*	B3*	X*	3-2	3-3
SiO_2	35.71	35.06	35.28	35.00	35.63	33.97	34.98	36.21	35.03
Al_2O_3	15.86	16.00	16.33	15.96	15.97	16.08	16.42	16.84	16.32
FeO	20.52	21.67	20.55	20.74	20.71	21.36	21.71	21.24	21.01
MgO	9.53	9.86	9.46	10.17	10.52	10.00	10.07	9.26	8.76
MnO	.69	.73	.73	.72	.71	.73	.66	.30	.25
ZnO	.03	.05	.08	.17	.07	.00	.08	.00	.00
TiO_2	3.19	2.70	2.74	2.48	2.51	2.75	2.82	2.35	2.43
CaO	.02	.07	.11	.30	.12	.10	.20	.13	.16
Na_2O	.09	.09	.08	.05	.04	.03	.13	.17	.10
K	9.39	9.15	8.91	7.82	9.12	8.46	8.04	9.64	9.56
F	.54	.69	.56	.74	.35	.47	.40	.12	.11
Cl	.02	.02	.02	.01	.01	.00	.02	.07	.07
TOTAL	95.59	96.09	94.85	94.16	95.76	93.95	95.40	96.29	93.80

Formula Based on 7 Octahedral + Tetrahedral Cations

	Y	A1*	A2*	B1*	B2*	B3*	X*	3-2	3-3
Si	2.816	2.744	2.788	2.755	2.771	2.690	2.713	2.828	2.820
Al^{iv}	1.184	1.256	1.212	1.245	1.229	1.310	1.287	1.172	1.180
Al^{vi}	.290	.221	.310	.236	.236	.192	.214	.378	.369
Fe	1.353	1.419	1.359	1.366	1.347	1.415	1.409	1.385	1.415
Mg	1.120	1.150	1.115	1.194	1.220	1.180	1.164	1.079	1.052
Mn	.046	.049	.049	.048	.047	.049	.044	.020	.017
Zn	.002	.003	.005	.010	.004	.000	.004	.000	.000
Ti	.189	.159	.163	.147	.147	.164	.164	.138	.147
Ca	.002	.006	.009	.025	.010	.008	.017	.011	.014
Na	.013	.013	.013	.007	.007	.004	.019	.026	.015
K	.945	.913	.899	.785	.905	.855	.795	.961	.982
F	.136	.169	.144	.184	.085	.118	.099	.029	.028
Cl	.002	.002	.003	.002	.002	.000	.002	.009	.009
Mg/Mg+Fe	.453	.448	.451	.466	.475	.455	.452	.438	.426
Charge	22.445	22.221	22.354	22.126	22.232	22.085	22.104	22.492	22.507
Remarks	C	C,D	C,D	F,D	F,D	F,D	C,D	M	M

* = Sheared Biotite

(Analyses of Biotite continued)

Sample	SG7-PGR					SG-6
Specimen	K	K-2	D	B	A-1	B
SiO_2	36.19	37.01	36.11	35.81	36.94	34.32
Al_2O_3	15.93	16.07	15.85	16.36	15.86	16.85
FeO	19.78	19.50	20.41	19.72	20.03	23.40
MgO	10.92	10.49	10.36	10.87	10.80	9.86
MnO	.27	.27	.32	.30	.26	.73
ZnO	.15	.04	.03	.27	.00	.00
TiO_2	3.15	3.35	2.92	2.74	3.19	2.04
CaO	.08	.26	.18	.17	.25	.09
Na_2O	.04	.05	.05	.06	.05	.06
K	9.09	8.91	8.28	8.47	7.18	7.77
F	.63	.52	1.07	.65	.52	.59
Cl	.03	.03	.03	.03	.03	.01
TOTAL	96.28	96.50	95.61	95.45	95.11	95.72
	Formula units per 7 Octahedral + Tetrahedral Cations					
Si	2.799	2.857	2.815	2.775	2.838	2.651
Al^{IV}	1.201	1.143	1.185	1.225	1.162	1.349
Al^{VI}	.251	.319	.271	.270	.274	.186
Fe	1.280	1.259	1.331	1.279	1.287	1.512
Mg	1.259	1.207	1.204	1.257	1.237	1.136
Mn	.002	.018	.021	.020	.017	.048
Zn	.009	.002	.002	.015	.000	.000
Ti	.183	.194	.171	.160	.184	.119
Ca	.006	.022	.015	.014	.020	.007
Na	.006	.007	.008	.010	.007	.009
K	.896	.878	.823	.838	.703	.766
F	.155	.127	.264	.159	.126	.144
Cl	.004	.004	.004	.004	.003	.001
Mg/Mg+Fe	.496	.489	.475	.496	.490	.429
Charge	22.331	22.493	22.289	22.240	22.23	21.863
Remarks	C, Int	F	C,D	C,D	D	C

TABLE 2E. Analyses of Chloritized Biotite From the San Gabriel Fault Zone

Sample	SG7-Pb			SG8-PGN			SG8-2			
Specimen	S-2	S-1	C	A	B-1	B-2	A-1	A-2	A-3	2-1
SiO_2	32.60	32.30	30.82	33.58	34.85	34.77	36.93	35.91	36.69	36.49
Al_2O_3	18.01	18.45	15.39	16.15	16.38	16.98	14.90	15.94	14.40	15.51
FeO[1]	25.50	26.08	23.31	22.94	21.58	22.25	16.45	17.39	15.49	15.58
MgO	8.02	8.98	13.22	12.74	11.08	11.74	14.55	14.32	14.50	13.62
MnO	.34	.23	.39	.42	.30	.30	.29	.22	.20	.23
ZnO	.03	.00	.05	.00	.10	.00	.00	.02	.04	.01
TiO_2	3.20	2.17	2.79	.06	.39	.11	1.62	1.56	1.44	1.37
CaO	.18	.16	.73	.12	.46	.18	.30	.70	.77	.27
Na_2O	.07	.11	.04	.07	.04	.26	.08	.06	.07	.10
K_2O	5.66	4.79	1.95	5.91	7.82	7.11	7.89	6.58	7.12	7.85
F	.15	.17	.28	.29	.16	.00	.76	.25	1.05	.41
Cl	.03	.08	.11	.06	.05	.08	.04	.05	.04	.06
TOTAL	93.79	93.52	89.08	92.34	93.21	93.78	93.81	93.00	91.77	91.51
Formula Based on 7 Total Oct. + Tet. Cations										
Si	2.540	2.482	2.380	2.577	2.730	2.667	2.828	2.733	2.869	2.859
Al^{iv}	1.460	1.518	1.402	1.423	1.270	1.333	1.172	1.267	1.131	1.141
Al^{vi}	.195	.154	.000	.038	.243	.203	.173	.163	.196	.291
Fe	1.662	1.677	1.506	1.473	1.414	1.428	1.054	1.107	1.013	1.021
Mg	.932	1.029	1.523	1.458	1.294	1.343	1.661	1.625	1.690	1.591
Mn	.022	.015	.025	.028	.020	.019	.019	.014	.013	.015
Zn	.002	.000	.003	.000	.006	.000	.000	.001	.002	.001
Ti	.187	.126	.162	.003	.023	.006	.093	.089	.085	.081
Ca	.015	.014	.060	.010	.038	.015	.025	.057	.064	.022
Na	.011	.016	.007	.010	.006	.039	.012	.008	.011	.015
K	.562	.470	.192	.578	.781	.696	.771	.639	.710	.785
F	.036	.041	.069	.070	.040	.000	.183	.061	.260	.101
Cl	.004	.011	.014	.007	.006	.010	.005	.006	.005	.008
Mg/Mg+Fe	.359	.380	.503	.497	.478	.485	.612	.595	.625	.609
Total Charge	21.711	21.400	20.805	21.231	21.883	21.648	22.020	21.837	22.085	22.46
Remarks[2]	D	D	D	F	F	F	M	I	M	M

[1] All Fe analysed as FeO

[2] D= deformed, F= fine grained, Fo=foliated, M= matrix
I= interstital, C= coarse grained.

(Analyses of Chloritized Biotite continued)

Sample	SG8-2		SG7-PGR		SG2-PGR	SG-5
Specimen			C	E	G	H
SiO_2	38.22	34.37	34.70	34.91	30.42	30.66
Al_2O_3	14.74	16.82	16.59	15.65	18.52	26.99
FeO	14.46	23.12	20.46	18.60	23.33	17.55
MgO	12.80	8.37	10.80	10.63	10.82	13.87
MnO	.23	.11	.33	.38	.32	.37
ZnO	.00	.00	.08	.13	.00	.00
TiO	1.31	2.61	3.09	2.92	1.15	.12
CaO	.94	.14	.57	.62	.62	.01
Na_2O	.18	.08	.05	.04	.04	.15
K_2O	7.56	7.62	6.54	6.49	2.48	2.52
F	.59	.44	.69	1.14	.02	.08
Cl	.05	.06	.03	.03	.03	.00
TOTAL	91.08	93.74	93.93	91.54	87.75	92.32
Formula Based on 7 Total Oct. + Tet. Cations						
Si	3.042	2.732	2.695	2.796	2.391	2.184
Al^{iv}	.958	1.268	1.305	1.204	1.609	1.816
Al^{vi}	.425	.308	.214	.274	.108	.451
Fe	.963	1.537	1.329	1.246	1.534	1.046
Mg	1.518	.992	1.250	1.270	1.268	1.474
Mn	015	.007	.021	.026	.022	.022
Zn	.000	.000	.004	.008	.000	.000
Ti	.078	.156	.180	.176	.068	.007
Ca	.080	.012	.047	.053	.052	.001
Na	.028	.012	.007	.006	.007	.021
K	.767	.773	.648	.663	.249	.229
F	.148	.111	.170	.290	.005	.017
Cl	.006	.008	.004	.004	.004	.000
Mg/Mg+Fe	.612	.392	.485	.505	.452	.585
Total Charge	22.579	22.160	22.019	22.198	20.996	20.900
Remarks	M	M	C	D	D	F,Fo

(Analyses of Chloritized Biotite continued)

Sample			SG-9C					SG-9A1		
Specimen	F-1	C	F-2	F-3	H	H	A	F-1	F	D
SiO_2	31.65	32.06	30.81	29.37	30.74	34.51	35.71	33.94	36.68	39.03
Al_2O_3	15.34	15.22	16.45	14.50	16.04	22.30	17.54	16.74	18.13	18.59
FeO^1	22.33	22.13	21.86	21.74	24.64	19.19	19.03	17.60	17.57	17.49
MgO	13.06	12.68	13.99	11.56	13.78	8.93	6.31	8.36	10.15	7.79
MnO	.33	.37	.42	.59	.48	.22	.24	.17	.26	.12
ZnO	.00	.01	.11	.10	.13	.11	.01	.00	.06	.15
TiO_2	3.67	3.46	2.53	4.60	2.12	.45	1.14	3.18	1.63	2.31
CaO	.51	1.07	1.12	3.17	.10	.25	.32	.23	.21	1.32
Na_2O	.04	.00	.03	.01	.04	.10	.17	.17	.11	.11
K_2O	3.31	2.01	1.33	.66	2.49	1.92	3.93	4.20	2.98	5.73
F	.00	.29	.35	.00	.00	.16	.09	.19	.15	.34
Cl	.05	.04	.08	.04	.03	.03	.03	.02	.02	.05
TOTAL	90.29	89.21	88.90	86.32	90.58	88.08	84.47	84.72	87.88	92.86
Si_{IV}	2.436	2.484	2.352	2.392	2.316	2.661	2.588	2.849	2.872	3.065
Al_{IV}	1.392	1.390	1.481	1.393	1.425	1.339	1.412	1.151	1.128	.935
Al_{VI}	.00	.00	.000	.000	.00	.689	.087	.505	.547	.786
Fe	1.438	1.434	1.396	1.482	1.553	1.238	1.154	1.236	1.151	1.149
Mg	1.499	1.464	1.593	1.404	1.548	1.026	.682	1.046	1.185	.912
Mn	.022	.024	.027	.040	.030	.014	.014	.012	.017	.008
Zn		.001	.006	.006	.007	.006	.001		.004	.008
Ti	.213	.202	.145	.282	.120	.026	.062		.096	.136
Ca	.042	.089	.092	.276	.008	.021	.025	.201	.018	.111
Na	.006		.005	.002	.240	.014	.023	.028	.017	.017
K	.325	.199	.130	.069		.189	.363	.450	.298	.574
F	.001	.071	.084			.038	.022	.051	.036	.085
Cl	.007	.006	.011	.005	.033	.003	.003	.003	.003	.006
Mg/Mg+Fe	.510	.505	.533	.487	.499	.453	.371	.458	.507	.443
Total Charge	21.105	21.139	20.793	21.366	20.560	21.647	19.237	22.274	21.961	22.937
Remarks	F,D	F,D	F,D	F,D	I	M	M	M	M	M

(Analyses of Chloritized Biotite continued)

Sample		SG-9A1	
Specimen	G	E-2	C
SiO_2	37.42	39.27	44.78
Al_2O_3	19.22	17.47	20.62
FeO[1]	16.40	13.06	10.48
MgO	6.27	7.26	3.65
MnO	.15	.08	.08
ZnO	.10	.08	.00
TiO_2	2.06	2.03	1.32
CaO	.41	.10	.85
Na_2O	.46	.12	.61
K_2O	5.13	7.68	5.50
F	.13	.42	.02
Cl	.04	.11	.03
TOTAL	87.71	87.47	87.92
Si	3.086	3.301	3.185
Al^{IV}	.914	.699	.815
Al^{VI}	.954	1.032	.914
Fe	1.131	.918	.623
Mg	.770	.910	.387
Mn	.010	.006	.005
Zn	.006	.005	
Ti	.128	.128	.071
Ca	.036	.009	.065
Na	.073	.019	.084
K	.540	.824	.499
F	.034	.113	.004
Cl	.006	.015	.004
Mg/Mg+Fe	.405	.498	.383
Total Charge	22.980	23.451	20.954
Remarks	M	M	M

TABLE 2F. Analyses of Chlorite From the San Gabriel Fault Zone

Sample	SG7-Pb		SG8-PGN	SG8-PGR	
Specimen	1	A	F	A	F
SiO_2	28.06	27.50	27.09	26.18	25.50
Al_2O_3	18.14	19.70	18.10	19.93	20.25
Cr_2O_3	.00	.00	.01	.02	.03
FeO[1]	23.20	27.75	28.22	26.04	25.92
MgO	15.46	13.43	12.61	15.30	15.41
MnO	.83	.48	.31	1.15	1.36
ZnO	.04	.00	.13	.11	.07
TiO	.01	.11	.11	.06	.05
CaO	.52	.38	.24	.04	.03
Na_2O	.00	.00	.00	.00	.00
F	.09	.00	.00	.00	.00
Cl	.04	.02	.00	.00	.00
TOTAL	86.39	89.37	86.81	88.84	88.61
			Formula Based on 10 Cations		
Si	3.028	2.911	2.967	2.744	2.675
Al^{iv}	.972	1.089	1.033	1.256	1.325
Al^{vi}	1.337	1.371	1.305	1.208	1.180
Cr	.000	.000	.001	.002	.002
Fe	2.094	2.458	2.586	2.283	2.276
Mg	2.488	2.120	2.060	2.392	2.412
Mn	.076	.043	.029	.102	.121
Zn	.003	.000	.010	.009	.006
Ti	.001	.009	.009	.005	.004
Ca	.060	.043	.028	.004	.003
Na	.000	.000	.000	.000	.000
F	.030	.000	.000	.000	.000
Cl	.007	.003	.000	.000	.000
Mg/Mg+Fe	.543	.463	.443	.512	.515
Total Charge	28.487	28.386	28.347	27.972	27.872
Remarks[2]	F	F	F	D	F

[1] All Fe analysed as FeO

[2] D = deformed, I= inclusion, F= fine grained, C= coarse grained, M= matrix
P = porphyroclast, Bn= brown, Gn= green, R= rim on biotite

(Analyses of Chlorite continued)

Sample	SG7-PGR	SG-6				
Specimen	J	B	F	H	I	J
SiO_2	27.61	27.11	27.97	27.36	27.37	29.14
Al_2O_3	19.49	17.04	17.32	16.08	17.46	16.86
Cr_2O_3	.08	.04	.00	.02	.00	.01
FeO	23.09	27.65	26.14	27.77	27.10	27.96
MgO	15.14	13.09	13.51	12.26	12.43	12.74
MnO	.58	.83	.85	1.00	.77	.84
ZnO	.02	.37	.14	.06	.23	.21
TiO_2	.06	.14	.09	.28	.47	.57
CaO	.26	.26	.30	.53	.34	.27
Na_2O	.01	.00	.00	.01	.05	.00
F	.00	.17	.17	.03	.20	.17
Cl	.02	.00	.00	.01	.01	.03
TOTAL	86.36	86.63	86.41	85.38	86.34	88.71
		Formula Based on 10 total Cations				
Si	2.966	2.980	3.064	3.076	3.029	3.143
Al^{IV}	1.034	1.020	.936	.924	.971	.857
Al^{VI}	1.435	1.189	1.301	1.208	1.308	1.287
Cr	.007	.003	.000	.002	.000	.001
Fe	2.074	2.543	2.395	2.612	2.510	2.523
Mg	2.425	2.146	2.206	2.054	2.052	2.049
Mn	.053	.077	.078	.096	.072	.076
Zn	.002	.030	.011	.005	.018	.017
Ti	.002	.012	.007	.024	.039	.005
Ca	.030	.030	.035	.063	.041	.031
Na	.003	.000	.000	.001	.011	.000
F	.000	.058	.058	.011	.068	.057
Cl	.003	.001	.000	.001	.000	.005
Mg/Mg+Fe	.539	.458	.479	.44	.450	.448
Total Charge	28.479	28.255	28.450	28.461	28.508	28.586
Remarks	Gn,F	R	Bn	Bn	D,Bn	D,Bn

(Analyses of Chlorite continued)

Sample	SG-5				SG-2				
Specimen	C	H-2	H-1	B	D	C	A4	A2	A1
SiO_2	25.17	24.88	24.97	24.82	25.89	25.60	26.03	25.99	25.61
Al_2O_3	22.85	22.73	23.31	23.84	19.90	19.37	20.06	18.97	18.98
Cr_2O_3	.00	.00	.03	.01	.00	.05	.06	.04	.01
FeO	20.58	21.52	21.03	20.56	26.86	26.05	27.94	27.59	27.28
MgO	18.54	18.01	18.45	18.20	14.83	15.05	14.73	14.39	14.52
MnO	.46	.43	.48	.52	.40	.39	.31	.44	.37
ZnO	.04	.01	.06	.12	.00	.07	.15	.00	.02
TiO	.07	.10	.13	.06	.04	.04	.09	.60	.03
CaO	.02	.04	.02	.00	.02	.04	.06	.58	.03
Na_2O	.00	.02	.00	.03	.00	.04	.00	.01	.00
F	.00	.12	.00	.00	.22	.00	.22	.13	.31
Cl	.01	.04	.02	.01	.02	.01	.01	.02	.01
TOTAL	87.73	87.84	88.49	88.17	88.18	86.72	89.57	88.68	87.03

Formula Based on 10 total Cations

Si	2.584	2.565	2.545	2.537	2.753	2.749	2.726	2.772	2.759
Al^{IV}	1.416	1.435	1.455	1.463	1.247	1.251	1.274	1.228	1.241
Al^{VI}	1.348	1.329	1.345	1.409	1.238	1.202	1.202	1.159	1.170
Cr	.000	.000	.003	.001	.000	.004	.005	.003	.001
Fe	1.767	1.856	1.793	1.758	2.381	2.340	2.447	2.462	2.459
Mg	2.836	2.769	2.803	2.773	2.342	2.410	2.300	2.289	2.333
Mn	.040	.038	.041	.045	.036	.035	.027	.040	.034
Zn	.003	.001	.004	.009	.000	.006	.011	.000	.001
Ti	.006	.007	.010	.005	.003	.003	.007	.048	.002
Ca	.002	.005	.002	.000	.003	.005	.007	.066	.004
Na	.000	.004	.000	.006	.000	.009	.000	.002	.000
F	.001	.040	.000	.000	.073	.001	.071	.043	.106
Cl	.002	.007	.004	.001	.003	.002	.002	.003	.001
Mg/Mg+Fe	.616	.599	.610	.612	.496	.507	.485	.482	.487
Total Charge	27.947	27.922	27.918	27.962	28.002	27.980	27.960	28.165	27.942
Remarks	F,I	F,Fo	F,Fo	F,Fo	M	M	P,F	P,F	P,F

(Analyses of Chlorite continued)

Sample	SG2-PGR						SG-9C
Specimen	D	G-2	F-3	A	F-1	1	G
SiO_2	22.16	22.97	24.54	24.09	23.97	23.89	30.79
Al_2O_3	22.34	21.75	21.32	21.75	21.70	21.59	15.73
Cr_2O_3	.00	.05	.00	.09	.04	.00	.00
FeO	40.54	40.23	32.33	32.52	33.96	34.57	23.78
MgO	4.17	5.26	11.19	10.35	9.18	8.34	14.62
MnO	.25	.13	.28	.24	.13	.18	.40
ZnO	.20	.09	.09	.00	.00	.00	.04
TiO	.08	.07	.04	.08	.06	.06	3.02
CaO	.00	.02	.00	.00	.02	.01	1.71
Na_2O	.02	.00	.00	.00	.01	.00	.00
F	.00	.00	.09	.00	.00	.00	.12
Cl	.01	.01	.00	.01	.01	.02	.04
TOTAL	89.76	90.57	89.84	89.12	89.07	88.66	90.19
			Formula Based on 10 total Cations				
Si	2.488	2.541	2.618	2.599	2.610	2.628	3.287
Al^{IV}	1.512	1.459	1.382	1.401	1.390	1.372	.713
Al^{VI}	1.446	1.379	1.299	1.366	1.396	1.429	1.267
Cr	.000	.004	.000	.008	.003	.000	
Fe	3.809	3.723	2.885	2.934	3.093	3.182	2.124
Mg	.070	.868	1.780	1.664	1.491	1.367	2.327
Mn	.023	.012	.025	.022	.012	.017	.036
Zn	.016	.007	.007	.000	.000	.000	.003
Ti	.007	.006	.003	.006	.005	.005	.242
Ca	.000	.002	.000	.000	.003	.002	.195
Na	.004	.000	.000	.000	.002	.000	
F	.000	.000	.031	.000	.000	.000	.039
Cl	.002	.001	.001	.002	.001	.003	.008
Mg/Mg+Fe	.155	.189	.382	.362	.325	.301	.523
Total Charge	21.951	27.941	27.923	27.985	28.026	28.071	29.430
Remarks	C	D	C	C	C	C	F

(Analyses of Chlorite continued)

Sample	SG-9B		SG-12A	
Specimen	C	F	B	A
SiO_2	26.85	28.39	29.37	30.53
Al_2O_3	19.05	17.72	18.52	18.29
Cr_2O_3	.00	.00	.03	.00
FeO	25.52	30.97	18.68	16.77
MgO	16.02	10.88	18.41	19.45
MnO	.44	.32	.25	.29
ZnO	.00	.00	.07	.07
TiO	.03	.04	1.19	.03
CaO	.14	.32	1.35	.61
Na_2O	.00	.00	.00	.24
F	.06	.11	.00	.00
Cl	.02	.00	.01	.02
TOTAL	88.09	88.71	87.87	86.29
Si	2.828	3.095	3.077	3.199
Al^{IV}	1.172	.905	.923	.801
Al^{VI}	1.194	1.374	1.364	1.459
Cr		.000	.002	
Fe	2.248	2.824	1.637	1.470
Mg	2.516	1.769	2.875	3.038
Mn	.039	.029	.022	.026
Zn			.005	.006
Ti	.002	.003	.094	.002
Ca	.016	.037	.151	.068
Na				.049
F	.019	.037		.001
Cl	.004		.002	.003
Mg/Mg+Fe	.528	.385	.637	.674
Total Charge	28.059	28.550	28.933	28.849
Remarks	C	F	M	M

TABLE 2G. Analyses of Amphibole From the San Gabriel Fault Zone

	SG8-A		SG8-2		SG-2PGR
	1	2	1	A	G
SiO_2	60.67	56.52	53.70	59.80	42.52
Al_2O_3	2.11	3.31	2.61	2.40	13.36
Cr_2O_3	.00	.00	.00	.14	.00
FeO[1]	12.74	13.32	15.20	10.11	19.61
MgO	9.83	11.29	13.42	13.94	8.38
MnO	.31	.25	.49	.21	.70
TiO	.30	.22	.15	.31	.35
CeO	10.01	12.27	11.66	11.05	11.74
Na_2O	.17	.13	.32	.25	1.18
K_2O	.05	.06	.05	.14	.74
F	.001	.00	.12	.27	.23
Cl	.01	.004	.02	.01	.10
TOTAL	96.20	97.38	97.72	98.63	98.91
		Formula Based on 15 Oct. + Tet. Cations			
Si	9.130	8.318	7.857	8.606	6.340
Al^{iv}	.000	.000	.143	.000	1.660
Al^{vi}	.375	.575	.307	.406	.688
Cr	.000	.000	.000	.016	.000
Fe	1.604	1.604	1.860	1.217	2.446
Mg	2.205	2.477	2.928	2.991	1.863
Mn	.039	.032	.060	.025	.089
Ti	.034	.024	.016	.033	.039
Ca	1.614	1.934	1.828	1.704	1.875
Na	.050	.038	.090	.069	.341
K	.009	.011	.010	.025	.141
F	.001	.000	.058	.123	.107
Cl	.002	.001	.005	.003	.025
Mg/Mg+Fe	.579	.602	.612	.711	.432
Charge	48.762	47.309	46.296	47.797	45.588
Remarks[2]	ACT,D	ACT,D	ACT,P	ACT,P	HBLD,D

[1] All Fe analysed as FeO
[2] ACT= actinolite, HBLD= hornblende, D= deformed, P= porphyroclast

(Analyses of Amphibole continued)

Sample			SG-9C		
Specimen	F	H	K	F	F
SiO_2	43.00	43.73	42.48	42.94	42.89
Al_2O_3	10.89	10.82	10.57	11.03	10.89
Cr_2O_3	.02	.03	.00	.00	.00
FeO[1]	17.95	17.79	17.58	18.06	18.02
MgO	10.25	10.47	9.91	10.21	10.26
MnO	.53	.59	.56	.57	.56
TiO	1.70	1.84	1.77	1.78	1.84
CaO	11.91	11.90	10.71	11.89	11.97
Na_2O	1.39	1.55	1.22	1.46	1.41
K_2O	1.53	1.36	1.25	1.44	1.48
F	.12	.07	.11	.16	.09
Cl	.07	.08	.08	.09	.07
TOTAL	99.28	100.17	96.16	99.54	99.42
Si	6.409	6.454	6.522	6.387	6.384
Al^{IV}	1.591	1.546	1.478	1.613	1.616
Al^{VI}	.323	.337	.435	.322	.295
Cr	.003	.003			
Fe	2.238	2.196	2.258	2.247	2.244
Mg	2.277	2.303	2.268	2.265	2.276
Mn	.067	.073	.073	.072	.070
Ti	.190	.204	.205	.199	.206
Ca	1.902	1.883	1.762	1.895	1.909
Na	.401	.445	.362	.420	.407
K	.054	.032	.053	.075	.044
F	.017	.019	.020	.023	.017
Cl					
Mg/Mg+Fe	.504	.512	.501	.502	.504
Charge	45.806	45.903	45.973	45.798	45.780
Remarks	HBLD,D	HBLD,D	HBLD,D	HBLD,D	HBLD,D

TABLE 2H. Analyses of Epidote From the San Gabriel Fault Zone

Sample		SG8-PGN		SG8-PGR	SG8-2		SG-7	SG7Pb
Specimen	F	B-1	B-2	E	C	1	1	A
SiO_2	36.48	37.66	38.23	36.99	38.70	37.21	37.02	37.32
Al_2O_3	22.91	22.98	22.89	22.61	23.98	23.95	23.60	23.96
Ce_2O_3	.05	.00	.05	.00	.05	.00	.00	.07
Y_2O_3	.00	.00	.00	.00	.00	.00	.00	.00
La_2O_3	.00	.00	.00	.00	.00	.00	.00	.00
Nd_2O_3	.00	.00	.00	.00	.00	.00	.00	.00
FeO[1]	12.19	11.82	12.81	11.24	10.39	12.59	11.86	11.85
MgO	.01	.00	.03	.03	.34	.00	.39	.00
MnO	.14	.18	.30	.46	.21	.11	.43	.27
TiO_2	.23	.01	.12	.19	.08	.03	.18	.08
CaO	22.89	22.96	23.28	22.50	22.08	23.72	22.50	23.40
F	.00	.00	.00	.00	.03	.002	.18	.06
TOTAL	94.90	95.61	97.71	94.02	95.86	97.61	96.00	97.01
				Formula Units Per 8 Cations				
Si	2.962	3.031	3.019	3.028	3.094	2.922	2.964	2.960
Al^{iv}	.038	.000	.000	.000	.000	.067	.036	.040
Al^{vi}	2.155	2.181	2.132	2.182	2.260	2.159	2.191	2.201
Ce	.001	.000	.000	.000	.001	.000	.000	.002
Y	.000	.000	.000	.000	.000	.000	.000	.000
La	.000	.000	.000	.000	.000	.000	.000	.000
Nd	.000	.000	.000	.000	.000	.000	.000	.000
Fe	.827	.796	.847	.769	.695	.830	.794	.786
Mg	.001	.000	.003	.003	.040	.000	.047	.000
Mn	.010	.012	.020	.032	.014	.007	.029	.018
Ti	.014	.001	.007	.012	.005	.001	.011	.005
Ca	1.991	1.979	1.970	1.973	1.891	2.003	1.929	1.989
F	.000	.000	.000	.000	.008	.0004	.047	.014
Remarks[2]	C	F	F		M	P	P	B

[1] All Fe analysed as FeO
[2] C= coarse grained, F= fine grained, M= matrix, P= porphyroclast, A= allanite,
V= vein, Th= thorium rich (E.D.S. scan)

(Analyses of Epidote continued)

Sample	SG-5	SG-2				SG-9C
Specimen	D	D	F	B	A	D
SiO_2	31.68	30.24	38.24	37.45	37.21	33.62
Al_2O_3	18.61	15.36	25.14	22.61	22.11	17.06
Ce_2O_3	.17	6.55	.06	.00	.06	8.67
Y_2O_3	.22	.44	.00	.00	.00	.03
La_2O_3	4.19	3.64	.00	.00	.00	5.52
Nd_2O_3	4.01	2.84	.00	.00	.00	2.44
FeO	12.34	10.38	10.99	13.34	13.96	13.05
MgO	.29	.62	.04	.12	.30	1.45
MnO	.67	.42	.69	.07	.10	.39
TiO_2	.00	.22	.10	.26	.17	.59
CaO	11.82	11.85	22.48	22.87	22.62	14.35
F	.13	.41	.00	.15	.00	.00
TOTAL	92.13	83.61	97.74	96.87	96.53	96.87
Formula units per 8 Cations						
Si	3.028	3.216	3.002	2.990	2.981	3.036
Al^{IV}						1.816
Al^{VI}						
Ce	.286	.250	.002	.000	.002	.286
Y	.011	.024	.000	.000	.000	.001
La	.148	.140	.000	.000	.000	.184
Nd	.137	.105	.000	.000	.000	.079
Fe	.987	.905	.722	.891	.935	.986
Mg	.041	.096	.004	.013	.036	.154
Mn	.054	.037	.046	.005	.007	.030
Ti	.000	.017	.006	.015	.010	.040
Ca	1.211	1.323	1.891	1.957	1.941	1.388
F	.039	.134	.000	.037	.000	
Remarks	P,A	P,A,Th	V	P	P	A,F

(Analyses of Epidote continued)

Sample	SG-9A1	
Specimen	D	J
SiO_2	30.93	33.02
Al_2O_3	15.36	17.82
Ce_2O_3	10.08	7.95
Y_2O_3	.34	.17
La_2O_3	5.59	3.94
Nd_2O_3	3.22	3.39
FeO	12.95	12.34
MgO	1.00	1.12
MnO	.98	.10
TiO_2	.37	.42
CaO	10.94	14.27
F	.27	.13
TOTAL	91.92	94.62
Si	3.044	3.023
Al^{IV}	1.783	1.924
Al^{VI}		
Ce	.363	.266
Y	.018	.008
La	.203	.133
Nd	.113	.111
Fe	1.066	.945
Mg	.146	.153
Mn	.082	.007
Ti	.028	.029
Ca	1.154	1.400
F	.084	.038
Remarks	A,P	A,P

TABLE 21. Analyses of Calcite From the San Gabriel Fault Zone

Sample	SG8-PGN				SG8A	SG8-2
Specimen	E	F-1	F-2	G	1	4
CaO	52.56	53.05	50.92	54.74	56.27	54.36
MgO	.16	.33	.34	.05	.00	.31
FeO	.44	.67	.62	.21	.08	.77
MnO	.90	.92	.81	.62	.03	.77
BaO	.00	.00	.00	.00	.00	.00
CO_2[1]	43.04	42.98	41.21	43.53	44.23	43.95
TOTAL	98.10	97.96	93.89	99.15	100.60	100.16
			Formula Based on 2 Cations			
Ca	1.953	1.937	1.940	1.974	1.997	1.941
Mg	.008	.017	.018	.002	.000	.016
Fe	.012	.019	.018	.006	.002	.021
Mn	.026	.027	.024	.018	.001	.022
Ba	.000	.000	.000	.000	.000	.000
CO_2	2.000	2.000	2.000	2.000	2.000	2.000
Xcc[2]	.977	.969	.970	.987	.999	.971
Remarks[3]	B	B	B	F	F,P	F,P

[1] CO_2 Determined from Stoichiometry

[2] Mole fraction $CaCO_3$

[3] B= in micro breccia zone, F= inclusion in feldspar (secondary), P= inclusion in porphyroclast.

(Analyses of Calcite continued)

Sample	SG-9B	SG-12A	SG-12A
Specimen	B	F	F
CaO	57.43	52.36	52.11
MgO	.18	.25	.33
FeO	.04	.74	.87
MnO	.03	.35	.53
BaO	.00	.00	.00
CO_2 [1]	45.31	42.04	42.11
TOTAL	102.98	95.74	95.94
Ca	1.990	1.955	1.942
Mg	.009	.013	.017
Fe	.001	.022	.025
Mn	.001	.010	.016
Ba	.000	.000	.000
CO_2	2.000	2.000	2.000
Xcc [2]	.995	.978	.971
Remarks	C	V,F	V,M

C = coarse fragment, VF = Vein in feldspar, VM = vein in matrix

TABLE 2J. Analyses of Apatite From the San Gabriel Fault Zone

Sample	SG8-PGN		SG8-PGR		SG7-PB
Specimen	A	B	A	E	A
SiO_2	.09	.57	.33	.17	.57
Al_2O_3	.00	.00	.00	.00	.00
Ce_2O_3	.31	.15	.00	.20	.31
Y_2O_3	.33	.29	.22	.38	.20
La_2O_3	.25	.10	.00	.00	.07
Nd_2O_3	.30	.16	.09	.04	.00
FeO	.10	.11	.00	.06	.11
MgO	.00	.00	.00	.00	.00
CaO	53.49	54.52	55.39	55.58	54.79
Na_2O	.00	.00	.00	.07	.00
P_2O_5	40.45	40.92	41.40	41.76	40.92
F	2.45	2.34	4.02	4.19	3.64
Cl	.20	.14	.01	.01	.06
TOTAL	98.57	99.30	101.46	102.46	100.69
			Formula Based on 8 Cations		
Si	.059	.048	.028	.014	.050
Al	.000	.000	.000	.000	.000
Ce	.010	.005	.000	.006	.010
Y	.015	.013	.010	.017	.009
La	.008	.003	.000	.000	.002
Nd	.009	.005	.003	.001	.000
Fe	.007	.008	.000	.004	.008
Mg	.000	.000	.000	.000	.000
Ca	4.939	4.970	5.004	4.986	4.981
Na	.000	.000	.000	.012	.000
P	2.952	2.949	2.956	2.960	2.940
F	.667	.630	1.072	1.108	.978
Cl	.029	.020	.002	.001	.009
Remarks[1]	E	E	E	E	P

[1] E= euhedral matrix phase, P= porphyroclast

TABLE 2K. Analyses of Magnetite From the San Gabriel Fault Zone

Sample	SG8-PGN	SG8-PGR	SG8-2		SG8-A	SG7Pb
Specimen	A	B	3-1	3-2	A	1
SiO_2	.11	.07	.27	.15	.10	.87
TiO_2	.11	.05	.08	.11	.71	10.80
ZrO_3	.00	.00	.00		.00	.07
Al_2O_3	.00	.00	.02	.00	.06	.24
Cr_2O_3	.00	.06	.49	.08	.02	.28
FeO[1]	94.91	94.35	92.91	93.12	92.84	83.09
MgO	.00	.01	.05	.00	.08	.02
MnO	.00	.18	.00	.00	.06	.78
ZnO	.08	.07	.00	.00	.00	.13
Nb_2O_5	.00	.03	.00	.00	.05	.00
TOTAL	95.20	94.82	93.83	93.46	93.93	96.28
			Formula Based on 3 Cations			
Si	.004	.003	.010	.006	.004	.033
Ti	.003	.001	.002	.003	.020	.305
Zr	.000	.000	.000	.000	.000	.001
Al	.000	.000	.001	.000	.003	.011
Cr	.000	.001	.015	.002	.001	.008
Fe	2.991	2.985	2.969	2.989	2.965	2.612
Mg	.000	.001	.003	.000	.005	.001
Mn	.000	.006	.000	.000	.002	.025
Zn	.002	.002	.000	.000	.000	.004
Nb	.000	.001	.000	.000	.001	.000
XM[2]	.995	.993	.993	.995	.969	.681
Remarks[3]	I	F	P	P	P	B

[1] All Fe analysed as FeO
[2] Mole fraction magnetite (Fe_3O_4)
[3] I= with ilmenite, F= fine grained, P= porphyroclast, B= brecciated, C= coarse grained

(Analyses of Magnetite continued)

Sample	SG-6	SG-5	SG2-PGR	SG-9C		
Specimen	K	G	F	B	D	E
SiO_2	.15	.16	.12	.16	.11	.37
TiO_2	.04	.05	.18	.10	.13	.31
ZrO_2	.02	.03	.00	.00	.00	.00
Al_2O_3	.00	.08	.05	.15	.23	.06
Cr_2O_3	.03	.16	.03	.00	.02	.06
FeO	94.17	93.91	94.42	90.88	93.09	89.25
MgO	.00	.00	.00	.00	.03	.00
MnO	.09	.02	.05	.17	.05	.07
ZnO	.00	.00	.00	.00	.07	.00
Nb_2O_5	.02	.00	.05	.00	.00	.00
TOTAL	94.52	94.40	94.89	91.45	93.73	90.124
	Formula Based on 3 Cations					
Si	.006	.006	.004	.006	.004	.015
Ti	.001	.002	.005	.003	.004	.009
Zr	.000	.001	.000			
Al	.000	.003	.002	.007	.010	.003
Cr	.001	.005	.001		.001	.002
Fe	2.989	2.983	2.985	2.979	2.976	2.969
Mg	.000	.000	.000		.002	
Mn	.003	.001	.002	.006	.002	.002
Zn	.000	.000	.000		.002	
Nb	.000	.000	.001			
XM	.999	.994	.994	.993	.990	.988
Remarks	B	P	C	C	F	F

TABLE 2L. Analyses of Ilmenite and Ferropseudobrookite From the San Gabriel Fault Zone

Ilmenite

Sample	SG8-PGN	SG8-2		SG6	SG-9C	SG-9A1
Specimen	A	1	3	I	F	E
SiO_2	.07	.20	.07	.11	.14	.08
TiO_2	50.43	51.11	51.31	47.36	47.81	45.87
ZrO_2	.02	.00	.02	.00	.00	.00
Al_2O_3	.00	.00	.00	.00	.00	.00
Cr_2O_3	.10	.00	.04	.00	.07	.06
FeO[1]	47.06	43.75	47.03	42.01	48.01	47.43
MgO	.07	.07	.03	.00	.00	.11
MnO	3.74	3.49	.60	10.09	.55	1.19
ZnO	.07	.00	.00	.28	.03	.21
Nb_2O_5	.05	.08	.04	.48	.02	.08
TOTAL	101.60	98.70	99.14	100.33	96.63	95.03
	Formula Based on 2 Cations					
Si	.002	.005	.002	.003	.005	.003
Ti	.939	.982	.982	1.359	1.405	1.368
Zr	.000	.000	.000	.000		
Al	.000	.000	.000	.000		
Cr	.002	.000	.001	.000	.002	.002
Fe	.974	.934	1.001	1.320	1.568	1.573
Mg	.003	.003	.001	.000		.007
Mn	.078	.076	.013	.321	.018	.040
Zn	.001	.000	.000	.008	.001	.006
Nb	.001	.001	.000	.008	.000	.001
XILM[2]	.859	.906	.961	.676	.926	.879
XHEM	.059	.015	.017	.104	.061	.086
XPYR	.079	.076	.013	.215	.012	.027
XGEIR	.003	.003	.001	.005	.001	.001
Remarks[3]	E	P	P	B	C	P

[1] All Fe analysed as FeO
[2] Mole fraction ilmenite ($FeTiO_3$), Hematite (Fe_2O_3), pyrophanite ($MnTiO_3$) and Geikielite ($MgTiO_3$), Pseudo brookite (Fe_2TiO_5), Ferropseudo brookite ($FeTi_2O_5$)
[3] E= euhedral, P= porphyroclast, B= brecciated

(Analyses of Ilmenite and Ferropseudobrookite continued)

	Ferropseudobrookite
Sample	SG7Pb
Specimen	A
SiO_2	.16
TiO_2	62.76
ZrO_2	.00
Al_2O_3	.03
Cr_2O_3	.03
FeO	30.36
MgO	.00
MnO	.00
ZnO	.00
Nb_2O_5	.08
TOTAL	93.39

Formula Based on 3 Cations

Si	.007
Ti	1.945
Zr	.000
Al	.000
Cr	.0001
Fe	1.046
Mg	.000
Mn	.000
Zn	.000
Nb	.001
XPB	.027
XFPB	.973

B

TABLE 2M. Analyses of Laumontite from the San Gabriel Fault Zone

Sample	SG-9C	
Specimen	D	E
SiO_2	54.58	52.87
TiO_2	.00	.00
Al_2O_3	22.03	21.89
FeO	.00	.42
MgO	.00	.05
MnO	.00	.01
CaO	11.86	11.59
Na_2O	.00	.00
K_2O	.36	.36
TOTAL	88.83	87.19
Formula per 12 oxygen		
Si	4.067	4.046
Al^{IV}	.000	.000
Al^{VI}	1.935	1.939
Ti	.000	.000
Fe	.000	.027
Mg	.000	.005
Mn	.000	.000
Ca	.947	.950
Na	.000	.000
K	.034	.035

TABLE 3. Whole Rock Analyses[1] of Cataclastic and Protolith Rock Samples from the San Gabriel Fault Zone

Sample	SG7	SG7-PGR	SG7-Pb	SG8	SG8-PGN	SG8-PGR
SiO_2[2]	61.45	67.82	68.60	58.69	60.40	67.46
TiO_2	.87	.63	.61	1.03	.32	1.29
Al_2O_3	16.68	15.78	13.58	14.09	12.76	16.27
FeO[3]	4.96	2.58	4.07	7.67	9.19	1.10
MgO	1.66	.68	1.39	3.58	2.37	.70
MnO	.075	.03	.06	.12	.14	.06
CaO	2.18	2.65	2.05	5.07	5.42	2.35
Na_2O	3.64	4.17	3.06	2.93	2.99	3.73
K_2O	3.04	3.53	4.24	1.77	1.90	5.27
L.O.I.[4]	4.45	1.44	2.14	3.18	2.78	.96
TOTAL	99.01	99.31	99.80	98.13	98.27	99.19
K_2O+Na_2O	6.68	7.70	7.30	4.70	4.89	9.00
FeO/(FeO+MgO)	.749	.791	.745	.682	.795	.611
Li	45.0	15	21	22	13	15
Rb	107	81.8	129	48.6	130	35.2
Sr	378	658	224	564	270	463
Ba	997	1399	983	803	610	1649
K/Rb	236	358	273	302	121	1243
Ba/Rb	9.32	17.1	7.62	16.5	46.9	46.8
Rb/Sr	.283	.124	.576	.0862	.482	.0760
Ba/Sr	2.64	2.13	4.39	1.42	2.26	3.56
		Analyses Recast on Volatile Free Basis				
SiO_2	64.99	69.30	70.24	61.81	63.25	68.68
TiO_2	.92	.64	.62	1.08	.34	1.31
Al_2O_3	17.64	16.12	13.91	14.84	13.36	16.56
FeO	5.25	2.64	4.17	8.08	9.62	1.12
MgO	1.76	.69	1.42	3.77	2.48	.71
MnO	.08	.03	.06	.13	.15	.06
CaO	2.31	2.71	2.10	5.34	5.68	2.39
Na_2O	3.85	4.26	3.13	3.09	3.13	3.80
K_2O	3.22	3.61	4.34	1.86	1.99	5.36
TOTAL	100.00	100.00	100.00	100.00	100.00	100.00
Li	47.6	15.3	21.5	23.2	13.6	15.3
Rb	113	83.6	132	51.2	136	35.8
Sr	400	672	229	594	283	471
Ba	1054	1429	1007	846	639	1679

(Analyses of Cataclastic and Protolith Rock Samples continued)

Sample	SG9A-1	SG9A-2	SG-9B	SG-9C	SG-11A	SG-11B
SiO_2	56.68	61.65	64.00	54.53	61.11	71.18
TiO_2	1.16	.90	.86	1.47	.74	.09
Al_2O_3	19.22	17.07	14.34	16.83	15.79	13.70
FeO	6.71	5.10	5.32	7.40	4.28	.84
MgO	3.39	2.32	1.70	2.70	2.81	.37
MnO	.084	.061	.089	.123	.069	.020
CaO	.83	1.76	3.20	4.99	3.53	2.53
Na_2O	.57	2.56	3.74	3.75	3.13	4.39
K_2O	5.06	3.46	3.50	2.13	2.89	4.66
L.O.I.	5.79	4.56	3.12	4.44	5.62	2.16
TOTAL	99.49	99.45	99.87	98.36	99.97	99.94
K_2O+Na_2O	5.63	6.02	7.24	5.88	6.02	9.05
FeO/(FeO+MgO)	.664	.687	.758	.733	.604	.694
Li	23.1	46.1	21.8	24.2	37.6	42.3
Rb	251	139	67.0	66.3	112	94.1
Sr	146	326	277	521	563	380
Ba	497	905	925	716	3141	1278
K/Rb	167	207	434	267	214	411
Ba/Rb	1.98	6.51	13.8	10.8	28.0	13.6
Rb/Sr	1.72	.426	.242	.127	.199	.248
Ba/Sr	3.40	2.78	3.34	1.37	5.58	3.36
Analyses Recast on Volatile Free Basis						
SiO_2	60.49	64.98	66.15	58.06	64.77	72.80
TiO_2	1.24	.95	.89	1.57	.78	.09
Al_2O_3	20.51	17.99	14.82	17.92	16.74	14.01
FeO	7.16	5.38	5.50	7.88	4.54	.86
MgO	3.62	2.45	1.76	2.87	2.98	.38
MnO	.09	.06	.09	.13	.07	.02
CaO	.89	1.85	3.31	5.31	3.74	2.59
Na_2O	.61	2.70	3.87	3.99	3.32	4.49
K_2O	5.40	3.65	3.62	2.27	3.06	4.77
TOTAL	100.00	100.00	100.00	100.00	100.00	100.00
Li	24.7	48.6	22.5	25.8	39.9	43.3
Rb	26.8	147	69.3	70.6	119	96.2
Sr	156	344	286	555	597	389
Ba	530	954	956	762	3329	1307

(Analyses of Cataclastic and Protolith Rock Samples continued)

Sample	SG-13A	SG-13ap	SG-13B	SG-13bp	SG-16a	SG-16D	SG-16E
SiO_2	67.73	66.09	63.05	44.67	56.25	61.97	72.07
TiO_2	.56	.54	1.04	2.41	1.52	1.01	.23
Al_2O_3	14.83	15.58	14.79	13.15	15.71	14.72	14.47
FeO	2.51	2.52	6.30	15.29	8.79	6.74	1.56
MgO	1.10	1.09	3.80	7.85	3.11	2.26	.55
MnO	.042	.044	.063	.203	.131	.147	.038
CaO	3.30	3.45	1.39	9.02	3.48	3.78	1.73
Na_2O	3.33	3.83	.75	1.03	1.80	2.46	3.72
K_2O	3.61	3.20	4.29	1.42	1.91	3.56	4.06
L.O.I.	2.98	1.73	3.66	2.20	6.42	2.55	.82
TOTAL	99.99	98.07	99.14	97.24	99.12	99.20	99.25
K_2O+Na_2O	6.94	7.03	5.05	2.45	2.71	6.02	7.78
FeO/(FeO+MgO)	.695	.698	.624	.661	.739	.749	.739
Li	18.9	16.5	44.2	12.9	41.8	16.0	18.8
Rb	103	85.9	220	20.3	55.3	147	78.3
Sr	487	590	345	146	288	208	380
Ba	1129	992	1194	104	958	754	988
K/Rb	291	309	162	581	287	201	430
Ba/Rb	11.0	11.5	5.43	5.12	17.3	5.13	12.6
Rb/Sr	.211	.146	.638	.139	.192	.707	.206
Ba/Sr	2.32	1.68	3.46	.712	3.33	3.63	2.60

Analyses Recast on Volatile Free Basis

	SG-13A	SG-13ap	SG-13B	SG-13bp	SG-16a	SG-16D	SG-16E
SiO_2	69.82	68.60	66.03	47.00	60.78	64.12	73.22
TiO_2	.58	.56	1.09	2.54	1.64	1.05	.23
Al_2O_3	15.29	16.17	15.49	13.84	16.95	15.23	14.70
FeO	2.59	2.62	6.60	16.09	9.48	6.97	1.58
MgO	1.13	1.13	3.98	8.26	3.35	2.34	.56
MnO	.04	.05	.07	.21	.14	.15	.04
CaO	3.40	3.58	1.46	9.49	3.75	3.91	1.76
Na_2O	3.43	3.98	.80	1.08	1.94	2.55	3.78
K_2O	3.72	3.32	4.49	1.49	2.06	3.68	4.12
TOTAL	100.00	100.00	100.00	100.00	100.00	100.00	100.00
Li	19.5	17.1	46.3	13.6	45.1	16.6	19.1
Rb	106	89.2	230	21.4	59.7	152	79.6
Sr	502	612	361	154	311	215	386
Ba	1163	1030	1251	109	1033	780	1004

[1] Analyses completed at U.S.C. Petrochemistry Laboratory by Whitney Moore and J. Lawford Anderson
[2] Major elements as wt. % oxide; trace elements Li, Rb, Ba, and Sr as ppm
[3] All Fe as FeO
[4] L.O.I. = Loss on ignition at 1000°C, includes $H_2O + CO_2$

TABLE 4. Summary of Textural results for Measurable Grains[1]

Grain-size classes		Sample Number — Values are listed as Frequency Percentages				
Millimeters	Phi (ϕ) units	SG2	SG5	SG6	SG7	SG8
1.00 to 1.41	-0.5 to 0.0	0.00	0.00	0.14	0.00	0.00
0.71 to 1.00	0.0 to 0.5	0.01	0.00	0.32	0.00	0.00
0.50 to 0.71	0.5 to 1.0	0.03	0.10	0.49	0.00	0.00
0.35 to 0.50	1.0 to 1.5	0.08	0.04	0.44	0.00	0.00
0.25 to 0.35	1.5 to 2.0	0.06	0.05	0.51	0.00	0.00
0.177 to 0.25	2.0 to 2.5	0.38	0.48	0.47	0.00	0.02
0.125 to 0.177	2.5 to 3.0	0.55	1.22	0.53	0.03	0.05
0.088 to 0.125	3.0 to 3.5	1.58	3.44	1.31	0.13	0.34
0.0625 to 0.088	3.5 to 4.0	4.69	10.21	2.94	0.47	0.99
0.044 to 0.0625	4.0 to 4.5	8.03	17.72	6.17	1.09	2.53
0.031 t0 0.044	4.5 to 5.0	16.45	25.61	10.72	3.12	5.77
0.0221 to 0.031	5.0 to 5.5	22.62	23.41	20.12	6.61	12.42
0.0156 to 0.0221	5.5 to 6.0	25.79	14.57	28.01	20.32	24.23
0.0110 to 0.0156	6.0 to 6.5	12.15	3.21	16.47	21.63	16.98
0.0078 to 0.0110	6.5 to 7.0	7.58	0.04	11.35	46.60	36.66
TOTAL		100.00	100.10	99.99	100.00	99.99
Percentage of measureble grains[1]		15.5	19.3	63.0	15.2	10.7

[1] Grains with diameter $\geq$ 0.0078 mm.

(Summary of Textural results for Measurable Grains continued)

Grain-size classes								Sample Number Values are listed as Frequency Percentages			
Millimeters			Phi (ϕ) units			SG-10A	SG-13A	SG-13B	SG-15A	SG-16A	SG-18A
1.00	to	1.41	-0.5	to	0.0	0.00	0.00	0.00	0.00	0.00	0.00
0.71	to	1.00	0.0	to	0.5	0.00	0.00	0.00	0.00	0.00	0.00
0.50	to	0.71	0.5	to	1.0	0.00	0.00	0.00	0.00	0.00	0.00
0.35	to	0.50	1.0	to	1.5	0.00	0.00	0.00	0.00	0.00	0.00
0.25	to	0.35	1.5	to	2.0	0.00	0.00	0.00	0.00	0.00	0.00
0.177	to	0.25	2.0	to	2.5	0.37	0.52	1.07	0.40	0.00	0.72
0.125	to	0.177	2.5	to	3.0	1.12	1.09	5.86	0.78	0.01	1.15
0.088	to	0.125	3.0	to	3.5	3.23	3.11	29.66	2.38	0.02	2.28
0.0625	to	0.088	3.5	to	4.0	9.90	7.15	27.87	6.25	0.16	5.49
0.0440	to	0.0625	4.0	to	4.5	14.91	12.18	21.47	10.52	0.83	9.32
0.0310	to	0.0440	4.5	to	5.0	22.17	18.42	8.52	17.63	3.77	16.35
0.0221	to	0.0310	5.0	to	5.5	23.38	23.72	3.83	24.78	14.37	21.58
0.0156	to	0.0221	5.5	to	6.0	18.35	22.40	1.16	26.02	45.45	28.07
0.0110	to	0.0156	6.0	to	6.5	4.62	7.66	0.42	8.32	23.20	12.37
0.0078	to	0.0110	6.5	to	7.0	1.94	3.74	0.14	2.92	12.20	2.68
TOTAL						99.99	99.99	100.00	100.00	100.01	100.01
Percentage of measurable grains[1]						25.0	42.7	23.4	29.6	9.9	33.4

[1] Grains with diameter $\geq$ 0.0078 mm.